Un-Coordinated Multi-User and Inter-Cell Interference Alignment based on Partial and Outdated Information for Large Cellular Networks

Von der Fakultät Informatik, Elektrotechnik und Informationstechnik der Universität Stuttgart zur Erlangung der Würde eines Doktor-Ingenieurs (Dr.-Ing.) genehmigte Abhandlung

Vorgelegt von

Danish Aziz

aus Karachi

Hauptberichter:	Prof. Dr.-Ing. Joachim Speidel
Erster Mitberichter:	Prof. Dr.-Ing. Andreas Kirstädter
Zweiter Mitberichter:	Prof. Dr.-Ing. Stephan ten Brink
Tag der mündlichen Prüfung:	18. Januar 2016

Institut für Nachrichtenübertragung der Universität Stuttgart

2016

Contents

Acknowledgements **vii**

Abstract **ix**

Kurzfassung **xi**

List of Acronyms **xiii**

List of Symbols **xvii**

1 Introduction **1**

1.1 Motivation and Focus 2

1.2 Thesis Outline and Contributions 5

2 Fundamentals **7**

2.1 Wireless Channel Models 7

2.1.1 Empirical Models 8

2.1.2 Shadow Fading Models 9

2.1.3 Multipath Fading Models 10

2.1.4 MIMO Spatial Channel Model 11

2.2 OFDM Based Wireless Access 15

2.3 Closed Loop Downlink MIMO Transmission Schemes 17

2.4 Interference in Cellular Networks 18

3 Coordinated Inter-Cell Interference Alignment **19**

3.1 Introduction 19

3.2 System Model 21

3.2.1 Coordination Clusters 22

3.3 Loss in Degrees of Freedom . . . 24
3.4 Transmit Precoding using Interference Alignment . . . 26
3.5 Baseline Transmit Precoding Schemes . . . 28
3.6 Linear Receiver Design . . . 29
3.7 CSI Sharing Requirements . . . 31
3.8 Performance with Ideal Channel Estimation . . . 32
3.8.1 Simulation Assumption and Parameters . . . 32
3.8.2 Spectral Efficiency Evaluation . . . 33
3.8.3 Impact of Receivers . . . 34
3.8.4 Impact of Residual Unaligned Interference . . . 34
3.9 Performance with Channel Estimation Errors . . . 37
3.10 User Selection Diversity for IA . . . 39
3.10.1 System Assumptions and Problem Formulation . . . 40
3.10.2 User Selection Algorithms . . . 41
3.10.3 Performance Analysis . . . 45
3.11 Conclusion . . . 47

4 Un-Coordinated Multi-User Inter-Cell Interference Alignment 49
4.1 Introduction . . . 49
4.2 Basic Idea . . . 52
4.2.1 Numerical Results . . . 57
4.3 Multi Cell Multi User MIMO System Model . . . 60
4.4 Transmit Precoding using Multi User Inter Cell Interference Alignment . . . 64
4.4.1 Based on Multiuser Inter Cell IA (MUICIA) . . . 64
4.4.2 Based on Multiuser Strongest Cell IA (MUSCIA) . . . 67
4.5 Baseline Transmit Precoding Schemes . . . 68
4.5.1 Egoism: Maximum Ratio Transmission (MRT) . . . 68
4.5.2 Altruism: Effective Zero forcing (EFZF) . . . 69
4.5.3 Balance: Signal to Leakage and Noise Ratio (SLNR) . . . 69
4.6 Rate Computation . . . 70
4.7 Performance Analysis of IA based Precoding Schemes . . . 70
4.7.1 Simulation Assumptions and Parameters . . . 70
4.7.2 Impact of Inter Cell Interference . . . 72

4.7.3 Impact of Receiver Realization . . . 73
4.8 Multi User Selection . . . 73
4.8.1 Pair Selection Algorithms . . . 74
4.8.2 Performance of MUICIA with User Selection . . . 78
4.9 Conclusion . . . 81

5 Un-Coordinated Interference Alignment with Practical Constraints 83
5.1 Performance with Imperfect Information . . . 83
5.1.1 Channel Estimation Errors at the Receiver . . . 84
5.1.2 Interference Estimation Errors at the Receiver . . . 88
5.1.3 Imperfect Information at the Transmitter . . . 89
5.1.4 Results with Imperfect Information . . . 91
5.2 Performance with Limited Feedback . . . 97
5.3 Performance with Measured Channels . . . 99
5.3.1 Technical Description for the Measurement Platform . . . 99
5.3.2 Precoding in Interfering Cells . . . 100
5.3.3 Transmit Processing . . . 102
5.3.4 Receive Processing . . . 105
5.3.5 Measurement Scenarios . . . 106
5.3.6 Measurement Results and Anaylsis . . . 107
5.4 Conclusion . . . 111

6 Performance of Un-Coordinated Alignment in Heterogeneous Networks 113
6.1 Introduction . . . 113
6.2 System Model and Performance Metric . . . 115
6.3 Important Aspects of Heterogeneous Networks . . . 117
6.3.1 Cell Association and Range Expansion . . . 117
6.3.2 Enhanced Inter Cell Interference Coordination (eICIC) . . . 117
6.3.3 User Scheduling during ABS . . . 118
6.4 Performance Results and Analysis . . . 120
6.4.1 Simulation Assumptions . . . 121
6.4.2 Impact of Heterogeneity . . . 122
6.4.3 Spectral Efficiency Gains in Macro Coverage Area . . . 123
6.4.4 Interference Alignment vs Interference Coordination . . . 124

6.4.5 Conclusion 126

7 Conclusion **127**

References **129**

Acknowledgements

This dissertation is a part of my research activities in the department of *Smart Wireless Networks* at Alcatel-Lucent Bell Labs, Germany in cooperation with the Institute of Telecommunications (INUE), University of Stuttgart, Germany.

My sincere gratitudes towards Prof. Dr.-Ing. Joachim Speidel for providing me the opportunity to complete this milestone and supervising me for the whole period of time.

I am grateful to Prof. Dr.-Ing. Andreas Kirstädter and to Prof. Dr.-Ing. Stephan ten Brink for being the second and the third reviewer and providing me the valuable comments and improvements.

My special thanks to the *Access Domain Leader* at Bell Labs, Dr. Theodore Sizer for encouraging me to carry out this disruptive research.

I express my deepest gratitude to the head of *Smart Wireless Networks* at Bell Labs, Ulrich Barth for making this cooperation with INUE possible and providing me all the required degrees of freedom. As my manager, Mr. Barth always supported me and guided me to the path that lead me to successfully achieve this goal in my professional career.

I extend a very heartfelt thank to Dr.-Ing. Andreas Weber for his constant support, extensive technical discussions, his guidance and his critic in many aspects of this work, in particular, for efficient simulation and modelling of large cellular networks.

My sincere thanks to Dr. Paolo Baracca, Dr. Federico Boccardi, Mr. Thorsten Wild, Dr. Gerhard Schreiber, Mr. Siegfried Klein, Mr. Osman Aydin and Mr. Lutz Schoenerstedt for their time and efforts to carry out valuable technical discussions that helped me define valid research problems and provide their successful solutions. I would also like to thank my fellow researchers at *Smart Wireless Networks* for providing me a friendly working environment specially, my room mate, Mr. Michael Wilhelm who always motivated me with his inspirational quotes and short moral stories.

Acknowledgements

I acknowledge and appreciate the work of all the students who carried out their *Master Thesis Projects* with me in this area of research.

My special thanks to my colleagues and friends who reviewed my thesis and provided me their valuable comments and suggestions.

I would like to thank Mr. Stephen Kaminski and Dr. Markus Gruber at Bell Labs who encouraged and motivated me to kick off this milestone.

With all my heart and countless gratitudes I express my thanks and grateful emotions to my whole family specially my parents, my siblings, my wife, my sweet little daughter and my lovely son for their abiding love and for providing me all the support that I needed.

Finally, I would like to thank all my beloved friends specially my two best friends, Faris and Ismail for their well wishes and their cherishing talks that kept me motivated to achieve this goal.

Abstract

The cellular networks have gone through rapid evolution during the past decade. However, their performance is still limited due to the problem of interference. Therefore, interference management in current and future cellular networks is still an ongoing research topic. Interference Alignment is one of the techniques to manage the interference efficiently by using "*align*" and "*suppression*" strategy.

In the first part of this thesis we focus on *Coordinated inter cell interference alignment* in a large cellular network. We assess the performance of interference alignment based transmit precoding under specific receiver strategies and coordination scenarios by comparing with different state of the art precoding schemes. We continue our assessment by considering imperfect channel state information at the transmitter. The results show that the gains of coordinated alignment based transmission are very sensitive to the receiver strategies and imperfections as compared to the other precoding schemes. However, in case of the availability of good channel conditions with very slow moving users, coordinated interference alignment outperforms the other baselines even with imperfect channel state information. In addition to that, we propose efficient user selection methods to enhance the performance of coordinated alignment. The results of our assessment draws important conclusions about the application of coordinated interference alignment in practical systems.

In the second part of the thesis we consider a cellular system where each cell is serving multiple users simultaneously using the same radio resource. In this scenario, we have to manage not only the inter cell interference but also the multi user interference. For this purpose, we propose a novel *Uncoordinated* transmit precoding scheme for multi user cellular networks which is based on the alignment of *multi user interference* with *partial and outdated inter cell interference*. We show analytically that our scheme approaches the performance optimal transmission scheme. With the help of simulations we show that our proposal outperforms the state of the art non-alignment based multi user transmit precoding schemes.

Abstract

We further propose user selection methods which exploit the diversity gains and improve the system spectral efficiency. In order to assess the feasibility of our proposal in a real system, we evaluate our scheme with practical constraints like imperfect information at the transmitter and limited feedback in uplink channel. For the proof of concept we also evaluate the performance of our scheme with measured channels using a software defined measurement platform. Finally, we also assess the application of our proposal in future heterogeneous networks. The outcome of our efforts states that as an interference alignment based transmission scheme, our scheme is a good candidate to manage the two dimensional interference in multi user cellular networks. It outperforms the non-alignment baselines in many scenarios even with practical constraints.

Kurzfassung

Die Mobilfunknetze haben sich während den letzten zehn Jahren sehr rasch entwickelt. Aber ihre Leistungsfähigkeit ist noch durch die Interferenz begrenzt. Für aktuelle und zukünftige Mobilfunknetze ist daher das Interferenzmanagement ein andauerndes Forschungsthema. *Interference Alignment* ist eine der Techniken, die die Interferenz durch räumliche Vorcodierung im Sender vektoriell ausrichtet, um sie im Empfänger unterdrücken zu können.

Im ersten Teil der Arbeit konzentrieren wir uns auf *Coordinated Inter Cell Interference Alignment* in einem großen Mobilfunknetz. Wir bewerten die Leistungsfähigkeit von Sendeverfahren basierend auf *Interference Alignment* unter Berücksichtigung spezifischer Empfangsalgorithmen und Koordinierungsszenarien mit verschiedenen Sendeverfahren die Stand der Technik sind. Unsere Beurteilung berücksichtigt unvollständige Kanalinformationen am Sender. Die Ergebnisse zeigen, dass die Gewinne der *Coordinated Interference Alignment* basierten Übertragungen sehr empfindlich hinsichtlich der Empfangsalgorithmen und unvollständigen Kanalinformationen sind im Vergleich zu bereits bekannten Sendeverfahren. Jedoch im Falle von guten Kanalbedingungen für sehr langsam bewegte Benutzer übertrifft *Interference Alignment* die anderen bekannten Sendeverfahren auch bei unvollständigem Kanalwissen. Zusätzlich schlagen wir effiziente Scheduler-Verfahren vor, die die Leistung von *Coordinated Interference Alignment* erhöhen. Die Ergebnisse unserer Untersuchung treffen wichtige Aussagen über die Anwendbarkeit von *Interference Alignment* in realen Systemen.

Im zweiten Teil der Arbeit betrachten wir ein zellulares System, in dem jede Zelle mehrere Mobilifunknutzer gleichzeitig mit der gleichen Funkressource bedient. In diesem Szenarium müssen wir nicht nur die *Inter Cell Interference*, sondern auch *Multi User Interference* berücksichtigen. Für diesen Zweck schlagen wir ein neues *Uncoordinated* Sendeverfahren für Mobilfunknetze mit mehreren Nutzern vor. Dieses Verfahren basiert auf *Alignment* von *Multi User Interference* mit *Partial and Outdated Inter Cell Interference*. Wir zeigen analytisch, dass die Leistungsfähigkeit unseres Systems sich dem optimalen Sendeverfahren annähert. Mit

Kurzfassung

Hilfe von Simulationen zeigen wir, dass unser Ansatz die Leistung anderer *Multi User* Sendeverfahren des Stands der Technik übertrifft. Weiterhin schlagen wir Nutzerauswahlmethoden vor, welche die Kanaldiversität ausnützen und die spektrale Effizienz des Systems verbessern. Um unseren Vorschlag in einem realen Systems zu bewerten, evaluieren wir unsere Methoden unter praxisnahen Bedingungen, wie dem senderseitig unvollständigen Kanalwissen und unter begrenztem Feedback auf dem Uplink-Kanal. In einer Machbarkeitsstudie bewerten wir auch die Leistungsfähigkeit unseres Verfahrens mit real gemessenen Kanälen und einem softwarebasierten Messaufbau. Am Ende der Arbeit haben wir die Anwendbarkeit unseres Vorschlags für zukünftige heterogene Netzwerke bewertet. Das Ergebnis unserer Arbeit zeigt, dass unter den *Interference Alignment* Sendeverfahren unser Verfahren ein guter Kandidat ist, um die zweidimensionale Interferenz in Mobilfunknetzen mit mehrerern Nutzern zu reduzieren. Unser Verfahren übertrifft andere *Multi User* Sendeverfahren in vielen Szenarien sogar unter realen Bedingungen.

List of Acronyms

ABS	Almost Blank Subframe
AoA	Angle of Arrival
AoD	Angle of Departure
BS	Base Station
CBW	Cell Border Window
CSI	Channel State Information
CSRS	Cell Specific Reference Signals
CP	Cyclic Prefix
CU	Central Unit
DoF	Degree of Freedom
DPC	Dirty Paper Coding
EFZF	Effective Zero Forcing
eICIC	Enhanced Inter Cell Interference Coordination
FDD	Frequency Division Duplex
HETNET	Heterogeneous Networks
ICI	Inter Cell Interference
IRC	Interference Rejection and Combining

IM	Interference Minimization
INCI	Intra Cluster Interference
INR	Interference to Noise Ratio
LMMSE	Linear Minimum Mean Square Error
LOS	Line Of Sight
LTE	Long Term Evolution
MIMO	Multiple Input Multiple Output
MISO	Multiple Input Single Output
MMSE	Minimum Mean Square Error
MRC	Maximum Ratio Combining
MRT	Maximum Ratio Transmission
MUI	Multi User Interference
MU-MIMO	Multi User MIMO
MUICIA	Multi User Inter Cell Interference Alignment
MUSCIA	Multi User Strongest Inter Cell Interference Alignment
NLOS	Non Line Of Sight
NF	Noise Factor
OCI	Out of Cluster Interference
OFDM	Orthogonal Frequency Division Multiplexing
PRB	Physical Resource Block
RE	Resource Element
RSS	Received Signal Strength

RSRP	Reference Signal Received Power
RX	Receiver
RVQ	Random Vector Quantization
SC	Sub Carrier
SCM	Spatial Channel Model
SICI	Strongest Inter Cell Interference
SINR	Signal to Interference and Noise Ratio
SIRC	Strongest Interference Rejection and Combining
SAIRC	Strongest and Average Interference and Noise Ratio
SNR	Signal to Noise Ratio
SLNR	Signal to Leakage and Noise Ratio
SUS	Semi-orthogonal User Selection
SVD	Singular Value Decomposition
TDD	Time Division Duplex
TTI	Transmission Time Interval
TX	Transmitter
UE	User Equipment
USRS	UE Specific Reference Signals
ZFBF	Zero Forcing Beamforming
3GPP	3rd Generation Partnership Project

List of Symbols

x:	scalar in $\mathbb{R}$ or $\mathbb{C}$
$\mathbf{x}$:	column vector
$\mathbf{X}$:	matrix $\mathbf{X}$
$\mathcal{A}$:	finite set
$(.)^T$:	transpose
$(.)^*$:	complex conjugate
$(.)^H$:	complex conjugate transpose (Hermitian)
$(.)^{-1}$:	inverse
$\mathbb{E}[.]$:	expectation
$(.)^\dagger$:	Moore-Penrose pseudoinverse
$\|x\|$:	absolute value of scalar x
$\|\mathbf{x}\|$:	Euclidean norm of vector $\mathbf{x}$
$\|\mathbf{X}\|_F$:	Frobenius norm of matrix $\mathbf{X}$
$\|\mathbf{X}\|$:	determinant of matrix $\mathbf{X}$
$\|\mathcal{A}\|$:	cardinality (size) of set $\mathcal{A}$
$Tr(\mathbf{X})$:	trace of matrix $\mathbf{X}$
$diag(\mathbf{X})$:	replace the non-diagonal entries of the Matrix $\mathbf{X}$ by 0

$\mathbf{I}_N$: identity matrix of size N

$\mathbf{o}$, $\mathbf{0}$: null vector and null matrix with all zero entries

$\mathcal{CN}\left(\mu, \eta^2\right)$: circularly symmetric complex Gaussian random variable with mean μ and variance η^2

$span(\mathbf{X})$: span of the column vectors of matrix $\mathbf{X}$

Chapter 1

Introduction

Wireless communication systems enable humans, sensors, machines or any two entities (commonly called as nodes or users) to communicate through wireless channels using electromagnetic waves. Like any other system in our daily life, one of the main objectives in the development of a wireless system is to improve the system efficiency. In general, the efficiency can be defined as the ratio of useful output to the given input resources. For a given amount of resources, the efficiency can be improved by increasing the system performance to enhance the useful output. The primary resource of a wireless communication system is the *frequency spectrum (bandwidth, expressed in Hertz)* and the desired output is the *rate of information (communication, expressed in bits per seconds)*. Therefore, the *information rate per Hertz* which is commonly known as *Spectral Efficiency* is our primary concern in this thesis. In particular, we are interested to achieve a higher spectral efficiency for a cellular wireless communication network.

As there may be many simultaneously active users in the network, there will be more than one wireless link that will share the limited resources over the wireless channel. If more than one link starts communicating actively, using the same frequency spectrum in a given time, they will interfere with each other and the information transfer for each individual link will suffer loss. This information loss due to the interference reduces the system efficiency. In order to allow loss-less communication of multiple links simultaneously, the interference between the links should be managed and treated if necessary. One way of managing would be to distribute the frequency spectrum between the links orthogonally in time. It resolves the problem of interference. However, it reduces the spectral efficiency of the system. The challenging goal of this work is to find advanced methods which deal with this interference

and maintain or improve the spectral efficiency of the system. Until now for cellular networks, there are many techniques that have been developed to approach this goal such as, frequency reuse [1], Code Division Multiple Access (CDMA) [2] and interference coordination ([3] and references there in). One of the recently developed techniques that deal with interference is called the ***Interference Alignment*** (IA) as proposed in [4] and [5]. Here we focus on this technique, as it promises the optimum achievable performance for a given interference network.

1.1 Motivation and Focus

The transmission from the network side towards the end user is generally referred as *downlink*. The basic transmitting entity in downlink transmission is commonly known as *base station*. The coverage area of a base station is known as a *cell*, therefore in literature, the term cell also refers to the base station or the network side transmitter. In a cellular network, many cells are deployed to cover a large geographical area with careful cellular planning. For efficient use of spectrum, typically the operator of the network would like to use the same frequency in all the cells. However, the problem of interference arises when the geographically neighbouring cells serve their users simultaneously on the same frequency resources. This interference is called the inter cell interference (ICI) and this problem makes the cellular networks inherently interference limited.

Frequency reuse [1] is one of the solutions to this problem. The spectrum is divided into subsets and each subset is allocated to the cell such that the subsets of geographically direct neighbouring cells are mutually exclusive. In Europe, the 2nd generation of the cellular systems (Global System for Mobile Communications (GSM)) employed this solution [6]. However, this solution reduces the spectral efficiency. Therefore, the next generations like Universal Mobile Telecommunication Systems (UMTS), Wideband CDMA (WCDMA), High Speed Packet Access (HSPA) [7], Long Term Evolution (LTE) and LTE-Advanced [8]) did not rely only on the frequency reuse. For these systems, other methods were adopted to overcome this problem and still maintain the requirements of achievable system spectral efficiency. Therefore, the 3rd generation systems, WCDMA/UMTS/HSPA, used spreading codes and combining techniques [7]. The 4th generation and beyond, LTE and LTE-Advanced, which are based on OFDM based radio interface, came up with fractional/soft frequency reuse [8].

However, it requires enormous effort of frequency planning. Furthermore, it needs coordination between the cells which comes with extra cost on backhaul. Great efforts have been put in the research to find optimum solutions for ICI problem and it is still an ongoing research topic (please refer to [9] and references therein).

Inspired by the antenna arrays in radars, multiple transmit and receive antennas were also introduced in the communication systems [10]. This started an era of research for Multiple Input and Multiple Output (MIMO) wireless communication. The initial objective of using multiple antennas was to exploit the spatial diversity of the wireless channel in order to achieve robustness in communication [11]. Later it lead to enhancement in the spectral efficiency. The work in [12, 13] showed that there can be a linear increase in spectral efficiency with the increase in the number of antennas in the system. The advancement in MIMO technology has also evolved the objectives of MIMO. At present, the MIMO transmission methods can be used to enhance the signal quality and robustness [14] or to mitigate the interference in the system [15]. On the basis of the use of channel state information (CSI) at the transmitter, MIMO methods can be categorized as *open loop methods* and *closed loop methods*. The *open loop methods* do not require any CSI at the transmitter. Their objective is mainly to achieve robustness against the errors induced by the channel using the channel diversity. The *closed loop methods* require the CSI at the transmitter. This CSI can be used to design the transmission such that a greater amount of desired signal energy reaches the desired receiver. It can also be used to ensure less interference at the desired receiver. Either way, the goal is to enhance the spectral efficiency of the system. These transmission methods, which use the spatial dimension (multiple antennas) to design the transmit signal are in general known as *transmit precoding methods*.

Jafar et al [5] presented the application of the interference alignment technique in the design of closed loop transmit precoding in a universal reuse fully coordinated cellular system to deal with the ICI problem. For this purpose, they considered multiple antennas as the spatial resource and showed that interference alignment is close to optimum even with universal reuse. The main idea behind interference alignment is to confine the interference at the desired receiver in a subspace non-overlapping to the desired signal space. Once the interference is confined, the receiver can suppress it with a proper design of receiver algorithm. We do not want to go into the details of the alignment technique now, but we would like to mention that it is a concept that can be applied using any resource dimension e.g. frequency or time. Initially, it was presented over time by symbol extension in [4].

Motivated by Jafar's approach, we focus on interference alignment using spatial dimension in cellular network. We start by analysing the fact that coordination in a network is possible only on a limited scale. It implies that the uncoordinated transmissions would perturb the optimality of alignment in a practical cellular network. Hence as a first step, in the first part of this thesis we investigate the realization of IA in a coordination-cluster based large cellular network. In line with the practical feasibility, we analyse the loss in the performance due to the channel estimation errors and various levels of interference suppression capabilities of present day receivers. Following the critical aspects of real world, we also exploit the opportunities provided by the practical conditions such as channel diversity. We explore user selection diversity and propose user selection methods to improve the system performance with IA as transmit precoding in a clustered cellular network.

The use of MIMO opens a new door of multiple access which is called Spatial Division Multiple Access (SDMA) and generally referred as Multi User MIMO (MU-MIMO) in literature. It enables the transmitter to schedule and transmit multiple users in a cell simultaneously on the same radio resource. However, this benefit does not come without a cost. The co-scheduling of multiple users on the same resource causes an extra dimension of interference in the system which can be called as *Intra Cell Interference*. To differentiate easily between the two interferences in this thesis, we call intra cell interference as *Multi User Interference* (MUI). There are many transmission methods and studies like [15, 16] and [17] which explore the potential of SDMA by designing the appropriate transmit precoding to deal with MUI but they neglect the impact of ICI by considering a single cell system. Therefore, after dealing with ICI through coordinated IA, we shift our focus to deal with both ICI and MUI. We propose an interference alignment based precoding technique which aligns the MUI and ICI in a multi cell system. Similar to the first part, we also analyse our approach with some practical constraints like feedback limitations, channel estimation errors and different receiver capabilities. As a proof of concept, we also demonstrate the performance of our scheme using measured channels on a software defined measurement test-bed. The results show that our proposed interference alignment based transmit precoding scheme outperforms the state of the art non-alignment based MU-MIMO transmit precoding schemes in the presence of ICI in a multi cell system.

We also exploit the user selection diversity for our scheme. Especially in the case of MU-MIMO, user selection improves the performance of the transmit precoding scheme. In principle, the users which are facing spatially orthogonal channels from its serving cell they

will cause least interference on each other and make the most of multi user transmission [16]. We propose user selection methods that bring sustainable gains to the system which is serving multiple antenna user equipments.

Due to the increasing demand of capacity and traffic density, it has been proposed to deploy an additional layer of cells on top of the macro cellular layer. Now the primitive approach of single layer is termed as *Homogeneous Network* and the multi layer approach is known as *Heterogeneous Network* (HetNets). The additional layer of cells can be deployed on the same or on additional frequency spectrum. The deployment on the same frequency is known as co-channel deployment. In either way the power is kept very small in order to reduce additional interference in the system and thus often the name *small cells* is used for the additional layer. The initial purpose of the small cells is to provide a good signal to noise ratio to the users present at the border of macro cells. Notice that the ICI characteristics in a co-channel deployed HetNet would be different than a plane homogeneous network. In principle, we have a two-layer universal frequency reuse in HetNets which imposes a big challenge to deal with the ICI. This gives us the motivation to study further the interference alignment and user selection algorithms in HetNets with MU-MIMO. Hence as a last part of the thesis we investigate the performance of our proposed multi user interference alignment technique in HetNet. We not only analyse interference alignment as a transmit precoding method but also as an interference management technique in HetNet. For this purpose, we also compare it with the state of the art interference coordination techniques and show that in relevant scenarios interference alignment out performs the interference coordination with respect to the system performance and system resource utilization.

1.2 Thesis Outline and Contributions

After explaining the major focus of the thesis, in this section we will explain briefly the structure in which we have distributed our efforts. The rest of the work is organized in six chapters. The brief description of each is given as follows;

In Chapter 2, we provide a short review of the essential characteristics and issues in a cellular wireless system that will help us understanding the approaches and results in later chapters. These essentials include the modelling of the wireless channel. We explain different types of channel models with extensive details to MIMO spatial channel model as we have used this model throughout the thesis for our simulation based analysis. Then we briefly

describe the OFDM based radio access as we have considered a MIMO-OFDM system in this thesis. An overview of the closed loop transmit precoding techniques is also given in order to develop the understanding of problems related to these techniques.

In Chapter 3, we mainly consider the interference alignment based transmit precoding as proposed in [5]. This precoding provides optimum performance in a fully coordinated cellular system. We assess the performance of this scheme in a coordination-cluster based downlink single user multi cell MIMO-OFDM transmission system with ideal assumptions on acquiring CSI at the transmiter and the ideal feedback. We also compare the performance with other baseline precodings and with different receiver algorithms. With the help of a simple channel estimation model we evaluate the performance of this scheme with channel estimation errors. After the step of rigorous performance analysis of the scheme we also provide some solutions for the performance improvement by exploiting the user selection diversity. Parts of this chapter are also published in [18] and [19].

In chapter 4, we propose the concept of an uncoordinated transmit precoding scheme based on multi user inter cell interference alignment. At first, we present the concept and prove it analytically. Then we assess the concept with system level simulations using spatial channel model and different receivers. Furthermore, we show the improvement in the performance by using the user selection diversity. We propose new methods for user-selection which support alignment based and non-alignment based transmit precodings. Parts of this chapter are also published in [20], [21], [22] and [23].

In Chapter 5, we assess our proposed scheme with practical constraints. At first we consider the limited feedback and evaluate the performance with random and hierarchical codebooks. Then we analyse the impact of channel estimation errors. Continuing the efforts with realistic environments we further evaluate the performance with measured channels. Parts of this chapter are published in [24] and submitted for peer review through [25].

In Chapter 6, we apply our scheme in HetNets. We show that alignment based precoding provides higher gains in HetNets. We explain the concept of enhanced inter cell interference coordination in HetNets and compare the performance of interference alignment and interference coordination. We show that until some resource utilization level in macro cell, our scheme outperforms the interference coordination. Parts of this chapter are published in [26] and [27].

In Chapter 7, we conclude with the highlights of our main findings and the possibilities for future works.

Chapter 2

Fundamentals

The purpose of this chapter is to provide an overview of the essentials which lay the basis for our assumptions and the concepts that follow further in this work. At first we talk about the characteristics and the modelling of the wireless channel which serves as the backbone to the analysis of any wireless access system. Then we present some details of an OFDM based wireless access design which is considered throughout this work. A brief review of closed loop downlink transmission schemes is also presented as we deal with these schemes. At the end we give a short overview on the characteristics of the interference in cellular systems. This helps us to understand and devise methods to mitigate this interference.

2.1 Wireless Channel Models

A simple example of wireless communication system consists of two nodes, a transmitter and a receiver communicating with each other over the wireless channel with the help of a transmit and a receive antenna respectively. The information signal over the wireless channel is carried by the electromagnetic waves which undergo the physical propagation phenomena of absorption, reflection, scattering and diffraction. Due to these propagation phenomena, the transmitted power of the information signal carried by the waves faces two types of effects which are generally categorized as long term (large scale) effects and short term (small scale) effects. The characterization of these effects requires modelling of the wireless channel. There are many approaches to model these effects. In the following we divide these approaches in three broad categories which provide us with *Deterministic Models*, *Empirical Models*, and *Statistical Models* of the wireless channels.

The deterministic models are mostly used in the wireless network planning stage and therefore they are based on the real world geographical information of a particular coverage area. The *Ray Tracing* is one of the examples of such models (please refer to [28] for details). For the purpose of analysis and research, such models are computationally complex and financially very expensive. Moreover, they are needed mostly when absolute system performance is required. When the objective is to perform a comparative analysis of the methods in a given environment, then the deterministic models are not needed. As the other two categories are sufficient enough for comparison of methods, they are most widely used in research and analysis studies. We also consider the later two models for further discussion.

2.1.1 Empirical Models

The communicating nodes are typically separated by a given distance d. Due to the absorption phenomena in the environment, the transmitted signal power suffers a loss over the path travelled by the waves to reach the receiving node. The transmit power dissipates even if there is a free space between the communicating nodes. The dissipation in free space is characterised by the well known *Free Space Loss* and is given by,

$$P_{rx} = \frac{P_{tx} G_{tx} G_{rx} \lambda^2}{(4\pi d)^2} \tag{2.1}$$

where, P_{rx} is the power received by the receive antenna with the antenna gain G_{rx} in free space at a distance d, P_{tx} is the power transmitted by the transmitter with antenna gain G_{tx}, λ is the wavelength of the electromagnetic waves.

This expression can be used to find the received power for a given location at a distance d in free space. However, in a real environment the path between the nodes is usually obstructed and surrounded by the real objects. Hence the received power depends upon many other parameters (in general known as propagation and environment parameters). Therefore, finding the received power at a given distance in real environments is not a simple task. However, if the average path loss can be characterized for a given location, the average received signal power can be predicted for that location provided the transmitted power is known. The ratio of the received signal power at a given location to the transmitted power is known as the path loss. Therefore, these models are also known as *Path Loss Prediction* models as they predict the average loss of transmitted signal power over the path travelled by the waves to reach the receiving node.

For the determination of path loss in our system-level simulation studies, we have used the path loss prediction models which are specified by 3GPP in [29]. The models are classified in different propagation scenarios, frequency ranges, Line-of-Sight (LOS), Non-Line-of-Sight (NLOS) situations and network layouts. These models are based on the extensive measurement campaigns within a European funded project which are reported in [30] and in standard studies available in literature. The general form for the path loss model that we have used can fit to different scenarios and parameters, it is given by,

$$P_{dB} = A + B\log_{10}(\frac{d}{1km}) + C + \kappa \tag{2.2}$$

where, P_{dB} represents the path loss in dB, d represents the separation between the communicating nodes in km, the parameters A, B and C depend on carrier frequency, antenna height and the scenario, κ can include any other losses specific to the environment or propagation characteristics such as indoor penetration losses.

The empirical models average their received power measurements in the proximity of a given distance to provide mean path loss. However, this averaging removes the random effects of the wireless channel which occur due to other propagation mechanisms. The averaged path loss values are good for planning a network and calculating a link budget but for the purpose of analysis and evaluation of new methods related to the transmission it is essential to take into account the random effects of the channel. Therefore, in the following we give an account of the models that characterize the random effects statistically.

2.1.2 Shadow Fading Models

Due to the effects of propagation mechanisms, the received power varies over a mean even for a fixed location. This phenomena is known as *shadowing* or *shadow fading* or *large scale fading*. The variations are mainly caused by the spatial structures, trees and moving obstacles present in the environment. Therefore, it is difficult to predict them empirically. However, the measurements of received power have shown that the impact of these variations can be modelled with log-normal distribution. That is why it is also called as *Log-normal Shadowing*. The effect of shadowing is typically the same in a close proximity of a given location. Therefore there should be a correlation between two points spatially close to each other suffering shadow fading. This effect is modelled by Gudmundson in [31] and it is widely used for accounting the shadowing effect.

The Gudmundson model is good to characterise the spatial correlation of the shadowing effect however, it is not possible to recreate the effect in a different time interval or for a different link at the same location. In reality, if two receivers are present at the same location, they should suffer the same shadowing effect. If the same user comes in the same location at a different time and there is no major change in environment then it should suffer the similar shadowing loss. Hence, the Gudmundson model is updated and a new model is developed which accounts for the two dimensional (2-D) correlation of shadowing. We also use the 2-D shadowing model for our system-level simulation studies. It provides better modelling of the shadowing effect. For the details of the model and the efficient generation of shadowing coefficients we refer to [32] and references therein.

2.1.3 Multipath Fading Models

So far we have learned about the models that predict the long term attenuation due to the propagation phenomena. In this section we learn more about the statistical modelling of the effects that cause the short term fading of the signal.

The scattering, reflection and diffraction not only cause the shadow fading attenuation but also cause multiple copies of the signal to arrive at a given receiving point with different powers and delays. This phenomenon is generally known as *Multipath Propagation*. The parameters characterising multipath propagation can be taken as random variables and their combined effect is a random process which can be modelled statistically. If we assume that each path is independent and can be characterised with an attenuation factor and a delay then the channel impulse response can be described as the sum of the impulses each arriving with time varying amplitudes and delays. In the absence of noise, the channel impulse response can be written in discrete representation form as follows:

$$h(t,\tau) = \sum_{i=1}^{L} a_i(t)\delta(\tau - \tau_i) \tag{2.3}$$

Where, $h(t,\tau)$ represents the time variant channel impulse response, i is the index of multipath, $a_i(t)$ is the time dependent amplitude (attenuation) of the ith path which accounts for the long term losses (path loss, shadowing) and τ_i is the delay corresponding to the ith path. Notice that we have limited the number of multipaths to L, in practice, we neglect the paths whose attenuation is around or below noise level. If a signal is transmitted through this time variant multipath channel in a very rich scattering environment with no LOS between the

communicating nodes and with a high number of independent multipaths, then using the central limit theorem, the channel can be modelled as zero mean complex Gaussian random coefficient. It is well known that the absolute value of this coefficient is Rayleigh distributed and the phase is uniformly distributed between 0 and 2π. For some of our simulation studies we have considered a highly scattered, uncorrelated environment and channel with Rayleigh distribution.

2.1.4 MIMO Spatial Channel Model

Until now we have discussed the models that characterize the fading behaviour of channel between transmitter and receiver each equipped with single antenna. With multiple antennas at both nodes, the channel is known as *Multiple Input Multiple Output* (MIMO) channel. For MIMO channel, the spatial diversity primarily depends upon the antenna array parameters and then secondarily on the environment and signal characteristics. Until now for single antenna case, we have considered only the latter two (secondary factors) for the modelling of wireless channel. For multiple antennas, we also need to account for the antenna related parameters in the modelling of the channel.

Many approaches to model MIMO channel are already available in the literature which provide the transfer function for MIMO channel. In [33] a detailed overview of these approaches and classification is given. Most of these approaches are antenna-centric and array-dependent. However, in this thesis we have considered a channel-centric, array-independent approach proposed by 3GPP in [34] for a given set of environments to facilitate system-level simulations with MIMO channels. It is also commonly known as *Spatial Channel Model* (SCM). Many of the concepts used in SCM were developed under the COST-259 European project which is well described in [35].

Modelling Methodology of SCM

The distinguishing feature of SCM is that it is a generic model which allows the generation of the channel coefficients by simply choosing a set of parameters separately for antenna array and propagation environment. Another salient feature of SCM is that the model already incorporates the simulation approach for both link and system level simulations. The approach is based on Monte-Carlo snapshots [36]. A simulation is based on multiple snapshots and there are several transmissions within each snapshot. The mobile users are uniformly dropped in the start of the snapshot over the simulation area (cellular coverage area). The long term effects such as path loss and shadow fading remain the same in the snapshot. However, the

short term multipath fading varies for each transmission within the snapshot. With respect to the long term and short term effects, the model parameters are broadly categorized in large scale and small scale parameters. The large scale parameters remain the same for a snapshot but the small scale parameters may change. In SCM, the snapshots are independent with respect to the parameters. The number of snapshots and the transmissions during each can be selected suitably for stable statistical results.

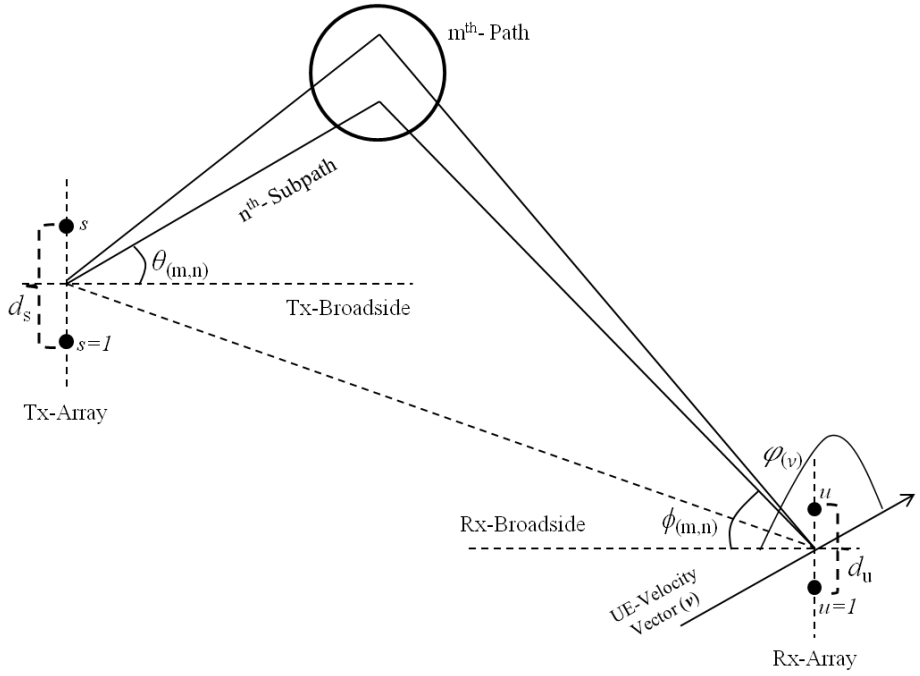

Figure 2.1: Geometrical representation of paths and sub-paths where each Tx and Rx are equipped with two antenna elements

Channel Matrix Generation

Figure 2.1 shows an example of the geometry of a multipath component due to the scattering in the environment between the transmitter and the receiver which are equipped with uniform linear antenna arrays. Each multipath component is further divided into a number of sub-paths. For a given environment, the average number of paths, sub-paths and other parameters required for random distributions have been estimated through extensive measurements [35].

For the linear arrays of transmitter and receiver as shown in figure 2.1 the expression for the channel impulse response of the *mth* path between the transmit antenna element s and

receive antenna element u from [34] is given as:

$$h_{(u,s,m)}(t,\tau) = \sqrt{\frac{P_m \sigma}{N}} \sum_{n=1}^{N} \Big(\sqrt{G_{tx}(\theta_{(m,n)})} e^{j(\frac{2\pi}{\lambda} d_s \sin\theta_{(m,n)} + \psi_{(m,n)})} \sqrt{G_{rx}(\phi_{(m,n)})} e^{j\frac{2\pi}{\lambda} d_u \sin\phi_{(m,n)}} e^{j\frac{2\pi}{\lambda}||\mathbf{v}||\cos(\phi_{(m,n)} - \varphi_v)t} \Big) \delta(\tau - \tau_{(m,n)}) \tag{2.4}$$

where,

- m: the index of mth path
- n: the index of nth subpath in mth path
- N: the total number of subpaths
- u: the index of uth antenna element of the receiver
- s: the index of sth antenna element of the transmitter
- P_m: mth path power
- σ: shadow fading value for the link
- $\theta_{(m,n)}$: angle of departure of the nth subpath
- $\phi_{(m,n)}$: angle of arrival of the nth subpath
- $\psi_{(m,n)}$: phase difference of the nth subpath
- G_{tx}: transmit antenna array response
- G_{rx}: receive antenna array response
- d_s: distance of transmit antenna element s from the reference transmit antenna element which is $s = 1$
- d_u: distance of receive antenna element u from the reference receive antenna element which is $u = 1$
- $||\mathbf{v}||$: magnitude of the receiver velocity vector
- φ_v: angle of the velocity vector

- $\tau_{(m,n)}$: delay corresponding to the nth subpath of the mth path

With an array of U receive and S transmit antennas, a $U \times S$ MIMO channel impulse response matrix is generated for each path and then the final MIMO channel matrix is formed with the sum over all the paths.

Our purpose is to establish an understanding of the modelling approach and the idea that SCM is an appropriate model which incorporates the important physical effects of the environment and the antenna geometry with proper modelling. For the detailed description of the environments, distributions of parameters and their dependencies, we refer to [29, 34]. However, for the basic understanding of the framework, we provide a brief overview of the major steps with the help of a flow chart as shown in figure 2.2.

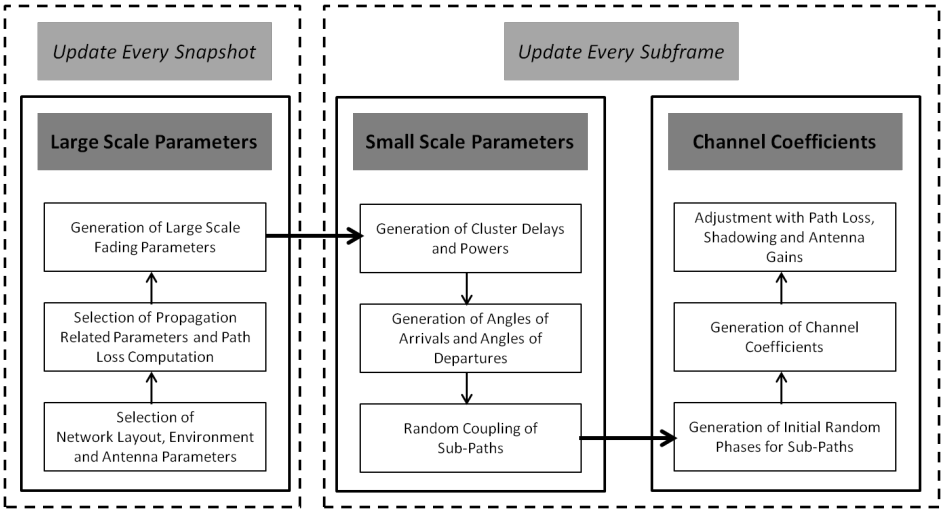

Figure 2.2: Steps for the generation of channel coefficients using SCM model

The steps are broadly categorized in the generation of *large scale parameters*, *small scale parameters* and *channel coefficients*. At first, we select the simulation scenario and the antenna geometry. The simulation scenario is based on a given environment (urban, rural, indoor, outdoor, etc.) and the network layout (hexagonal arrangement, network size, etc.). After the deployment of the network, the mobile users are dropped in the simulation area according to a given distribution function. Once the locations of the transmitters and the receivers are fixed then we determine the path losses and large scale parameters for all the channels in the system. This process of dropping users and generating large scale parameters is updated in the beginning of each snapshot (also known as *drop* with respect to user dropping). In the beginning of each subframe, small scale parameters are updated and channel

coefficients are generated by following the steps listed in figure 2.2 for all the channels in the system.

2.2 OFDM Based Wireless Access

The choice for the modulation of an information signal mainly depends upon the quantification of the time varying nature of the two properties of multipath channel namely the time-dispersion and the frequency-dispersion. The channel coherence bandwidth (a measure of frequency dispersiveness) in a micro cellular environment with carrier frequency around *2 GHz* is typically of the order of *100-300 kHz*. If we choose a wideband single carrier modulation with the transmission bandwidth *e.g. 1.25 MHz*, then it is greater than the channel coherence bandwidth. The communication will suffer with frequency selective channel fading. Hence in most of the current wireless systems, *Orthogonal Frequency Division Multiplexing* (OFDM) based narrowband multi carrier modulation and access is used. The OFDM is a special case of multi-carrier system which was proposed by the Bell Labs researchers [37]. The current multi user wireless systems employ OFDM for radio interface e.g. IEEE-WiMax (WLAN), 3GPP-LTE (Cellular). In the following we take an example of LTE-FDD Downlink and explain how the physical transmission layer for radio access is designed using the OFDM.

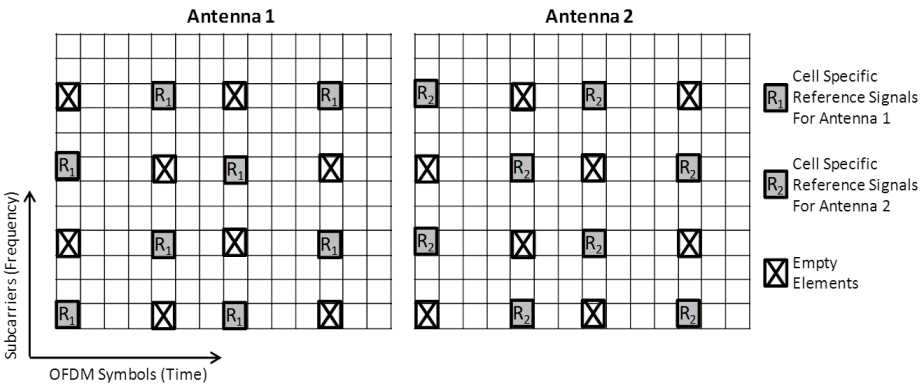

Figure 2.3: Representation of time-frequency OFDM resources in a PRB for the case of two transmit antenna elements

LTE Downlink Physical Layer Parameters

The LTE based cellular system supports a range of bandwidth from 1.25 MHz to 20 MHz without carrier aggregation. The complete bandwidth is divided into a number of equally

spaced sub carriers. The sub carrier spacing is set to be 15 kHz. Each sub carrier carries a number of OFDM symbols which is defined with the help of a radio frame structure. The duration of one radio transmission frame is 10 ms. Each frame consists of 10 subframes which are also known as *Transmission Time Intervals* (TTIs). Each subframe has two slots. Each slot is further divided in a number of OFDM symbols which depends upon the length of the Cyclic Prefix (CP) which is used to mitigate inter symbol interference. Two types of CP settings are possible namely *Normal* and *Extended*. With normal CP which is mostly used in urban and dense urban environments, there are 7 OFDM symbols in a slot. One OFDM symbol on a sub carrier represents a radio *Resource Element* (RE) which defines the allocation of wireless channel in time and frequency dimension. The radio resource allocation can be done on subframe basis. For the ease of scheduling, a set of REs in a subframe over 12 consecutive sub carriers is further classified as a *Physical Resource Block* (PRB). Figure 2.3 illustrates an example of downlink OFDM resource structure in a PRB for transmit antenna array of 2 elements.

Three symbols in each subframe over the whole bandwidth are reserved to carry the control information. Rest of the symbols are used for data and reference signals. The reference signals are used for multiple purposes. Here we highlight two main types of reference signals which are *Cell Specific Reference Signals* (CSRS) and *User Specific Reference Signals* (USRS). The CSRS are commonly known as *Pilot Signals* and they are used for channel estimation. In case of multiple antennas, they are defined with respect to each antenna element. They are also shown in figure 2.3. The CSRS are common for all the users in the cell. The USRS are dedicated to each user and used by the user to find out the transmission details e.g. transmit precoding. For further details on the complete set of signalling information we refer to [38]

In our system level simulations, we have modelled the OFDM resources with the help of LTE specifications. We assume that the channel is block faded over the PRB. The channels have temporal correlations which depend upon the speed of the users. In a real network, special pilot sequences are used to generate orthogonal pilots in the system which improve the performance of channel estimation. However, to compute the achievable performance bounds, we assume ideal channel estimation and therefore we do not use any pilot sequences. For the simulation analysis with imperfect channel estimation, we still do not use the pilot sequences rather we only model the error due to the imperfect channel information. Further details on modelling the imperfect channel estimation are given in chapters 3 and 5.

2.3 Closed Loop Downlink MIMO Transmission Schemes

In a broad sense, the term *Closed Loop Downlink* refers to the aspect of the wireless network which allows the network to perform optimization of any network process in the communication link chain based on the user feedback. In this thesis, we refer to the *closed loop downlink* in the context of MIMO transmit precoding schemes. If the instantaneous channel response is known at the transmitter then it can be used to adaptively design the transmit precoding to overcome the effects of the channel. Figure 2.4 shows the application of the MIMO transmit precoding in the downlink communication chain of LTE based systems.

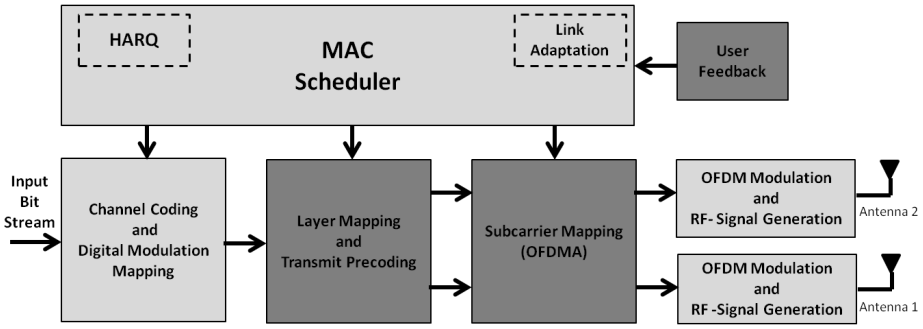

Figure 2.4: Representation of transmit precoding and layer mapping in the downlink

In the past decade, closed loop MIMO transmission has been extensively investigated. For simple understanding, we broadly categorize the transmission schemes based on *the usage of radio resource* and based on *the coordination among the cells*. Based on the resource usage, we can further classify the transmission schemes as *single user* and *multi user* MIMO transmissions. The basic single user transmission scheme (with multiple streams) was applied by [13] to find optimum capacity with the perfect CSI known at the transmitter. Now the spatial multiplexing of multiple independent data streams for single user is even possible in the commercial systems like LTE [38]. However, in the presence of spatial correlation, the multiplexing of independent streams does not bring gains for single user MIMO. This gives rise to the idea of multi user transmission. If there are spatially orthogonal users present in the system then multiple streams for different users can be multiplexed and transmitted if the CSI of both users is known at the transmitter. Zero-forcing based precoding for single antenna users is one of the famous schemes [15]. The system antenna constraints of zero-forcing with multiple antenna users are very well overcome by two different proposals namely *Effective Zero-forcing* in [39] and *Leakage Based Transmit Precoding* [17]. We explicitly mention these

two proposals as we are going to consider them as baselines for our proposed un-coordinated multi user transmit precoding scheme in chapter 4. For further details on this classification of closed loop schemes we refer to a comprehensive survey of single user and multi user transmission in [40].

Now we proceed to the next class which is based on the coordination between the cells. The coordinated transmission schemes are themselves a rich area of research. They are further classified based on their level of information sharing between the cells and the formation of coordination clusters in a cellular network. In chapter 3 we deal with the single user coordinated transmit precoding schemes where coordination clusters are fixed and only the channel state information is shared between the cells in the cluster. For further details on the coordinated tranmission schemes we refer to [41].

2.4 Interference in Cellular Networks

Figure 2.5 shows the surface plot of average received signal to inter cell interference and noise ratio (SINR) over the area covered by 7 sites arranged in a hexagonal grid in a frequency reuse 1 system, where each site consists of three *sectorized* antennas, each sector represents a cell and bears a unique cell identification. We see a high SINR in the direction of the

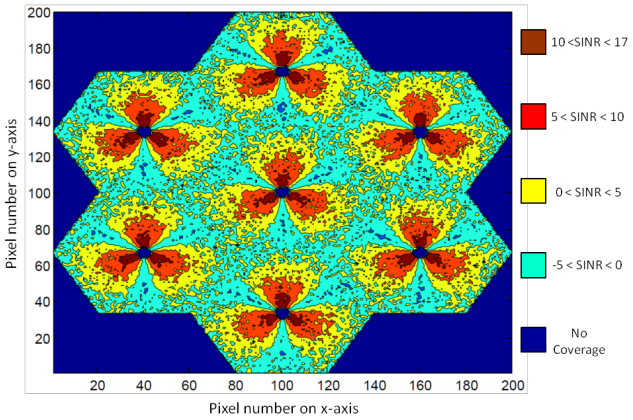

Figure 2.5: Contour plot for the average received SINR by the users in the coverage area of a universal frequency reuse cellular network with 7 sites and 21 cells

antenna. As we go far away from the antenna, the path loss increases and the ICI increases due to which the SINR decreases. This shows that even if the users have a low path-loss, the performance of the system is limited due to the ICI.

Chapter 3

Coordinated Inter-Cell Interference Alignment

In this chapter we describe briefly the concept of interference alignment (IA) as presented in [4] and its application as transmit precoding [5] for a coordinated cellular system. We explain the importance of IA in characterizing the achievable system capacity. Then we assess the loss in maximum achievable capacity in a cluster-based coordinated cellular network. We extend our performance assessment by taking into account different practical receiver algorithms and the impact of channel estimation errors. In the last section of the chapter, we discuss the improvements to the IA based system performance through user selection diversity. We propose sub optimal but computationally less complex user selection algorithms that target the enhancement of system spectral efficiency.

3.1 Introduction

The optimality of IA in terms of achievable capacity has been proved with the help of spatial degrees of freedom (DoF) in the network. Therefore, at first we discuss the role of DoF in the characterization of the capacity of networks facing co-channel interference.

The bandwidth limited (universal frequency reuse) multi-user cellular wireless network is inherently also interference limited. When a cell transmits to the desired user on a given radio resource, it also generates interference to the users of other cells that are using the same radio resource for transmission. Hence the network faces interfering channels for the communications. In literature, the communication link between a transmitter-receiver (Tx-Rx)

pair in such a scenario is termed as interference channel. Unlike point to point communication link (where noise is the major concern), the precise characterization of the capacity of interference channels is still an open problem. Until now, a great effort has been done to characterize the capacity of two-user interference channel. At very high signal to noise ratios (SNR), the capacity for MIMO Tx-Rx pair with M and N antennas (respectively for Tx and Rx) is proportional to $min(M, N)log(SNR)$ [12]. This pre-log factor (scaling factor) is also known as the multiplexing gain and in this case, it represents the spatial DoF [42]. This gain comes due to the fact that the new dimension of space provides extra DoF to the communicating pair. Hence it infers that in cases where precise capacity characterization is difficult, the performance can be approximately characterized using the notion of DoF. Following the objective of performance characterisation, interestingly [4] showed that for a given radio resource (time-frequency), in a fully cooperative network with two single antenna Tx-Rx pairs, 4/3 DoF can be achieved. The transmission scheme to achieve the DoF was based on message splitting and IA over the symbol extension in time dimension. Although spatial dimensions were not used, but the work in [4] introduced the concept of IA which lead to characterize the spatial DoF.

In [5] Jafar et al. first used the IA to achieve maximum spatial DoF in a *K-user* interference network. In contrast to [4], more generalized results over the characterization of the capacity were presented in [5]. Using the IA based transmit precoding scheme, Jafar et al. showed that "$MK/2$" DoF can be achieved at high signal to noise ratio (SNR) in a *K-user* coordinated interference network when each node is equipped with M antennas. The key in achieving this result is the idea of IA. It is based on the effort of limiting the interference over half of the signal space whereas leaving the other half for the desired signal space. At the receiver node, if the interferences are confined in a subspace which is possibly be non-overlapping to the desired signal space then zero forcing the interference subspace will simply let the receiver to successfully decode its desired signal.

One of the critical assumption in [5] is the cooperation of all the cells for the design of transmit precoding. For a small network consisting of small number of cells, the size of cooperation cluster and the overheads of CSI and computational complexity are acceptable. However, in a real-world cellular network with very high number of cells, the realization of fully coordinated IA would be an impossible task. The first efforts towards the realization of IA based precoding in real-world were carried out by the contributions in [43] and [44]. In [43], IA is evaluated with measured MIMO-OFDM interference channels. However, the

assessments were carried out assuming a set-up with only three Tx-Rx pairs without any interference outside the coordination area. The numerical study in [44] investigated a larger cellular setup, under the assumption of zero forcing receivers. The large network is divided into coordination clusters and IA is used within each cluster. However, the focus is to compare the IA with a non-coordinated baseline employing eigen-mode transmission and fractional frequency reuse. The contribution in this chapter is another step down the path marked by these references, with a threefold objective.

Our first objective is to evaluate the loss in DoF due to the consideration of practical limitations in the system and the impairments in the assumptions considered by [5]. Eventually, the loss in DoF infers the loss in the network capacity due to these impairments. We achieve this goal by assessing the impact of: a) Out-of-Cluster Interference (OCI), b) different receiver algorithms and c) imperfect CSI.

Our second objective is to compare the performance of IA with the state of the art baseline presented in [45] performing coordinated beamforming based on signal to leakage and noise ratio (SLNR) optimization [17]. We emphasize that the references [43] and [44] are instead comparing IA (that needs a degree of coordination between cells) with non-coordinated baselines.

The third objective after the analysis of real world impairments is to explore the real world opportunities. For this purpose, we exploit the user selection diversity. We propose user selection methods that improve the performance of IA based transmission scheme.

3.2 System Model

We consider a MIMO-OFDM based downlink cellular system such as LTE [29], with I base stations (BSs)(please note that in this document, the terms *BS* and *cell* are equivalent) equipped with M transmit antennas each serving a single user equippment (UE) equipped with N receive antennas with r_i independent data streams on a single time-frequency resource element. We refer to the ith UE as to the UE served by the ith BS. Each BS covers an area of a cell and a UE is dropped randomly in the coverage area of the BS. An example of such a system with $I = 21$ BSs is shown in figure 3.1. We assume the narrowband flat fading channel between each pair of BS and UE. The OFDM based system lets us make this assumption and carry out our analysis for single time-frequency resource element, whereas the simulation

results will be given for a wideband system. The received signal by the *ith* UE, $\mathbf{y}_i \in \mathbb{C}^{N\times 1}$ is given as:

$$\mathbf{y}_i = \mathbf{H}_{ii}\mathbf{F}_i\mathbf{s}_i + \sum_{j\neq i, j=1}^{I} \mathbf{H}_{ij}\mathbf{F}_j\mathbf{s}_j + \mathbf{n}_i \tag{3.1}$$

Where, $\mathbf{H}_{ii} \in \mathbb{C}^{N\times M}$ is the channel matrix between the *ith* BS and the corresponding UE, $\mathbf{F}_i \in \mathbb{C}^{M\times r_i}$ is the precoding matrix used by the *ith* BS for the transmission of $\mathbf{s}_i \in \mathbb{C}^{r_i\times 1}$ vector of symbols corresponding to r_i independent data steams, ($\sum_{j\neq i, j=1}^{I} \mathbf{H}_{ij}\mathbf{F}_j\mathbf{s}_j$) is the interfering term due to the transmission of the other $(I-1)$ BSs to their corresponding UEs and $\mathbf{n}_i \sim \mathcal{CN}(0, \eta^2)$ is the $N \times 1$ complex Gaussian noise vector. We assume total power constraint at each BS, equal power is allocated to each stream and the precoding matrices are with unit norm. The signal after receive combining, $\mathbf{y}_i^{'} \in \mathbb{C}^{r_i\times 1}$ is obtained as,

$$\mathbf{y}_i^{'} = \mathbf{G}_i^H\mathbf{y}_i \tag{3.2}$$

where, $\mathbf{G}_i \in \mathbb{C}^{N\times r_i}$ is the receive combiner matrix which is also unit norm.

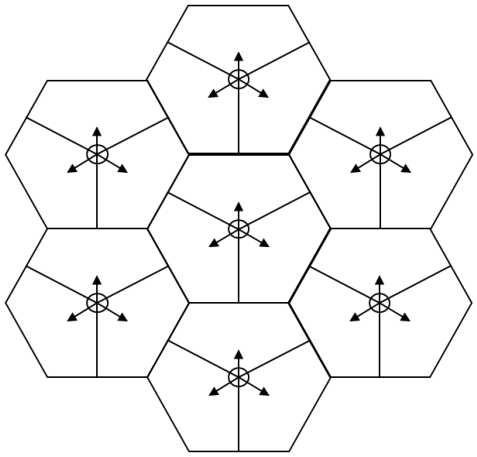

Figure 3.1: Example of a system with *I=21* BSs arranged in a hexagonal grid. The arrow represents the antenna bore-sight

3.2.1 Coordination Clusters

To realize IA based transmit precoding in a large cellular network like in figure 3.1, we define the sets of coordinating cells which are called clusters. The optimum cluster design is itself a separate problem to deal with in a large network. Our target here is to find a nominal

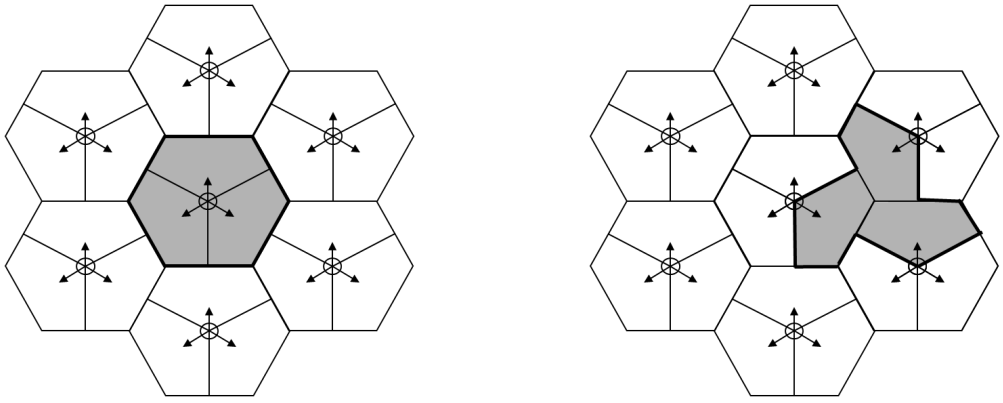

(a) Intra-Site cluster (b) Inter-Site cluster

Figure 3.2: Examples of clustering scenarios in a network of 21 BSs with $N_c = 1$ and $K = 3$

cluster size to realize IA. Therefore, we simply choose two types of static clusters to analyse the performance of clustered network with IA based transmit precoding.

Clustering Requirements: As our primary focus is to analyse the IA based solution in a large cellular network, the clustering arrangement is derived on the basis of the feasibility conditions given for IA in [46]. Let the considered network of I BSs be divided into N_c clusters. Let Π_l $(l = 1, 2, 3...N_c)$ be the set containing indices of BSs belonging to the lth cluster such that $|\Pi_l| = K$ where, K represents the size of the cluster i.e. total number of BSs in a cluster. When all the channel matrices in the cluster are full rank then the size of a cluster is limited by the following inequality [46].

$$M + N \geqslant (K + 1)r_i \tag{3.3}$$

For the ease of analysis, we assume $M = N = 2$ and each BS can send at least $r_i = 1$ independent data stream towards the desired UE. The required size of cluster for the feasibility of IA can be found from equation (3.3) as $K = 3$. For the purpose of the analysis of IA in a large cellular network, we limit ourselves to this cluster size because of two reasons. The first is the number of alignment constraints which will increase quickly with the size of cluster. The second is the high amount of CSI sharing among the cluster for the design of precoding. High amount of CSI would also require the consideration of the feedback issues, the delay tolerance at backhaul and backhaul-capacity.

Clustering Scenarios: Here we consider two types of clusters which can be differentiated based on the coordination feasibility within the cluster. We refer to them as *intra-site cluster*

and *inter-site cluster*. Figures 3.2(a) and 3.2(b) show the two cluster formations. With *intra-site cluster*, three BSs belonging to the same site form a coordination cluster. CSI sharing and centralized processing comes natural, as BSs belong to the same site. With *inter-site cluster*, three BSs belonging to different sites form a coordination cluster. Clearly, this case implies some high requirements on the backhaul. CSI sharing and precoding design can be realized either by a centralized entity or by choosing a master BS within the cluster. Let the *ith* BS belongs to the *lth* cluster. Now we can re-write equation (3.1) as,

$$\mathbf{y}_i = \mathbf{H}_{ii}\mathbf{F}_i\mathbf{s}_i + \sum_{\forall j, j\in\Pi_l, j\neq i} \mathbf{H}_{ij}\mathbf{F}_j\mathbf{s}_j + \sum_{\forall m, m\notin\Pi_l} \mathbf{H}_{im}\mathbf{F}_m\mathbf{s}_m + \mathbf{n}_i \tag{3.4}$$

where, $(\sum_{\forall m, m\notin\Pi_l} \mathbf{H}_{im}\mathbf{F}_m\mathbf{s}_m)$ represents the interference term due to the out-of-cluster BSs.

3.3 Loss in Degrees of Freedom

As we have described the cellular network that we consider and the clustering requirements, now we proceed towards the loss in DoF due to the OCI in the network. We characterize the loss in DoF or the lower bound on maximum achievable DoF of any cluster Π_l in a cellular network which consists of N_c such clusters. The transmitters in the cluster are coordinating to design IA based transmit precoding and the receivers are independently zero-forcing the aligned interference.

Based on the "*Corollary 1 of Theorem 3*" in [47], the maximum achievable spatial DoF on a time-frequency resource element in a cluster Π_l are exactly characterized by $MK/2$. Where, K is the number of Tx-Rx pairs in the cluster and M is the number of antennas on each node. We extend these results further by formulating the following statement:

Theorem 3.1: *In a cluster based cellular network, if interference alignment is applied within a cluster to achieve $MK/2$ maximum achievable spatial DoF, then a cluster can be considered as a point to point communication link even though the receivers within the cluster are independent and distributed.*

The proof of above theorem is given with the help of following corollaries.

Corollary 3.1.1: *The lower bound on the maximum achievable spatial DoF of lth cluster on single time-frequency resource element in a network of N_c uncoordinated clusters is given by,*

$$\varkappa_l = (\frac{MK}{2}).\frac{1}{N_c} \tag{3.5}$$

where, $\varkappa_l$ represents the lower bound on maximum achievable DoF by lth cluster.

Proof: The proof is rather trivial. An orthogonal scheme over the clusters can achieve this lower bound. Consider the orthogonal allocation of N_c time-frequency resource samples to all the clusters such that in each resource only one cluster performs transmission. Then the DoF of each cluster normalized over the N_c resources will be $(\frac{MK}{2}).\frac{1}{N_c}$.

Corollary 3.1.2: *The lower bound on the maximum achievable spatial DoF of a clustered cellular network on single time-frequency resource element is independent of the size of the network and is given by,*

$$\varrho = \sum_{l=1}^{N_c} \varkappa_l$$
$$= \sum_{l=1}^{N_c} (\frac{MK}{2}).\frac{1}{N_c}$$

$$\varrho = (\frac{MK}{2}) \tag{3.6}$$

where, ϱ represents the lower bound on maximum achievable DoF by the network of N_c clusters. The proof of the corollary is straight forward.

Corollary 3.1.3: *The theoretical upper bound on the maximum achievable spatial DoF in a clustered cellular network is directly related to the number of clusters in the network and is given by,*

$$\varsigma = (\frac{MK}{2}).N_c \tag{3.7}$$

where, ς represents the theoretical upper bound on maximum achievable spatial DoF by the network of N_c clusters. It implies that if for instance, the fading realizations in the network occur coincidently in such a way that all the inter cluster interference in the network vanishes, then all the clusters can achieve their maximum DoF when IA is applied within the cluster. On the other hand if the coordination between all the nodes of the network is possible and IA is feasible in the network, then as per [47] there will be (KN_c) Tx-Rx pairs and $(\frac{MK}{2}.N_c)$ DoF can be achieved. This also proves Theorem 3.1. The Dirty Paper Coding (DPC) [48] can achieve this DoF theoretically but, practically there is no scheme available at hand which achieves this limit. Moreover, in the absence of such a scheme it is not an easy task to characterize the DoF or the capacity of such network. The achievable system performance then depends upon the fading realizations in the network. Therefore, in the next sections,

we characterize the rate expression for this network with the help of transceiver design and heuristically find out the system performance.

3.4 Transmit Precoding using Interference Alignment

The IA based transmit precoding scheme [5] adjusts the interference space at the ith UE, such that the UE has enough DoF to cancel the interference. For example, assuming r_i be the number of independent data streams for the ith UE, then the interference signal space should be confined to $N - r_i$ dimensions. In other words, the transmitters in the coordination cluster Π_l design their precoding matrices for each time-frequency resource element in such a way that the interference at the undesired receivers in Π_l is aligned in a subspace non overlapping to the desired signal subspace. We refer to [5] for a detailed description of the IA concept. In the following, we only briefly recall the precoding-matrix and receiver-matrix construction for the case of a coordination cluster with $K = 3$ BSs, $r_i = 1$ and $M = N = 2$, as this case is relevant for our coordination setup described in subsection 3.2.1. Let $\Pi_l = \{i, j, k\}$ be the set representing the cluster of coordinating BSs and contains their indices. The BS index also corresponds to the UE served by the BS.

- The alignment condition for the ith UE side assuming BSs j and k as interferers can be written as:

$$\begin{aligned} span(\mathbf{H}_{ij}\mathbf{F}_j) &= span(\mathbf{H}_{ik}\mathbf{F}_k) \\ span(\mathbf{F}_j) &= span(\mathbf{H}_{ij}^{-1}\mathbf{H}_{ik}\mathbf{F}_k) \end{aligned} \tag{3.8}$$

The corresponding conditions for UEs j and k can be given with an equivalent formulation.

- The condition for the jth UE:

$$\begin{aligned} span(\mathbf{H}_{ji}\mathbf{F}_i) &= span(\mathbf{H}_{jk}\mathbf{F}_k) \\ span(\mathbf{F}_i) &= span(\mathbf{H}_{ji}^{-1}\mathbf{H}_{jk}\mathbf{F}_k) \end{aligned} \tag{3.9}$$

- The condition for the kth UE:

$$span(\mathbf{H}_{ki}\mathbf{F}_i) = span(\mathbf{H}_{kj}\mathbf{F}_j) \tag{3.10}$$

By combining the alignment conditions in (3.8), (3.9) and (3.10) we get:

$$span(\mathbf{H}_{ki}\mathbf{H}_{ji}^{-1}\mathbf{H}_{jk}\mathbf{F}_k) = span(\mathbf{H}_{kj}\mathbf{H}_{ij}^{-1}\mathbf{H}_{ik}\mathbf{F}_k)$$
$$span(\mathbf{F}_k) = span(\mathbf{H}_{ki}^{-1}\mathbf{H}_{ji}\mathbf{H}_{jk}^{-1}\mathbf{H}_{kj}\mathbf{H}_{ij}^{-1}\mathbf{H}_{ik}\mathbf{F}_k) \tag{3.11}$$

Let $\mathbf{E} = \mathbf{H}_{ki}^{-1}\mathbf{H}_{ji}\mathbf{H}_{jk}^{-1}\mathbf{H}_{kj}\mathbf{H}_{ij}^{-1}\mathbf{H}_{ik}$ be the $N \times M$ matrix with $N = M$ then (3.11) can be written as:

$$span(\mathbf{F}_k) = span(\mathbf{E}\mathbf{F}_k) \tag{3.12}$$

From (3.12) $\mathbf{F}_k \in \mathbb{C}^{M\times r_k}$ can be obtained by taking the dominant r_k eigenvectors of $\mathbf{E}$. With the help of $\mathbf{F}_k$, (3.8) and (3.9) the calculation of $\mathbf{F}_i \in \mathbb{C}^{M\times r_i}$ and $\mathbf{F}_j \in \mathbb{C}^{M\times r_j}$ is straight forward. The design of precoding matrices enables us to align the interference on the undesired UEs within the cluster. For example, the interference from the *jth* and *kth* BSs on the *ith* UE will be aligned. To ensure the suppression of the aligned interference at the receiver of the *ith* UE, weights for zero-forcing receiver are computed in [5] using the following conditions:

$$\mathbf{G}_i^H\mathbf{H}_{ij}\mathbf{F}_j = 0, \forall j \neq i \tag{3.13}$$

$$rank(\mathbf{G}_i^H\mathbf{H}_{ii}\mathbf{F}_i) = r_i \tag{3.14}$$

Under the assumption of non-degenerate (full rank) channels, the condition in (3.13) will always be fulfilled. Some parts of signal energy present in the interference space will be lost due to zero-forcing operation. However, due to rich-scattering environment enough energy for detection will be available in a non overlapping desired signal space and the condition in (3.14) will also be almost surely satisfied. Let $\mathbf{H}_{ZF_i} \in \mathbb{C}^{N\times(r_i+r_j)}$ be the combined matrix of the effective serving channel and any one effective interfering channel (from the cluster) seen by the *ith* UE.

$$\mathbf{H}_{ZF_i} = \begin{bmatrix} \mathbf{H}_{ii}\mathbf{F}_i & \mathbf{H}_{ij}\mathbf{F}_j \end{bmatrix}$$

Let $\mathbf{H}_{ZF_i}^{\dagger} \in \mathbb{C}^{(r_i+r_j)\times N}$ be the pseudo inverse of $\mathbf{H}_{ZF_i}$ and it can be written as:

$$\mathbf{H}_{ZF_i}^{\dagger} = \mathbf{H}_{ZF_i}^H(\mathbf{H}_{ZF_i}\mathbf{H}_{ZF_i}^H)^{-1} = \begin{bmatrix} \mathbf{G}_{ZF_1} & \mathbf{G}_{ZF_2} \end{bmatrix}^T$$

$$\mathbf{G}_i^H = (\mathbf{G}_{ZF_1})^T \tag{3.15}$$

We call the receiver algorithm fulfilling the conditions in (3.13) and (3.14) as **ZF-IA**. It will be used only for IA based transmit precoding. We emphasize that in the following we will refer to IA as a precoding technique independently of the receiver technique used. In section 3.6 we will discuss in detail about different receiver algorithms available at hand.

3.5 Baseline Transmit Precoding Schemes

In this section we present the baseline transmit precoding schemes. We have considered two types of baselines. One is based on the clustered network processing like IA and the other is based on the single cell processing.

Coordinated Precoding based on SLNR: We consider a state-of-the-art Coordinated Precoding (CP) scheme which is applied in [45, 49] based on Signal to Leakage-Interference and Noise Ratio (SLNR) criterion given in [17]. The optimization function can be written as:

$$\mathbf{F}_i = \arg \max_{F_i:||F_i||^2=1} \frac{||\mathbf{H}_{ii}\mathbf{F}_i||^2}{\sum\limits_{\forall j \in \Pi_l, j \neq i} ||\mathbf{H}_{ji}\mathbf{F}_i||^2 + M\eta^2} \tag{3.16}$$

Where, $\mathbf{H}_{ji} \in \mathbb{C}^{N \times M}$ is the channel between the ith BS and the UE served by the jth BS, Π_l is the set of indices of BSs belonging to the same cluster. It is shown in [17] and references therein that the optimization in (3.16) is a generalized eigenvalue problem for which the solution is given as:

$$\mathbf{F}_i = \xi \left(\left(\sum_{\forall j \in \Pi_l, j \neq i} \mathbf{H}_{ji}^H \mathbf{H}_{ji} + M\eta^2 \mathbf{I}_N \right)^{-1} \mathbf{H}_{ii}^H \mathbf{H}_{ii} \right) \tag{3.17}$$

The function 'ξ' gives the matrix of r_i dominant eigenvectors. The power constraint and normalization of the precoder has been taken care of. We emphasize that, in general, CP via SLNR is more flexible than the IA with respect to the constraints on the number of BSs in the coordination set. However, in this work we fix the number of BSs and the data streams per UE for both the schemes then the amount and type of feedback required for the design of their precoders is the same. This gives us a fair comparison between the performance.

Uncoordinated Maximum Ratio Transmission: For the sake of comparison, we have considered the well known single cell, single user eigen-beamforming based transmission for which the optimization function can be written as:

$$\mathbf{F}_i = \arg \max_{F_i:||F_i||^2=1} ||\mathbf{H}_{ii}\mathbf{F}_i||^2 \tag{3.18}$$

The optimal solution to the (3.18) can be found by taking the r_i dominant right singular vectors of the desired channel which is obtained through Singular Value Decomposition (SVD) of $\mathbf{H}_{ii}$. Please note that in the following we refer to single cell processing as SVD only with respect to the precoding scheme irrespective of the reciever technique.

3.6 Linear Receiver Design

We consider four different types of receivers. The objective of this receiver study is to capture real-world effects into our analysis. As a matter of fact, commercial UEs are characterized by large differences between receiver implementations, ranging from very simple algorithms implemented in low-end terminals to sophisticated algorithms implemented in high-end terminals.

Signal Maximization: Based on the maximization of the desired signal power at the receiver (using multiple antennas) we consider the well-known Maximum Ratio Combining **(MRC)** receiver for which the receive matrix is calculated as follows:

$$\mathbf{G}_i^H = (\mathbf{H}_{ii}\mathbf{F}_i)^H \tag{3.19}$$

Interference Minimization: We assume that each UE is able to perfectly estimate the total interference covariance matrix $\mathbf{Q}_i \in \mathbb{C}^{N\times N}$ which can be written as the sum of the Intra Cluster Interference (INCI) covariance matrix $\mathbf{R}_{i_{(INCI)}} \in \mathbb{C}^{N\times N}$ and the OCI covariance matrix $\mathbf{R}_{i_{(OCI)}} \in \mathbb{C}^{N\times N}$.

$$\mathbf{Q}_i = \mathbf{R}_{i_{(INCI)}} + \mathbf{R}_{i_{(OCI)}} \tag{3.20}$$

Where, $\mathbf{R}_{i_{(INCI)}}$ is given by:

$$\mathbf{R}_{i_{(INCI)}} = \sum_{\forall j, j\in\Pi_l, j\neq i} \mathbb{E}[(\mathbf{H}_{ij}\mathbf{F}_j\mathbf{s}_j)(\mathbf{H}_{ij}\mathbf{F}_j\mathbf{s}_j)^H] \tag{3.21}$$

We assume that the $\mathbf{H}_{ij}\mathbf{F}_j$ and $\mathbf{H}_{im}\mathbf{F}_m$ are known at the receiver. Moreover, independent data streams are transmitted towards each UE and the data streams from interfering BSs are also independent which leads to $\mathbb{E}[\mathbf{s}_j\mathbf{s}_j^H] = (P_j/r_j)\mathbf{I}_{r_j}$, where, $\mathbf{s}_j \in \mathbb{C}^{r_j\times 1}$, r_j is the number of independent streams transmitted by the BS j, $\mathbf{I}_{r_j}$ represents the $r_j \times r_j$ identity matrix and P_j is the total power transmitted by BS j. We assume unit power transmission by all

the BSs (i.e. $P_j = 1$) and $r_j = 1$. With these assumptions we proceed further to simplify $\mathbf{R}_{i_{(INCI)}}$ as follows:

$$\mathbf{R}_{i_{(INCI)}} = \sum_{\forall j, j \in \Pi_l, j \neq i} (\mathbf{H}_{ij}\mathbf{F}_j)\mathbb{E}[\mathbf{s}_j\mathbf{s}_j^H](\mathbf{H}_{ij}\mathbf{F}_j)^H$$
$$\mathbf{R}_{i_{(INCI)}} = \sum_{\forall j, j \in \Pi_l, j \neq i} (\mathbf{H}_{ij}\mathbf{F}_j)(\mathbf{H}_{ij}\mathbf{F}_j)^H \tag{3.22}$$

Similarly, we can write $\mathbf{R}_{i_{(OCI)}}$ as follows:

$$\mathbf{R}_{i_{(OCI)}} = \sum_{\forall m \notin \Pi_l} (\mathbf{H}_{im}\mathbf{F}_m)(\mathbf{H}_{im}\mathbf{F}_m)^H \tag{3.23}$$

Substituting equations (3.22) and (3.23) in (3.20) we get:

$$\mathbf{Q}_i = \sum_{\forall j \in \Pi_l, j \neq i} (\mathbf{H}_{ij}\mathbf{F}_j)(\mathbf{H}_{ij}\mathbf{F}_j)^H + \sum_{\forall m \notin \Pi_l} (\mathbf{H}_{im}\mathbf{F}_m)(\mathbf{H}_{im}\mathbf{F}_m)^H \tag{3.24}$$

The desired signal can be recovered by projecting the received signal on to the subspace occupied by minimum interference. The subspace spanned by the eigenvectors corresponding to the r_i lowest eigenvalues of $\mathbf{Q}_i$ is the subspace where we have minimum interference [50]. Hence, the receiver matrix can be calculated as follows:

$$\mathbf{G}_i^H = (arc\xi(\mathbf{Q}_i))^H \tag{3.25}$$

The function $arc\xi$ provides the eigenvectors corresponding to the r_i lowest eigenvalues of $\mathbf{Q}_i$. As we are not perfectly zero forcing the interference but only minimising it so we call it the Interference Minimization **(IM)** receiver.

SINR Maximization: At medium and high SNR values, we expect to get high performance with IM receiver. However, for low SNR values, the desired signal at the receiver is weak. In this case a better optimization is to maximize the output SINR at the receiver. This objective can be achieved by Minimizing the Mean Square Error (MMSE) in the detected symbol at the receiver. This is a well known objective function and the solution is given by:

$$\mathbf{G}_i^H = \left(\left(\mathbf{Q}_i + \eta^2\mathbf{I}_N\right)^{-1}\mathbf{H}_{ii}\mathbf{F}_i\right)^H \tag{3.26}$$

Like the IM receiver, the receive matrix in (3.26) requires ideal calculation of $\mathbf{Q}_i$. With this respect we name this as **MMSE-I** receiver. Calculating the perfect interference covariance depends upon the method of interference estimation at the receiver. One method could be

to estimate the interference components via the corresponding reference signals (when pilots are orthogonal). This task is not trivial in real world receivers, for different reasons. First, estimating the channel of a high number of interferences involves a high computational-complexity and a high overhead due to the reference signals. Second, the strength of the reference signals received from weak interferences, usually does not allow a precise estimation. Third, the interference is by nature highly time-variant, in particular when multiple antennas are used at the base station side. To incorporate the influence of these problems in practice, we compute an approximated total interference covariance matrix $\tilde{\mathbf{Q}}_i \in \mathbb{C}^{N \times N}$ such that:

$$\tilde{\mathbf{Q}}_i = diag(\mathbf{Q}_i) \tag{3.27}$$

Where, $\tilde{\mathbf{Q}}_i$ is a diagonal matrix where each diagonal element represents the total average interference power received by the corresponding receive antenna element. The expression for $\mathbf{G}_i$ with approximated interference information can be written as follows:

$$\mathbf{G}_i^H = \left(\left(\tilde{\mathbf{Q}}_i + \eta^2 \mathbf{I}_N \right)^{-1} \mathbf{H}_{ii} \mathbf{F}_i \right)^H \tag{3.28}$$

We refer to the receiver given by equation (3.28) as **MMSE-A**.

3.7 CSI Sharing Requirements

We assume that there is perfect CSI available in the coordination cluster. Both the IA algorithm described in section 3.4 and the CP via SLNR algorithm described in section 3.5 require a certain degree of CSI sharing between the BSs in the same coordination cluster. For IA it is assumed that a logical central unit gathers the channel samples within Π_l where, Π_l has already been defined as the set of indices of BSs belonging to a given coordination cluster. This means that the calculation of the IA precoding matrices must be carried out in this logical central unit and cannot be realized using a distributed implementation. For CP via SLNR it is required that the BS i gathers the channel samples $\mathbf{H}_{ji}$, $\forall j \in \Pi_l, j \neq i$. Based on this information, the precoding matrix design can be realized in a distributed way, without the need of any logical central unit. In other words, each BS is able to calculate its precoding coefficients independently from the other BSs in the coordination cluster.

3.8 Performance with Ideal Channel Estimation

In this section, we present the heuristic evaluation of the ergodic capacity of the clustered cellular network with IA based precoding applied within each cluster. At first we show the impact of the receive algorithm on the performance of transmission scheme and on the achievable DoF in a cluster. Then we further strengthen our understanding by analysing this impact in a clustered cellular network. Our second focus is on the impact of OCI. This causes the loss in alignment gains and eventually loss in DoF. All the results are based on the availability of perfect CSI at the BSs. The effects of imperfect CSI will be considered in section 3.9.

3.8.1 Simulation Assumption and Parameters

The performance evaluation is based on a system level simulator which is compliant (mainly in deployment, propagation scenarios, channels generation) with 3GPP [29]. For the 3 BSs case, we use one site with 3 sectorized antennas with inter antenna angle of 120 °. This is specified as the baseline scenario for the evaluation of clustered based transmission scheme in [29]. For the 21 BSs case, a central site is surrounded by 6 other sites arranged in a hexagonal gird. In order to obtain reliable results, we apply wraparound with 6 mirrors system. The salient simulation parameters are depicted in Table 1. For the complete set of simulation parameters we refer to [29].

Parameters	**Values**
TX x RX Antennas	2 x 2
Channel Model	Spatial Channel Model, Urban Micro
Channel Structure	600 subcarriers used, subcarrier spacing f = 15 kHz
Transmission Layers	1
Speed	3 km/h

Table 3.1: Salient simulation parameters for the performance evaluation

During a simulation run several Monte Carlo drops are performed. At the start of a drop, the position of all the UEs is randomly chosen with uniform distribution. Furthermore, the realization of all time and frequency selective spatial channels is calculated according to [34]. During each drop an event driven simulation is performed with sufficient duration in order to obtain reliable results. All channels are sampled with sufficient resolution in frequency and

time. The number of transmit layers is set to one. The UEs are scheduled randomly on each resource block. The SINR for unit transmit power after the receiver processing is measured for each allocated OFDM resource element as given in equation (3.29). A Mutual Information Effective SINR Mapping (MIESM) based virtual decoder is used in order to translate the SINR time/frequency samples delivered by the receiver into BLER. The adaptation of Modulation and Coding Schemes (MCS) to the channel quality (link adaptation) is performed ideally, i.e. the decision for a certain MCS is done at the reception time. However, for the single site case we preferred a Shannon estimation of the throughput due to the extremely high SINR values that would cut the performance differences between the investigated algorithms when using our virtual decoder, even when choosing the highest possible 64-QAM based MCS with the highest code rate. Perfect channel estimation and instantaneous feedback of CSI without delay to all the BSs in a cluster is assumed. Furthermore, it is also assumed that the feedback is error free. We emphasize on the fact that for comparative analysis, all the baseline schemes are also implemented in the same simulation system and evaluated like IA.

3.8.2 Spectral Efficiency Evaluation

Assuming single stream transmission with unit power by all the BSs in the network, the SINR for *ith* UE after receive combiner can be written as:

$$SINR_i = \frac{|\mathbf{G}_i^H \mathbf{H}_{ii} \mathbf{F}_i|^2}{\sum\limits_{\forall j \in \Pi_l, j \neq i} |\mathbf{G}_i^H \mathbf{H}_{ij} \mathbf{F}_j|^2 + \sum\limits_{\forall m \notin \Pi_l} |\mathbf{G}_i^H \mathbf{H}_{im} \mathbf{F}_m|^2 + ||\mathbf{G}_i^H||^2 \eta^2} \tag{3.29}$$

In case of SINR to Shannon Mapping, the Shannon formula is used to calculate the rate for the *ith* UE as $R_i = log_2(1 + SINR_i)$ and the network spectral efficiency in terms of mean cell rate is given as:

$$R_{system} = \frac{1}{I} \sum_{i=1}^{I} R_i \tag{3.30}$$

When the IA is applied with zero-forcing receiver then the expression in (3.29) will be reduced to the following:

$$SINR_i^{IA-ZF} = \frac{|\mathbf{G}_i^H \mathbf{H}_{ii} \mathbf{F}_i|^2}{\sum\limits_{\forall m \notin \Pi_l} |\mathbf{G}_i^H \mathbf{H}_{im} \mathbf{F}_m|^2 + ||\mathbf{G}_i^H||^2 \eta^2} \tag{3.31}$$

In case of only 3BSs, the OCI in equations (3.29) and (3.31) is zero.

3.8.3 Impact of Receivers

At first, we consider the scenario where a cluster is based on a single site (with only 3 BSs as shown in figure 3.2(a) and take IA only as a transmission technique. We analyse the performance of five different receiver algorithms given in section 3.6 along with the zero-forcing receiver.

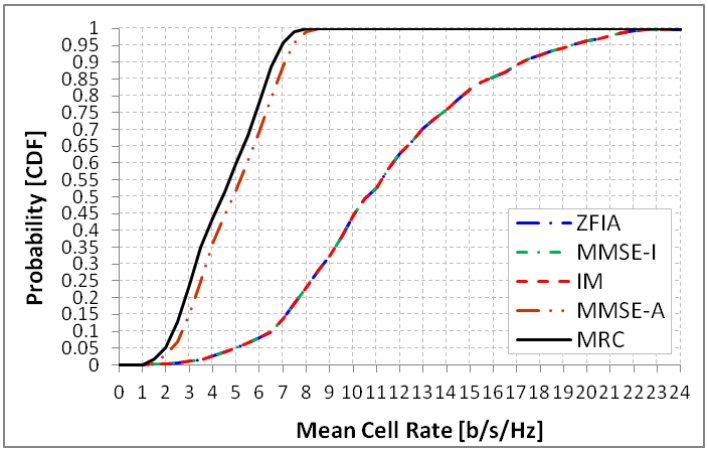

Figure 3.3: Performance comparison of receivers with IA for 3BSs

Figure 3.3 shows the CDF of mean cell rate. Due to the absence of OCI and due to the ideal and unlimited Shannon (SINR-to-RATE) mapping, we obtain a very high absolute system performance. We observe that, in the absence of OCI, the three receiver techniques namely ZF-IA, MMSE-I and IM overlap with each other. All these three receivers perfectly calculate and suppress the aligned interference and achieve the optimum performance. However, the other two receivers, MMSE-A and MRC are far away from reaching the optimum performance due to their inability to suppress the aligned interference. This outcome indicates that in a practical system, IA can be applied when the network would have the knowledge of the receivers' architecture. Moreover, the performance of MMSE-A shows that the optimum performance is highly sensitive to the accuracy of the estimated interference at the receiver. For further results on the comparison of IA with other precoding schemes under different receiver algorithms we refer to [18].

3.8.4 Impact of Residual Unaligned Interference

In the absence of OCI (due to single site network), the receiver is perfectly able to suppress the well aligned intra cluster interference. However, in a large cellular network there will

be OCI. The presence of unaligned OCI results in a residual interference part in the desired signal space even after the receive processing. This is the main reason for the loss of DoF in a clustered network. The residual unaligned interference part behaves like an increase in the total noise floor. Therefore, at first we analyse the impact of residual unaligned OCI on the performance of precoding schemes. For this purpose, we model a hypothetical unaligned residual OCI in the simulation of a 3 BS single site cluster with the help of a simple input parameter "Ψ". The value $\Psi = 0\ dB$ represents no unaligned interference whereas higher values of Ψ represent otherwise.

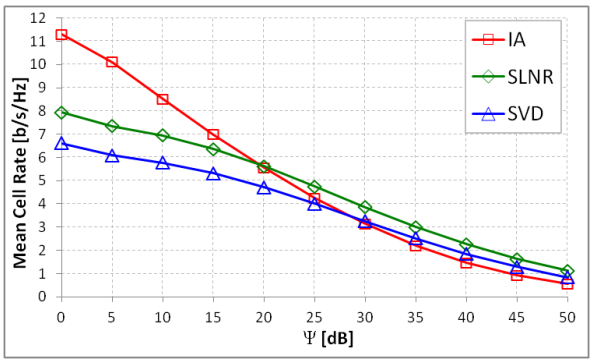

Figure 3.4: Impact of OCI on the performance of precodings with MMSE-I receiver

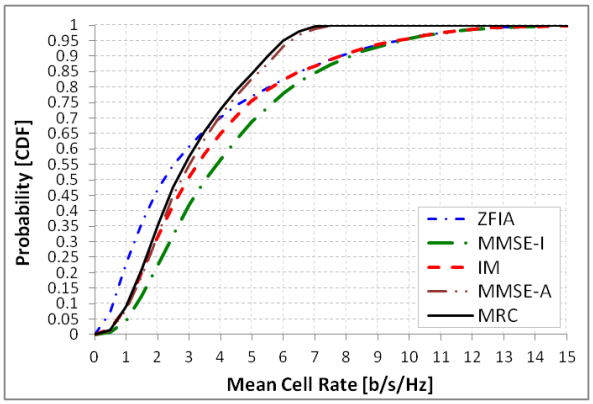

Figure 3.5: Mean cell rate CDF comparison of receivers with IA for 21BSs

Figure 3.4 shows the loss in mean cell rate performance in fully coordinated 3 BSs scenario with the increase in Ψ for IA and other baselines using the MMSE-I receiver. We have chosen this receiver as it is optimum for all precoding schemes. We can clearly see that for lower values of Ψ, IA completely outperforms other precodings because the UEs in the cluster face

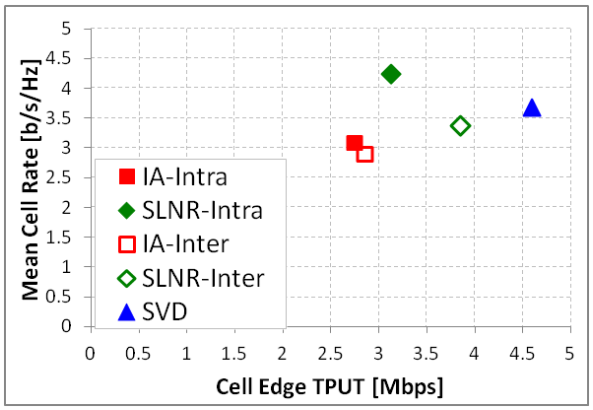

Figure 3.6: Performance comparison of different precoders with intra and inter site clustering in a 21 BSs scenario and under the assumption of a MMSE-A receiver

only INCI which can be perfectly aligned and suppressed. On the other hand, for higher values of Ψ, the performance is even worse than the SVD based single cell processing due to the fact that the system is now limited by the residual unaligned interference. In this case alignment and suppression of the INCI is not enough.

Now we consider the impact of OCI on the performance of IA precoding in 21 BS scenario with intra site clustering and with different receivers. Figure 3.5 presents the simulation results which clearly show that MMSE-I and IM receivers completely outperform the ZF-IA algorithm. The ZF-IA suppresses successfully only the intra cluster interference. Hence we can see that it approaches the performance of MMSE-I and IM for 75-percentile and above. This region of CDF represents the users near the cell center and with high signal strength which face mostly the intra cluster interference.

For the impact of OCI on the performance of all the precodings in small and large cellular networks we refer to the results in our publication [18]. For the sake of practical importance, here we only report the results in large cellular networks with MMSE-A receiver and the two clustering scenarios.

Figure 3.6 shows the tradeoff between mean cell rate and cell border throughput for the simple, but realistic, MMSE-A receiver. Here we compare the performance for the IA and SLNR precoders and for intra and inter site clusters as well as for the uncoordinated SVD precoder. We note that SLNR shows the best mean cell rate performance. As a matter of fact, with intra site clustering and SLNR precoding, we obtain approx. 25% gain in mean cell rate over SVD. However, SVD outperforms the other schemes on cell edge performance.

Concerning IA, it is outperformed by the other techniques. However, here we have considered fixed clustering and random user scheduling. We expect to have higher gains through IA when efficient clustering and user scheduling algorithms are used. In section 3.10 we address the topic of user selection for the enhancement in the performance of IA.

3.9 Performance with Channel Estimation Errors

Until now our focus in this chapter was to analyse the effect of OCI, therefore, we have assumed that the perfect CSI is available to design the transmit precoding. However, in practice, the availability of ideal CSI at the transmitter is not possible due to the inherent feedback delays and channel estimation errors. Therefore, in the following we intend to perform a system level simulation based assessment of the performance of IA and other baselines including the effect of channel estimation errors. The very initial study dealing with the CSI imperfections for IA can be found in [51]. A very good information-theoretic ground is given there for the performance of IA with imperfect CSI using zero-forcing receiver and an empirical model of erroneous channels applied on Gaussian channels. In contrast to [51], our study gives a detailed insight of the performance of IA considering near-to-practical issues by realizing a pilot-aided OFDM based downlink system. Another recent work over the impact of imperfect CSI on the performance of IA can be found in [52]. This work is focused on a special parametric study for the performance of IA with correlated channels using a zero-forcing receiver.

The focus of our study is to assess and compare the performance of IA with imperfect CSI at the transmitter due to the channel estimation errors in a receiver. We consider a general scattering environment where we have the probability of both LOS and NLOS reception with uncorrelated channels. At first we derive a simple channel estimation error model for system level simulations. This model is an extension of the model introduced in [45]. We apply this model to the channels generated by the spatial channel model [34] which considers realistic effects of environment in the simulations and is also recommended by 3GPP. Additionally, our model provides the possibility to realize the availability of instantaneous and average information of interference to be used by the estimator. In practice, the performance of real estimators is influenced by this information. Furthermore, we have evaluated and compared the impact of estimated interference at the receiver by realizing two different MMSE based receiver algorithms as given in subsection 3.6. The receiver study circumscribes the fact

that in reality we have a range (from efficient and complex to simple) of receive algorithms implemented in high-end and low-end user terminals. Moreover, we have also compared the performance of IA with other baseline coordinated and non-coordinated transmit precoding schemes to state that when and where it makes sense to use IA for transmission.

For the complete description of the model and detailed assessment of the performance we refer to our publication [19] and the master thesis report in [53]. With the help of selective results, here we show the sensitivity of coordinated alignment to the imperfections in the CSI.

Figure 3.7 presents the performance comparison of IA with other baselines in a scenario with 3 BSs and MMSE-I receiver with two bias factor models (Inst-β and Avg-β) for channel estimation as described in [19]. Notice that, the percentage loss in the performance of IA with CSI imperfections is higher than other baselines. With Inst-β based model the performance of IA is similar to the SVD whereas with Avg-β, IA is outperformed by the SVD. It implies that to utilize the gains of IA we require very high channel estimation accuracy. It appears from the figure that in this scenario, SLNR based precoding outperforms others in non-ideal conditions and with any model of estimation errors. The number of effective pilots considered here for estimation is $T = 10$. This parameters plays an important role in channel estimation. For further results illustrating the impact of effective pilots on the performance we refer to our publication [19] and the master thesis report in [53].

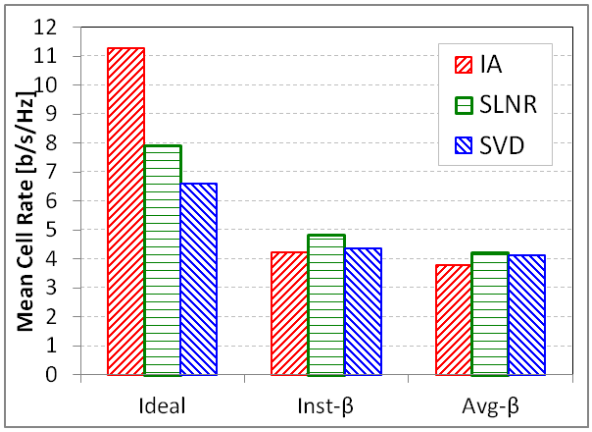

Figure 3.7: Performance of precoders with different scaling factors, T=10

The results have shown that IA promises very high gains and outperforms the other transmit precoding strategies with MMSE-I receiver algorithm in all SINR regions with perfect

CSI. However, these gains are receiver dependent and even with perfect CSI, IA is outperformed by other precodings if MMSE-A receiver is used. The MMSE-I receiver, relative to MMSE-A receiver comes under very high loss with channel imperfections but still outperforms the MMSE-A receiver. The comparison of the two bias factor models shows that the channel estimation errors can be reduced if bias factor can be adjusted to the instantaneous situation of the channel. The comparison of the precoding schemes shows that even with MMSE-I receiver, the IA is outperformed by SLNR with channel imperfections in all SINR regions under channel conditions with a nominal value of T=10. Another strong conclusion can be drawn that IA can only be applied in very limited practical scenarios with very low or almost zero mobility as it requires high estimation accuracy.

3.10 User Selection Diversity for IA

Until now our focus was the evaluation of the loss in the DoFs and the system performance due to the unaligned OCI and channel impairments in a clustered cellular network. Now we shift our focus towards methods that bring the improvement in achievable performance. On one hand, the existence of multiple active users in a network with the limited resources (e.g. frequency spectrum) increases the probability of congestion and delays. On the other hand, multiple users provide an additional opportunistic dimension (selection diversity) for the enhancement of system performance in the presence of limited resources. For the later reason, the user selection in a multi user system is of paramount importance. Therefore, in this section we ignore the practical limitations and put our efforts in finding the achievable performance limits of IA based precoding with user selection algorithms.

When the number of users is higher than the available radio resources, one of the easiest way is to select the user randomly or in a round robin fashion. However, random selection of users is not an optimum way to improve the system spectral efficiency. Hence in practice, to increase the system spectral efficiency and to maintain a given user fairness, the users are selected for transmission on the basis of a given metric. For this purpose, the decision is made by the network on the basis of a selection criteria. For example, to improve the spectral efficiency of the system, one of the criteria is to select the user with best radio channel quality.

In principle, IA is applied with the help of BS-coordination, several user selection methods have been proposed in literature for coordinated-multi cell system (please refer to [54] and references therein). We emphasize that most of these studies focus on user selection methods

either with zero-forcing beamforming, eigen beamforming or random beamforming. To the best of our knowledge there are no studies which have considered strict IA based precoding from [5] with user selection diversity in a cellular network given in section 3.2. However, the contributions in [55, 56, 57] show that the trend in research is to adopt user selection diversity for opportunistic interference alignment or mitigation. The work in [55] uses zeroforcing beamforming on a set of selected users in a Coordinated Multi Point (CoMP) setup with two cells. In [55], the users are selected jointly in the coordinated cluster based on channel norms. The contribution in [56] uses random beamformers for all the users in the system and then perform user selection for opportunistic inter cell interference alignment. An iterative algorithm to design optimal precoders and receiver filters in conjunction with user selection for a cellular network is proposed in [57].

The contributions in some of the studies even consider joint user selection and clustering problem [58] but our objective is to realize the gains of user selection diversity when the clusters are fixed. For this purpose, we analyse different user selection methods. These methods can be differentiated with respect to the complexity and the level of feedback information required at the BS for the evaluation of selection criteria.

3.10.1 System Assumptions and Problem Formulation

Let us consider the same system as given in section 3.2 with I BSs divided into N_c clusters each comprising of $K = 3$ BSs each equipped with $M = 2$ antennas and serving UEs with $r_i = 1$ data stream which are equipped with $N = 2$ antennas. We extend our assumption towards the number of active users present in the coverage area of each BS. Let N_u be the number of active users to be served by each BS ($N_u > 1$). Given these system dimensions, the number of users that a BS can serve on a single time-frequency resource is constrained by the condition in (3.3). It means that each BS can serve one UE out of N_u for the transmission on one resource element.

In the following we define the following sets containing the indices of the users:

- $\mathcal{U}_t$: all active UEs in the system with $|\mathcal{U}_t| = IN_u$
- $\mathcal{S}_t$: all selected UEs in the system for one transmission, $\mathcal{S}_t \subseteq \mathcal{U}_t$ with $|\mathcal{S}_t| = I$
- $\mathcal{U}_c$: all active UEs in a cluster, $\mathcal{U}_c \subset \mathcal{U}_t$ with $|\mathcal{U}_c| = KN_u$
- $\mathcal{S}_c$: all selected UEs in a cluster for one transmission, $\mathcal{S}_c \subseteq \mathcal{U}_c$, $\mathcal{S}_c \subset \mathcal{S}_t$ with $|\mathcal{S}_c| = K$

- $\mathcal{U}$: all active UEs to be served by a BS, $\mathcal{U} \subset \mathcal{U}_c \subset \mathcal{U}_t$ with $|\mathcal{U}| = N_u$
- $\mathcal{S}$: index of the UE selected by a BS for one transmission, with $|\mathcal{S}| = 1$ and such that $\mathcal{S} \subseteq \mathcal{U}$, $\mathcal{S} \subset \mathcal{S}_c \subset \mathcal{S}_t$

As our objective is to maximize the system spectral efficiency, we optimise the system sum rate for the optimal selection of users for each transmission. The optimisation problem can be written as follows:

$$\begin{aligned} \mathcal{S}_t &= \arg \max_{\mathcal{S}_t \subseteq \mathcal{U}_t, |\mathcal{S}_t| = I} R_{system} \\ \mathcal{S}_t &= \arg \max_{i \in \mathcal{S}_t, \mathcal{S}_t \subseteq \mathcal{U}_t, |\mathcal{S}_t| = I} \sum_{i=1}^{I} R_i \\ \mathcal{S}_t &= \arg \max_{i \in \mathcal{S}_t, \mathcal{S}_t \subseteq \mathcal{U}_t, |\mathcal{S}_t| = I} \sum_{i=1}^{I} \log_2(1 + SINR_i) \end{aligned} \tag{3.32}$$

The expression of $SINR_i$ in (3.29) expalins that the optimization in (3.32) firstly requires the full cooperation in the system which is difficult to realize practically. Therefore, in the following we provide reduced complexity suboptimal solutions that can be used to improve the system performance.

3.10.2 User Selection Algorithms

We divide our user selection methods in two different categories. The first category is based on the selection within the cluster. We assume that the Central Unit (CU) or the master BS has information of all users in the cluster and it performs the user selection. Here we further differentiate between exhaustive and greedy selection within the cluster. The second category assumes that each BS selects the user for transmission and informs the CU for the design of precoding. These methods simply differ on the basis of the trade off between the performance (spectral efficiency and user fairness) and the overhead (computational complexity, amount of required information and delay). At first we consider our first strategy where the selection is being done by the CU and all the active UEs in the cluster provide the required information to CU through their serving BSs.

Exhaustive Selection In the Cluster (CL-ER)

We simplify the problem in (3.32) by considering the maximization of rate in the cluster only. We consider the user selection in *lth* cluster, the optimisation problem is reduced to

the following form,

$$\mathcal{S}_c = \arg \max_{i \in \mathcal{S}_c, \mathcal{S}_c \subseteq \mathcal{U}_c, |\mathcal{S}_c| = K} \sum_{i=1}^{K} \widehat{R_i}$$

$$\mathcal{S}_c = \arg \max_{i \in \mathcal{S}_c, \mathcal{S}_c \subseteq \mathcal{U}_c, |\mathcal{S}_c| = K} \sum_{i=1}^{K} \log_2(1 + \widehat{SINR_i}) \tag{3.33}$$

where, $\widehat{R}_i$ and $\widehat{SINR}_i$ respectively represent the rate and SINR estimated by the CU before the transmission for the UE $i \in \mathcal{S}_c$ to be served by the BS i in lth cluster. The expression for the post receiver estimated $\widehat{SINR}_i$ is written as:

$$\widehat{SINR_i} = \frac{|\hat{\mathbf{G}}_i^H \mathbf{H}_{ii} \mathbf{F}_i|^2}{\sum\limits_{\forall j \in \Pi_l, j \neq i} |\hat{\mathbf{G}}_i^H \mathbf{H}_{ij} \mathbf{F}_j|^2 + \Omega_i^2 + ||\hat{\mathbf{G}}_i^H||^2 \eta^2} \tag{3.34}$$

The matrices $(\mathbf{F}_i, \mathbf{F}_j) \in C^{r_i \times M}$ are the precoding matrices that can be computed in the cluster for the considered combination as in section 3.4. The matrix $\hat{\mathbf{G}}_i \in C^{N \times r_i}$ is the receive matrix estimated by the CU for the ith UE. We will discuss about $\hat{\mathbf{G}}_i$ later in this section but first let us consider the term Ω_i^2 in equation (3.34). This term represents our approximation for the OCI. In principle, estimation of this term for the current transmission is a coupled problem as the clusters are uncoordinated and it depends upon the users selected in the other clusters. Therefore, we use this quantity under the following possible assumption which is easily realizable in practice.

- ***Average Out-of-Cluster Interference***: The average signal power received by UE i from any arbitrary interfering BSs depends upon the long term losses which are mainly *distance dependent path-loss, antenna gains, penetration losses and shadow fading.* For a UE moving with a slow speed, this power varies over a longer period of time. Hence, whatever is the set of selected UEs in the out-of-cluster BSs in the current transmission time, in average this power would remain the same if the UE is moving with a slow speed. Let γ_{im} denotes the average received interference power by the ith UE from the mth BS, the total average OCI received by the ith UE is represented by Γ_i and is given by:

$$\Gamma_i = \sum_{\forall m \notin \Pi_l} \gamma_{im}$$

The residual OCI after the receiver processing is given by:

$$\Omega_i^2 = ||\hat{\mathbf{G}}_i^H||^2 \Gamma_i \tag{3.35}$$

Now we consider the estimation of $\hat{\mathbf{G}}_i$ at the CU. We assume on the basis of the standardized systems like LTE, that a BS is aware of the receiver algorithm used by its served UEs. In practice, this assumption is realized by defining UE-categories as given in [59]. In fact a UE with multiple antennas falls in a category which can be further classified by the receiver algorithms. In previous section we have already evaluated the performance of IA based precoding with different receiver algorithms. For the purpose of user selection, we consider only the receiver algorithm based on SINR maximization and compute the expression for receive vector $\hat{\mathbf{G}}_i$ as follows:

$$\hat{\mathbf{G}}_i^H = \left(\left(\mathbf{R}_{i_{(INCI)}} + 0.5\Gamma_i \mathbf{I}_N + \eta^2 \mathbf{I}_N \right)^{-1} \mathbf{H}_{ii} \mathbf{F}_i \right)^H \tag{3.36}$$

Remarks about the Computational Complexity and Amount of Feedback: In the above paragraphs we have presented the user selection method that optimizes the system performance. However, it comes with some cost. Each active UE in the system has to send the required CSI to the CU. Moreover, for the estimation of rate, each has to send an extra OCI information. The CU has to perform an exhaustive search over all possible combinations in the cluster. For this purpose, at first the CU has to calculate the receive vectors and then the rates for all the UEs with respect to all possible combinations in the cluster. With N_u number of active UEs per BS, there will be $(N_u)^K$ number of possible combinations. If $N_u >> K$ the exhaustive search would become prohibitive.

Greedy Selection In the Cluster

In the sequel we provide a solution to simplify the complexity problem. We propose a greedy approach based on [16, 60] to reduce the size of the search space. The main idea is to select the first UE in the cluster through a different metric. Then further UEs are selected to maximize the expected sum rate as in equation (3.33). With the greedy approach, the total number of combinations is reduced to $(N_u)^{(K-1)}$ In the following, we present three possible criteria for the selection of the first UE.

- ***Round Robin Selection (GR-RR)*** The first user is selected simply by round robin approach. We refer this method as *Greedy Round Robin* (GR-RR). This method is very simple and it would provide high fairness but we expect a decrease in spectral efficiency.

- ***Proportional Fair Selection (GR-PF)*** In order to improve both fairness and spectral efficiency, we select the first user with proportional fair metric. We refer this method as *Greedy Proportional Fair* (GR-PF). The details of the metric will be given in the following.

- ***Maximum Channel Norm based Selection (GR-CN)*** This method simply takes the user with highest instantaneous channel gain in the cluster. We refer this method as *Greedy Maximum Channel Norm* (GR-CN).

Cell based Selection

Now we consider our second selection strategy in which each BS selects its own users (please note that in this document, the terms *BS*, *sector* and *cell* are equivalent). For this purpose, we simply process the selection metric in each BS over the set $\mathcal{U}$. This for sure reduces the computational complexity as well as the amount of information sharing in the system. As there will be no combinatorial problem to deal with, so a simple sorting process over $\mathcal{U}$ with respect to the selection metric in each BS will be enough. The following metrics are considered.

- ***Cell based Round Robin Selection (BS-RR)*** The users are selected simply by the round robin approach applied by each cell. We denote this method by (BS-RR). Only the selected users send the required information in the feedback to each serving BS. With respect to the complexity and feedback overhead, this is the simplest user selection method. It provides high fairness but no gains in spectral efficiency from selection diversity. This method serves as one of our baseline method.

- ***Cell based Proportional Fair Selection (BS-PF)*** In this method all the users in a BS (sector or cell) send the channel information to the serving BS and the BS computes the proportional fair metric. We denote this method as (BS-PF). The user with the highest metric is selected as through sorting process. The selection can be written as,

$$\mathcal{S} = \arg \max_{i \in \mathcal{S}, \mathcal{S} \subset \mathcal{U}, |\mathcal{S}|=1} \alpha_i \tag{3.37}$$

  where, α_i represents the proportional fairness weight of the ith UE among the set $\mathcal{U}$ and is given as:

$$\alpha_i = \frac{R_i^{'}}{1 + R_{i(avg)}(t)} \tag{3.38}$$

Where, $R_i^{'}$ represents the possible rate of UE i in current transmission. The $R_i^{'}$ is estimated only from the channel information without considering any precoding and receiver algorithms as $R_i^{'} = \log_2(1 + \tilde{\nu_i})$, where, $\tilde{\nu_i}$ is given as follows:

$$\tilde{\nu_i} = \frac{||\mathbf{H}_{ii}^H \mathbf{H}_{ii}||^2}{\sum\limits_{\forall j \in \Pi_l, j \neq i} ||\mathbf{H}_{ij}^H \mathbf{H}_{ij}||^2 + \sum\limits_{\forall m \notin \Pi_l} ||\mathbf{H}_{im}^H \mathbf{H}_{im}||^2} \tag{3.39}$$

The $R_{i(avg)}(t)$ is the mean rate of UE i until the current transmission time t. The unit summation in the denominator helps to schedule the UEs with $R_i^{'}$ when $R_{i(avg)}(t)$ is zero. The same metric is used for the selection of first UE in GR-PF.

- ***Cell based Maximum Channel Norm Selection (BS-CN)*** This method simply takes the user with highest instantaneous serving channel gain in the cell. We denote this method as (BS-CN).

$$\mathcal{S} = \arg \max_{i \in \mathcal{S}, \mathcal{S} \subset \mathcal{U}, |\mathcal{S}|=1} ||\mathbf{H}_{ii}^H \mathbf{H}_{ii}||^2 \tag{3.40}$$

This is highly unfair but we expect it to provide better spectral efficiency. The same metric is used for the selection of first UE in GR-CN.

3.10.3 Performance Analysis

Here we demonstrate the performance of the user selection algorithms presented in previous subsection with the help of system simulations. We have simulated the same system as described in subsection 3.8.1 with ideal channel assumptions and only with MMSE-I receiver. As earlier, we consider two types of static clustering which is intra-site cluster and inter-site cluster. There are 7 sites in the simulation area each with three cells. We distribute N_u users uniformly over the coverage area of each BS. Full buffer traffic is modelled which means there is always data available at the BS for each active UE. In each transmission, at first the user selection is performed and then the precoding is designed for the selected set of users.

Figure 3.8(a) and figure 3.8(b) show the mean cell rate performance with all the user selection methods respectively for intra-site and inter-site clusters. Notice that there is a great improvement in the performance with user selection in both clustering approaches. The best spectral efficiency is achieved by CL-ER method. The performance with GR-CN is very close to the CL-ER which means with a little compromise in the performance we can reduce the complexity and overhead. The percentage gains with user selection methods are

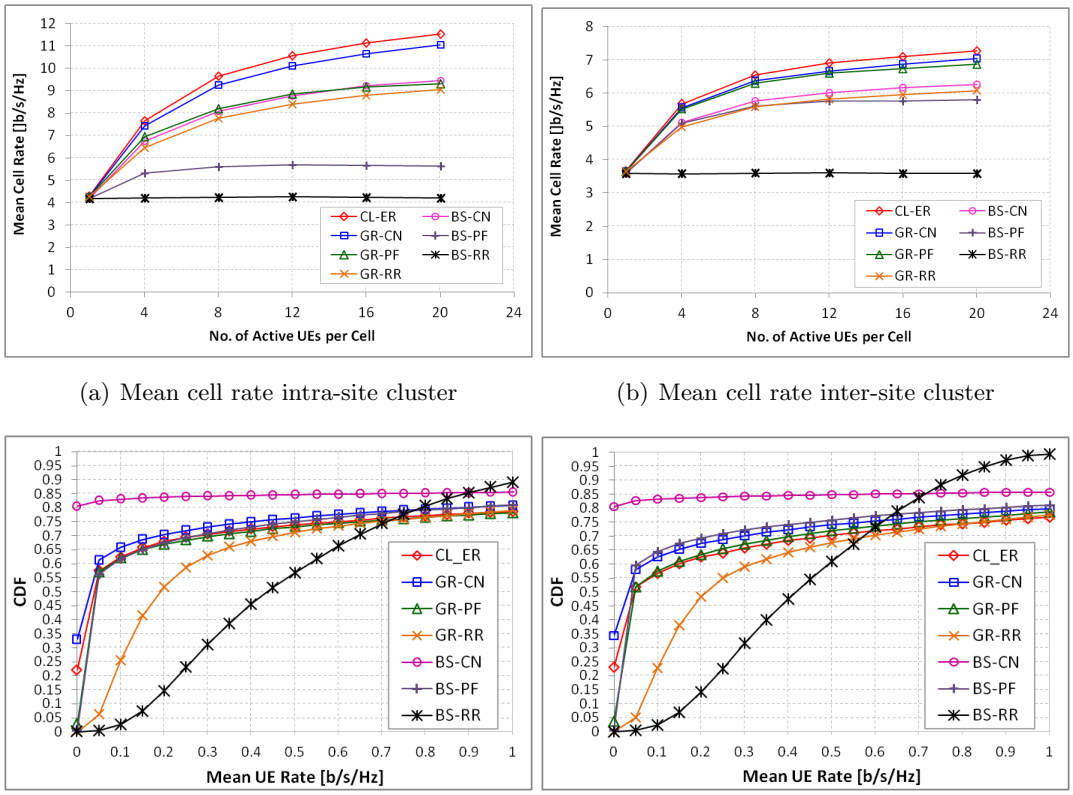

(a) Mean cell rate intra-site cluster

(b) Mean cell rate inter-site cluster

(c) CDF of mean UE rate intra-site cluster, 8 UEs

(d) CDF of mean UE rate inter-site cluster, 8 UEs

Figure 3.8: Performance of IA with different user selection methods

higher in intra-site clustering than inter-site clustering. Because of the hexagonal arrangement and sectorized antennas, intra-site clustering benefits most from IA based precoding. With uniform distribution of users, a sector of the same site is mostly the strongest interferer and this helps to align and suppress the interference in intra-site clustering.

Now let us focus on figure 3.8(a). The performance of BS-CN is almost overlapping the GR-PF and BS-CN outperforms the GR-RR. It implies that if we target the system spectral efficiency, then BS-CN can provide very high performance with negligible overhead. However, BS-CN neglects the user fairness. The complexity of GR-PF is higher than BS-CN and GR-RR and the performance gain is marginal. Hence for intra-site clustering, we recommend to use GR-RR which provides better user fairness with marginal compromise on system performance as well as it provides lower computational complexity. The BS-PF and BS-RR do not provide very high system rate but we expect to get higher user fairness with

these methods.

If we focus on figure 3.8(b), the behaviour of PF based methods are different than in figure 3.8(a). The GR-PF is close to GR-CN and BS-PF is very close to BS-CN. This behaviour could be understood with the influence of clustering approach on equation (3.38). In the light of these results, we state that with inter-site clustering, GR-PF and BS-PF provide considerable system performance with acceptable user fairness maintaining lower complexity.

Now we analyse the mean UE rates with all the selection methods to have a view on the user fairness. Figure 3.8(c) and figure 3.8(d) show the initial part of the CDF of mean UE rates (8 active UEs per cell) with all the user selection methods respectively for intra-site and inter-site clusters. We observe similar trend for all the selection methods in both figures. The drop duration for these results is 1 sec which means the results compare the fairness over 1 sec. The best fairness is achieved with BS-RR and the worst is with BS-CN. Here we can see that GR-RR provides higher fairness than BS-CN. The GR-PF and BS-PF provide almost similar fairness. The CL-ER has higher fairness than GR-CN.

The overall results show that we have a very high gain in spectral efficiency with user selection diversity. If we compromise on the spectral efficiency we can also provide user fairness. If we compare BS-CN and GR-CN for 20 active UEs, we get approximately 12-16 % gains in spectral efficiency and higher fairness with GR-CN based user selection. If higher fairness is required with a little compromise on system performance then GR-RR can be used in intra-site clustering whereas GR-PF can be used in inter-site clustering. Note that this user selection will help further improving the performance of IA in situations where IA is suitable. We suggest a future study to compare IA with the state of the art precoding with user selection methods.

3.11 Conclusion

In the first part of the study we have assessed the performance of IA based precoding in clustered cellular network by comparing it with state of the art transmit precoding schemes and with different receivers. We have carried out this assessment with both ideal and imperfect CSI at the transmitter. The results have shown that the application of IA is very limited with respect to the practical scenarios. In the second part we have exploited the user selection diversity to improve the performance of IA in cellular systems. The GR-PF based

user selection algorithm is suitable with respect to a good trade-off between system spectral efficiency and user fairness.

Chapter 4

Un-Coordinated Multi-User Inter-Cell Interference Alignment

In this chapter we propose a new transmit precoding scheme which exploits the concept of interference alignment in a cellular system which is affected by the intra cell (multi user) and inter cell interference. We show analytically that our scheme is close to optimal under certain conditions. Then we consider an un-coordinated large cellular system and show heuristically that our scheme outperforms other state of the art schemes. Further in the chapter, we exploit the multi user diversity and propose heuristic user selection methods for multi user multi cell MIMO systems.

4.1 Introduction

We consider the downlink of cellular system where each cell serves multiple users on the same channel use. A channel over which multiple antenna transmitter is serving many single or multiple antenna users is referred as MIMO-broadcast channel in the literature. It is well known that the Dirty Paper Coding (DPC) is the optimal scheme for MIMO-broadcast channel. However, it is not practical to realize DPC for real systems. The work in [16] presented that zero-forcing beamforming (ZFBF) [15] is closed to optimum and can also be used practically to mitigate the multi user interference (MUI) when the UEs are equipped with single antenna. However, the zero-forcing solution is still constrained by the single antenna UEs. The contributions in [39, 61] overcame this problem by introducing effective zero-forcing. Another issue with zero-forcing based precoding is that it does not take desired

signal optimization into account, therefore, it is optimum only in high SNR regime. The optimization method proposed in [17] solved both the problems of multiple antenna UEs and signal maximization. A balance objective function is used to design the transmit precoding. It maximizes the ratio between the signal towards the desired UE to the leakage interference towards the victim UEs. However, all these contributions consider the multi user system (broadcast channel) with only the single cell which is suffered by only the MUI and the Gaussian noise.

In a cellular system, we not only deal with the MUI (intra cell interference) but also with the inter-cell interference (ICI). Some recent research contributions deal the two dimensions of interference with the help of medium access solutions but our focus is based on the design of a transceiver scheme. We consider multiple antenna receivers, so the signal space at the receiving antennas can be divided into two subspaces containing desired signal and interference (MUI and ICI). Motivated by this fact, we apply the concept of IA with the intention to align ICI with MUI so that they are confined in the same subspace.

One of the earliest contributions dealing with MUI and as well as ICI on the basis of alignment is presented in [62]. The work in [62] proposes MUI and ICI alignment on a two-dimensional fixed plane. Extra signalling between the BS and the UEs is used to find that plane. This approach requires a predetermined precoder that is used by the cells involved in transmission. The UEs measure these precoded channels and find a receive processing vector in the null space of the precoded channel from interfering cells. The product of this receive vector with the precoded channel of the serving cell is termed as effective channel and it is fed back by the UE to the serving cell. Using these effective channels the serving cell designs the zero-forcing precoding to mitigate the MUI. We would like to mention here some points about the scheme in [62]. From our understanding it is two sided zero-forcing with the help of extra signalling. The ICI is zero-forced by the receiver and intra cell interference is zero-forced by the precoder. Moreover, this approach requires $K+1$ signalling dimensions to transmit K independent streams. For example, to serve $K=2$ independent streams to 2 users, it requires $K+1=3$ dimensions which implies 3 antennas on either transmit or receive side.

The contribution in [63] came up with a similar idea like [62]. In fact the authors in [63] have stated that their work is similar to [62] except that they avoid extra signaling (for effective channels) by using a pre-determined reference vector for the alignment. Moreover, their work is limited only to a two-cell scenario.

Unlike [62] and [63], our idea is to use *partial and outdated ICI* for alignment. Our inspiration is based on the work presented in [64] and on the characteristics of the interference in the cellular system. With the help of simulations, we show that under some conditions, the interference subspaces at the receiver in two consecutive transmissions are very close to each other. Hence the ICI from the previous transmission is still useful and can be used to design the transmit precoding for the current transmission. We design the precoding such that the ICI subspace from the last transmission is aligned at the intended receiver with the MUI subspace of the current transmission. In contrast to [62] and [63] we require neither extra signalling for a fixed plane nor a predetermined reference vector. In addition to that we decouple the problem of ICI by using the outdated information. It also helps us to avoid iterative method. As the number of interfering cells is higher than the available antennas at the receiver, this implies that the number of interfering terms are higher than the available dimensions to deal with. Therefore, we take only the dominant ICI subspace to align with MUI subspace. Due to the usage of partial and outdated ICI information, our scheme is suboptimal and it cannot achieve the maximum degrees of freedom. However, with a good receiver design it suppresses a major portion of ICI and MUI which helps our scheme to outperform the baseline transmission schemes. Moreover, it is valid for any number of interfering cells in a cellular network.

Generally, the performance of alignment based transmission schemes is highly dependent upon the receiver design. Likewise our scheme also requires a good estimation of the interference by the receiver. Improvements in receiver design with the help of interference estimation and cancellation are already an ongoing research topic. The 3GPP has already open a separate study item for *Network Assisted Interference Cancellation for LTE* [65]. Therefore, initially we assume that the receiver can perfectly estimate the interference covariance for MUI and ICI. Additionally, we release the tight requirement on the receiver by proposing a modified precoding scheme. This modified approach aligns only the strongest cell interference to the MUI. In this case, the receiver needs to perfectly estimate the covariance of only the strongest interfering cell/cells which is realizable even in current networks. The results show that our approach still provides considerable gains over the other schemes.

Another important aspect of our approach is that it requires only the local information i.e. no inter-cell coordination is required. Each user sends the required information only to its serving cell which is very attractive when we consider the latency requirements on backhaul. Due to this, we believe that our contribution gives an efficient and simple transmission scheme

and a useful insight on the applicability and feasibility of IA based MU-precoding in real-world cellular networks. At first we have assumed perfect channel estimation without feedback delay (except for the outdated ICI) and without feedback error for the performance evaluations. Later in the next chapter we will further investigate the performance with all these practical issues.

We distribute our contribution in this chapter in three stages. We start with the explanation of basic idea with the help of a system which is affected by MUI and ICI. Initially we assume a Rayleigh Fading channel in a perfectly uncorrelated environment. Later for the proof of concept, we use system level simulations with multiple cells and multiple active UEs in the system and validate our results by using spatial channel model (SCM). The SCM is more close to realistic scenarios as it considers the probabilities of LOS and NLOS and other important parameters. We also investigate the impact of different receiver algorithms on the performance of our scheme. We extend our work and show the increase in the performance of proposed transmission scheme by exploiting multi user selection diversity. As most of the user selection methods until now are valid for single antenna UEs and optimal for ZFBF, therefore, we propose new methods for user selection with multiple antenna users. Moreover, we show the impact of selection method on the performance of closed loop transmission schemes.

4.2 Basic Idea

Let us focus on a coverage area in a cellular network where two multiple antenna UEs a and b each with N receive antennas are served by a multiple antenna transmitter with M transmit antennas on the same OFDM resource as shown in figure 4.1. Assume that the transmitter uses the precoding vectors $\mathbf{p}_a \in \mathbb{C}^{M\times 1}$ and $\mathbf{p}_b \in \mathbb{C}^{M\times 1}$ to transmit independent scalar complex symbols s_a and s_b towards UE a and UE b respectively. Let $\mathbf{y}_a \in \mathbb{C}^{N\times 1}$ and $\mathbf{y}_b \in \mathbb{C}^{N\times 1}$ be the signals received by UE a and b respectively. With narrowband OFDM assumption, the expressions for the received signals in discrete time representation can be written as,

$$\mathbf{y}_a = \mathbf{H}_a\mathbf{p}_a s_a + \mathbf{H}_a\mathbf{p}_b s_b + \sqrt{\lambda_a}\mathbf{q}_a + \mathbf{n}_a \tag{4.1}$$

$$\mathbf{y}_b = \mathbf{H}_b\mathbf{p}_b s_b + \mathbf{H}_b\mathbf{p}_a s_a + \sqrt{\lambda_b}\mathbf{q}_b + \mathbf{n}_b \tag{4.2}$$

where, $\mathbf{H}_a \in \mathbb{C}^{N\times M}$ and $\mathbf{H}_b \in \mathbb{C}^{N\times M}$ are the MIMO channel matrices of UE a and b respectively to their serving transmitter with all the complex coefficients are independent

and drawn from a random Gaussian distribution with $\mathcal{CN}(0,1)$. The vectors, $\mathbf{q}_a \in \mathbb{C}^{N\times 1}$ and $\mathbf{q}_b \in \mathbb{C}^{N\times 1}$ represent the directions of major ICI components received by the UE a and the UE b respectively due to the transmission in the strongest interfering cell, λ_a and λ_b represent the average ICI power in the directions of $\mathbf{q}_a$ and $\mathbf{q}_b$ respectively such that ($||\mathbf{q}_a||= 1, ||\mathbf{q}_b||= 1$). We assume that the accumulated interference power due to the weak interfering cells in the network is adding up to the noise floor therefore it is treated as noise. The vectors, $\mathbf{n}_a \in \mathbb{C}^{N\times 1}$ and $\mathbf{n}_b \in \mathbb{C}^{N\times 1}$ are the Gaussian noise vectors with $\mathcal{CN}(0,\eta^2)$ respectively for UE a and b.

We assume that the average ICI power remains the same over time but the direction of major ICI component is changing slowly in time. This assumption is valid when the users in the system are experiencing slow time variant channels and the users are scheduled over multiple subframes. Based on the assumption, the directions of major components of ICI can be modelled by using the first order autoregressive process model from [66]:

$$\mathbf{q}_a(t) = \cos\phi_a \mathbf{q}_a(t-1) + \sin\phi_a \mathbf{q}_{a_\perp}(t-1) \tag{4.3}$$

$$\mathbf{q}_b(t) = \cos\phi_b \mathbf{q}_b(t-1) + \sin\phi_b \mathbf{q}_{b_\perp}(t-1) \tag{4.4}$$

Where, t represents the discrete time index, ϕ_a is the *Hermitian Angle* [67] between $\mathbf{q}_a(t)$ and $\mathbf{q}_a(t-1)$, similarly, ϕ_b is between $\mathbf{q}_b(t)$ and $\mathbf{q}_b(t-1)$. The angles ϕ_a and ϕ_b are uniformly distributed between $[0, \phi_{max}]$ where, $\phi_{max} \leq \pi/2$, $\mathbf{q}_{a_\perp}(t-1) \in \mathbb{C}^{N\times 1}$ and $\mathbf{q}_{b_\perp}(t-1) \in \mathbb{C}^{N\times 1}$ are the vectors orthogonal to $\mathbf{q}_a(t-1)$ and $\mathbf{q}_b(t-1)$ respectively.

The second part in equations (4.1) and (4.2) represents the MUI and the third part represents the ICI experienced by the UEs. We assume that the UEs a and b are capable of perfectly estimating the ICI. We also assume that each UE provides a perfect feedback over the channel and interference information to the serving transmitter in time t. Our idea is to design the precoding at the transmitter such that the MUI subspace and the ICI subspace at the desired UE is aligned. With the help of proper receiver design, the UE can cancel the aligned interference. However, the ICI information for current transmission is not available before the transmission. Therefore, the transmitter designs the precoding such that at each UE, the current MUI in time t is aligned with ICI subspace of previous transmission $(t-1)$. Following our idea, the alignment conditions for UE a and UE b can be written as:

$$span(\mathbf{H}_a(t)\mathbf{p}_b(t)) = span(\mathbf{q}_a(t-1)) \tag{4.5}$$

$$span(\mathbf{H}_b(t)\mathbf{p}_a(t)) = span(\mathbf{q}_b(t-1)) \tag{4.6}$$

From the conditions in equations (4.5) and (4.6) we can write the precoding vectors as follows:

$$\mathbf{p}_a(t) = \mathbf{H}_b^{-1}(t)\mathbf{q}_b(t-1) \tag{4.7}$$

$$\mathbf{p}_b(t) = \mathbf{H}_a^{-1}(t)\mathbf{q}_a(t-1) \tag{4.8}$$

Remark on the feasibility: As the coefficients of channel matrices are independent so the channels are of full rank and therefore with $M = N$ the inverse exist with probability one. However, in case of $N > M$, pseudo-inverse of the channel matrix will be required. Hence the application is feasible when inverse exists therefore it is limited to the scenarios with $N \geq M$.

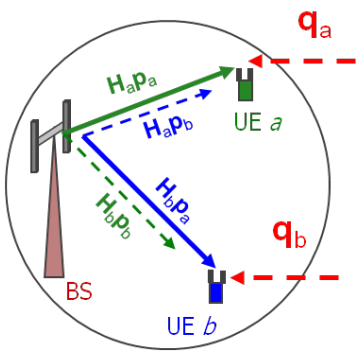

Figure 4.1: MU-MIMO where each UE is experiencing strong ICI

In order to meet the transmit power constraint, we further normalize the precoding vectors as follows,

$$\mathbf{p}_a(t) = \frac{1}{\gamma_a}\mathbf{H}_b^{-1}(t)\mathbf{q}_b(t-1)$$

$$\mathbf{p}_b(t) = \frac{1}{\gamma_b}\mathbf{H}_a^{-1}(t)\mathbf{q}_a(t-1)$$

where, $\gamma_a = ||\mathbf{H}_b^{-1}(t)\mathbf{q}_b(t-1)||$ and $\gamma_b = ||\mathbf{H}_a^{-1}(t)\mathbf{q}_a(t-1)||$. Let us consider the signal received by UE a in time t. Substituting the above precoding vectors in equation (4.1), we get the following form:

$$\mathbf{y}_a(t) = \frac{1}{\gamma_a}\mathbf{H}_a(t)(\mathbf{H}_b^{-1}(t)\mathbf{q}_b(t-1))s_a + \frac{1}{\gamma_b}\mathbf{H}_a(t)(\mathbf{H}_a^{-1}(t)\mathbf{q}_a(t-1))s_b + \sqrt{\lambda_a}\mathbf{q}_a(t) + \mathbf{n}_a(t)$$

$$\mathbf{y}_a(t) = \frac{1}{\gamma_a}(\mathbf{H}_a(t)\mathbf{H}_b^{-1}(t))\mathbf{q}_b(t-1)s_a + \frac{1}{\gamma_b}(\mathbf{I})\mathbf{q}_a(t-1)s_b + \sqrt{\lambda_a}\mathbf{q}_a(t) + \mathbf{n}_a(t) \tag{4.9}$$

Assume that the direction of major interference is unchanged in two consecutive transmissions. It implies that:

$$\mathbf{q}_a(t) = \mathbf{q}_a(t-1)$$
$$\mathbf{q}_b(t) = \mathbf{q}_b(t-1)$$

With this assumption, we can drop the time index in equation (4.9) and re-write it for time t as follows:

$$\mathbf{y}_a = \frac{1}{\gamma_a}(\mathbf{H}_a\mathbf{H}_b^{-1})\mathbf{q}_b s_a + \frac{1}{\gamma_b}\mathbf{q}_a s_b + \sqrt{\lambda_a}\mathbf{q}_a + \mathbf{n}_a \tag{4.10}$$

From equation (4.10) we already see that MUI subspace is aligned with ICI subspace and we only need one dimension to deal with the interference subspace. In order to suppress the aligned interference, the received signal by UE a can be projected to the subspace corresponding to the minimum ICI experienced by UE a. The vector orthogonal to $\mathbf{q}_a$ represents this subspace and we denote it by $\mathbf{q}_{a_\perp}$. The signal after receive processing can be written as,

$$\mathbf{q}_{a_\perp}^H\mathbf{y}_a = \frac{1}{\gamma_a}\mathbf{q}_{a_\perp}^H(\mathbf{H}_a\mathbf{H}_b^{-1})\mathbf{q}_b s_a + \frac{1}{\gamma_b}\mathbf{q}_{a_\perp}^H\mathbf{q}_a s_b + \sqrt{\lambda_a}\mathbf{q}_{a_\perp}^H\mathbf{q}_a + \mathbf{q}_{a_\perp}^H\mathbf{n}_a \tag{4.11}$$

$$y_a^{'} = \mathbf{q}_{a_\perp}^H\mathbf{y}_a = \frac{1}{\gamma_a}\mathbf{q}_{a_\perp}^H(\mathbf{H}_a\mathbf{H}_b^{-1})\mathbf{q}_b s_a + \mathbf{q}_{a_\perp}^H\mathbf{n}_a \tag{4.12}$$

where, $y_a^{'}$ is the signal received by the UE a after the receive processing. The equation (4.12) shows that the received signal by UE a is free from interference. Similar expression can be derived for the signal received by UE b. We assume that the serving cell is transmitting with unit power to both UEs, with $\mathbb{E}[||\mathbf{n}_a||^2] = \eta^2$ the signal to noise ratio can be written as:

$$SINR_a = \frac{|(1/\gamma_a)\mathbf{q}_{a_\perp}^H(\mathbf{H}_a\mathbf{H}_b^{-1})\mathbf{q}_b|^2}{||\mathbf{q}_{a_\perp}^H||^2\eta^2} \tag{4.13}$$

As $||\mathbf{q}_{a_\perp}^H||^2 = 1$, so the noise variance is unchanged even after the receive processing and the SINR expression in equation (4.13) can be written as follows:

$$SINR_a = \frac{(1/\gamma_a^2)|\mathbf{q}_{a_\perp}^H(\mathbf{H}_a\mathbf{H}_b^{-1})\mathbf{q}_b|^2}{\eta^2} \tag{4.14}$$

Proof: $|\mathbf{q}_{a_\perp}^H(\mathbf{H}_a\mathbf{H}_b^{-1})\mathbf{q}_b|^2 > 0$

The condition for numerator $|\mathbf{q}_{a_\perp}^H(\mathbf{H}_a\mathbf{H}_b^{-1})\mathbf{q}_b|^2 > 0$ in equation (4.14) holds good with probability one. The proof is trivial. The only possibility when $|\mathbf{q}_{a_\perp}^H(\mathbf{H}_a\mathbf{H}_b^{-1})\mathbf{q}_b|^2 = 0$ is when

$(\mathbf{H}_a\mathbf{H}_b^{-1}) = \mathbf{I}$ and $\mathbf{q}_{a_\perp}^H\mathbf{q}_b = 0$. This implies that $\mathbf{H}_a = \mathbf{H}_b$ and $\mathbf{q}_a = \mathbf{q}_b$. This condition is possible when the antennas of UE a and UE b are perfectly overlapping which means we have only one UE in the system.

The expression of SINR in equation (4.14) is based on the assumption that the direction of ICI is time-invariant. In practice, it is not the case and even in slow time variant channels, the direction of interference differs in consecutive transmissions. We re-write the equation (4.11) with time index as follows:

$$\begin{aligned}\underbrace{\mathbf{q}_{a_\perp}^H(t)\mathbf{y}_a(t)}_{=y_a^{'}(t)} = \frac{1}{\gamma_a}\mathbf{q}_{a_\perp}^H(t)\mathbf{H}_a(t)\mathbf{H}_b^{-1}(t)\mathbf{q}_b(t-1)s_a + \frac{1}{\gamma_b}\mathbf{q}_{a_\perp}^H(t)\mathbf{q}_a(t-1)s_b \\ + \sqrt{\lambda_a}\mathbf{q}_{a_\perp}^H(t)\mathbf{q}_a(t) + \mathbf{q}_{a_\perp}^H(t)\mathbf{n}_a(t)\end{aligned} \tag{4.15}$$

$$\begin{aligned}y_a^{'}(t) = \frac{1}{\gamma_a}\mathbf{q}_{a_\perp}^H(t)\mathbf{H}_a(t)\mathbf{H}_b^{-1}(t)\mathbf{q}_b(t-1)s_a + \\ \frac{1}{\gamma_b}\mathbf{q}_{a_\perp}^H(t)\mathbf{q}_a(t-1)s_b + \mathbf{q}_{a_\perp}^H(t)\mathbf{n}_a(t)\end{aligned} \tag{4.16}$$

Equation (4.16) implies that we get rid of ICI but there is still residual MUI in the desired signal space given by second term in (4.16). For this case, we obtain the following from equation (4.16):

$$SINR_a(t) = \frac{(1/\gamma_a^2)|\mathbf{q}_{a_\perp}^H(t)\mathbf{H}_a(t)\mathbf{H}_b^{-1}(t)\mathbf{q}_b(t-1)|^2}{(1/\gamma_b^2)|\mathbf{q}_{a_\perp}^H(t)\mathbf{q}_a(t-1)|^2+\eta^2} \tag{4.17}$$

The absolute value of the product $|\mathbf{q}_{a_\perp}^H(t)\mathbf{q}_a(t-1)|$ in equation (4.17) basically represents the *Hermitian Angle* $(0 \leq \phi_a^{'} \leq \pi/2)$ between $\mathbf{q}_{a_\perp}(t)$ and $\mathbf{q}_a(t-1)$ and is given by:

$$\cos\phi_a^{'} = \frac{\mathbf{q}_{a_\perp}^H(t)\mathbf{q}_a(t-1)}{||\mathbf{q}_{a_\perp}^H(t)||\ ||\mathbf{q}_a(t-1)||} = |\mathbf{q}_{a_\perp}^H(t)\mathbf{q}_a(t-1)| \tag{4.18}$$

Since $(0 \leq \phi_a \leq \pi/2)$ is the *Hermitian Angle* between $\mathbf{q}_a(t)$ and $\mathbf{q}_a(t-1)$ and $\mathbf{q}_{a_\perp}(t)$ is orthogonal to $\mathbf{q}_a(t)$ we obtain the following:

$$|\mathbf{q}_{a_\perp}^H(t)\mathbf{q}_a(t-1)| = \cos\phi_a^{'} = \cos(\pi/2-\phi_a) = \sin(\phi_a) \tag{4.19}$$

From equation (4.19) we get $\phi_a^{'} = (\pi/2-\phi_a)$ and equation (4.17) can be written as:

$$SINR_a(t) = \frac{(1/\gamma_a^2)|\mathbf{q}_{a_\perp}^H(t)\mathbf{H}_a(t)\mathbf{H}_b^{-1}(t)\mathbf{q}_b(t-1)|^2}{(1/\gamma_b^2)sin^2(\phi_a)+\eta^2} \tag{4.20}$$

From equation (4.3) with $\phi_a = \pi/2$, $\mathbf{q}_a(t) = \mathbf{q}_{a_\perp}^H(t-1)$, we have the highest residual MUI in desired signal space and the expression for SINR is given as:

$$SINR_a(t)|_{\phi_a=\pi/2} = \frac{(1/\gamma_a^2)|\mathbf{q}_{a_\perp}^H(t)\mathbf{H}_a(t)\mathbf{H}_b^{-1}(t)\mathbf{q}_b(t-1)|^2}{(1/\gamma_b^2)+\eta^2} \tag{4.21}$$

On the other hand, from equation (4.3) with $\phi_a = 0$, $\mathbf{q}_a(t) = \mathbf{q}_a(t-1)$, the residual MUI in desired signal space is zero and the expression for SINR is already given by equation (4.14). In the following we analyse the impact of alignment loss on the performance of our proposed precoding technique with the help of numerical simulations. We also consider the impact of interference power which is treated as noise power.

4.2.1 Numerical Results

We consider the system as shown in figure 4.1 for the simulation of 5000 channel realizations with Rayleigh fading. In order to align the interference subspaces, the ICI should have a strong dominant direction. We refer to this characteristic of ICI as *spatial colouredness* with respect to the white noise. If the UE will experience ICI equally from all the directions isotropically like white noise, then the alignment gains will be minimal. In a real system, the ICI power from direct neighbouring cells is stronger (dominant) and the individual power from other interfering cells is weaker. However, the accumulated power of the weak cells has an effect of increasing the noise floor in the system. We define a parameter called as Interference to Noise Ratio (INR) to control the impact of ICI. Higher values of INR represent strongly directed ICI and an ICI-limited system. Lower values of INR represent a noise limited system. In a real system, the condition number of ICI covariance matrix gives the indication about the colourdness of ICI.

As we have observed from equation (4.20) that the post receiver SINR for UE a depends upon ϕ_a i.e. the direction of arrival of major component of ICI in two consecutive transmissions. The same observation holds for UE b. Therefore, we control ϕ_a and ϕ_b for the simulation of our considered system. We model ϕ_a and ϕ_b as uniformly distributed random variables in the interval $[0, \phi_{max}]$. For each simulation run we fix the value of ϕ_{max} as given input parameter and for each channel realization within a simulation we take a value for each ϕ_a and ϕ_b uniformly between 0 and ϕ_{max}. Figure 4.2 presents the performance of our proposed alignment based precoding scheme using equations (4.8) and (4.9). We call our scheme as Multi User Inter Cell Interference Alignment (MUICIA). Additionally, we compare the

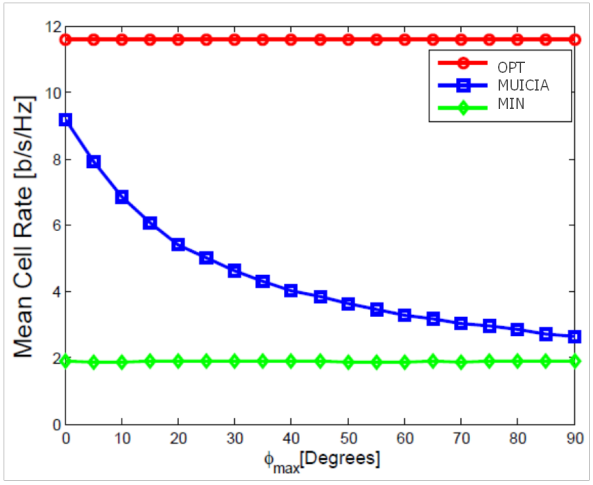

Figure 4.2: Performance comparison of MUICIA with OPT and MIN over ϕ_{max}, SINR=10dB and INR=20dB

performance of MUICIA with two other schemes (represented as OPT and MIN in figure 4.2) which can be seen as an upper bound and a lower bound for the considered system. The OPT is a hypothetical scheme which transmits equal power to both the UEs in their eigenmodes and the receiver perfectly nullifies both MUI and ICI. The MIN also transmits the power in the eigenmodes but the receiver does not treat the interference, it simply uses the MRC combiner.

Figure 4.2 shows the performance of these schemes for the range of ϕ_{max} which is varying from 0 to 90 degrees. We compute mean cell rate with the help of SINR to Shannon Rate mapping. When $\phi_{max} = 0$, our scheme is close to OPT meaning that MUICIA is able to cancel most of the ICI and MUI. With the increase in ϕ_{max} the performance of MUICIA drops drastically because the alignment of MUI and ICI is not perfect and there remains residual MUI in the desired signal space. However, even with very high values of ϕ_{max} the performance is noticeably above MIN.

Figure 4.3 presents the performance over the range of input SINR for different values of ϕ_{max}. For lower values of ϕ_{max}, the performance increases with the increase in SINR due to the improvement in average received signal energy. However, higher values of ϕ_{max} show a very low increase of performance with SINR. It is because the misalignment loss due to the increase in ϕ_{max} is dominant.

Now we consider, another important aspect which is the *colouredness* of ICI. Figure 4.4 shows the numerical performance results over the variation of INR from 0 to 30 dB, for SINR

= 10 dB and for different values of ϕ_{max}. Note that for any value of ϕ_{max}, the performance depends upon how coloured is the ICI. It increases with the increase in INR. Higher values of INR help to align the ICI and as well as suppress the ICI at the receiver. Higher values of ϕ_{max} represent the misalignment and MUI leakage in the desired signal space which causes the loss in the performance. However, still there is a noticeable increase in performance with the increase in INR at higher values of ϕ_{max}. These results show that even if the ICI is outdated, it is still useful to align the MUI with the ICI and deal with both interferences in a multi user cellular system.

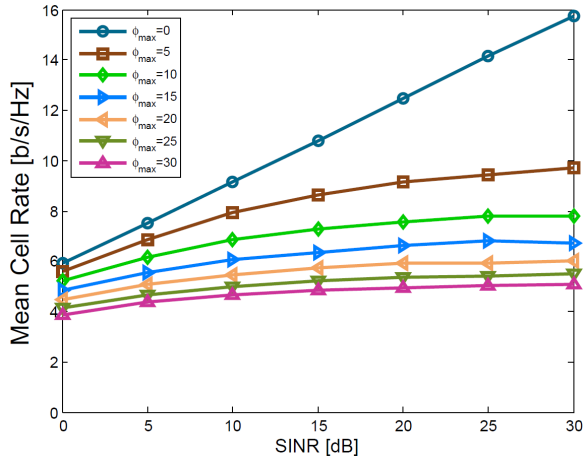

Figure 4.3: Performance of MUICIA over SINR for different ϕ_{max}, INR=20dB

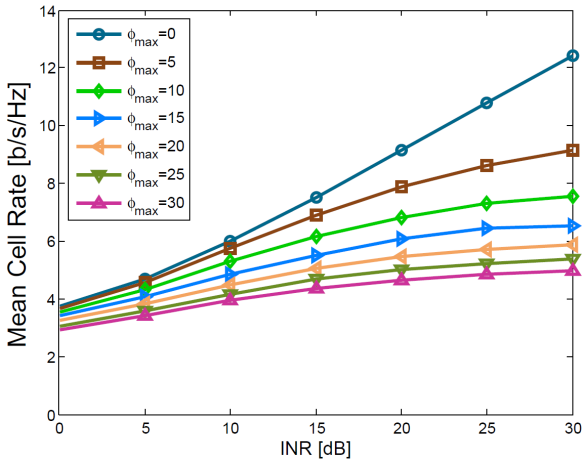

Figure 4.4: Performance of MUICIA over INR for different ϕ_{max}, SINR=10dB

4.3 Multi Cell Multi User MIMO System Model

After the description of our basic idea with the help of a simple system model, now we consider a MIMO-OFDM based cellular system which consists of I BSs (with M transmit antennas) where ith BS schedules a set of users $\mathcal{S}_i$ (each with N receive antennas) simultaneously on the same resource. Let $\mathcal{B}$ be the set which contains the indices of the BSs such that $|\mathcal{B}|= I$. At first, with the help of simulations, we investigate our assumption made in section 4.2 about the ICI. For this purpose, we consider the mth UE served by the ith BS. We consider a typical dense urban scenario where the users are moving with low speed and experiencing slow time varying channels. We assume block fading channel in time and frequency (with temporal correlation) and use spatial channel model [34] to generate the channel realizations for the MIMO system simulations. The total ICI impinging on the receive antennas of mth UE for an OFDM resource block, can be represented by the ICI covariance matrix $\mathbf{Q}_m^{ICI} \in \mathbb{C}^{N\times N}$and is given as follows:

$$\mathbf{Q}_m^{ICI} = \mathbb{E}[\mathbf{f}_m \mathbf{f}_m^H] \tag{4.22}$$

where, $\mathbf{f}_m \in \mathbb{C}^{N\times 1}$ represents the ICI received by UE m and is given by:

$$\mathbf{f}_m = \sum_{j\neq i, j=1}^{I} \sum_{\forall h, h\in\mathcal{S}_j} \mathbf{H}_{mj}\mathbf{p}_{hj}s_{hj} \tag{4.23}$$

Where, $\mathbf{H}_{mj} \in \mathbb{C}^{N\times M}$ represents the channel matrix between the mth UE and the jth interfering BS, $\mathcal{S}_j$ is the set of users scheduled by the jth BS, $\mathbf{p}_{hj} \in \mathbb{C}^{M\times 1}$ is the precoding vector (in this case, $\mathbf{p}_{hj}$ is based on[68]) used by the jth BS for the UE h. The interfering symbols to UE m which are transmitted by the jth BS for the UE h are represented by s_{hj}. The symbol sequences transmitted from each BS are independent and uncorrelated with average allocated power of $\mathbb{E}[s_{hj}s_{hj}^*] = \mathbb{E}[|s_{hj}|^2] = P_{hj}$. Please note that here we intend to focus only on the ICI experienced by the mth UE, a full system description with desired signal and MUI is given in equation (4.26). With equation (4.23) and the assumption that $\mathbf{H}_{mj}\mathbf{p}_{hj}$ is known at the receiver, we can write the ICI covariance matrix $\mathbf{Q}_m^{ICI}$ and simplify it as follows:

$$\mathbf{Q}_m^{ICI} = \sum_{j\neq i, j=1}^{I} \sum_{\forall h, h\in\mathcal{S}_j} \mathbb{E}[(\mathbf{H}_{mj}\mathbf{p}_{hj}s_{hj})(\mathbf{H}_{mj}\mathbf{p}_{hj}s_{hj})^H]$$

$$= \sum_{j\neq i, j=1}^{I} \sum_{\forall h, h\in\mathcal{S}_j} (\mathbf{H}_{mj}\mathbf{p}_{hj})\mathbb{E}[s_{hj}s_{hj}^*](\mathbf{H}_{mj}\mathbf{p}_{hj})^H$$

$$\mathbf{Q}_m^{ICI} = \sum_{j\neq i, j=1}^{I} \sum_{\forall h, h\in\mathcal{S}_j} P_{hj}(\mathbf{H}_{mj}\mathbf{p}_{hj})(\mathbf{H}_{mj}\mathbf{p}_{hj})^H \tag{4.24}$$

The matrix given by equation (4.24) is a positive definite Hermitian matrix whose eigenvectors represent the direction of arrival of average interference towards the UE and the corresponding eigenvalues represent the amount of average power in these directions. The eigenvector corresponding to the maximum eigenvalue represents the direction of arrival of maximum amount of interference towards the UE. Let $\mathbf{q}_m(t) \in \mathbb{C}^{N\times 1}$ and $\mathbf{q}_m(t-1) \in \mathbb{C}^{N\times 1}$ represent the eigenvectors of ICI for the current transmission (t) and previous transmission $(t-1)$ respectively. The *Hermitian Angle* between these eigenvectors can be represented by $(0 \leq \phi_m \leq \pi/2)$ and is given by [67].

$$\phi_m = \arccos\left(\left|\frac{(\mathbf{q}_m(t))^H(\mathbf{q}_m(t-1))}{\|(\mathbf{q}_m(t))^H\|\|(\mathbf{q}_m(t-1))\|}\right|\right) \tag{4.25}$$

This angle represents the change in the major component of ICI. Using the spatial channel model, we draw following observations from simple simulations for the statistics of ϕ_m. This gives us an insight about the dependency of ϕ_m in a realistic network scenario.

- **Time Variance:** Figure 4.5 shows the trace of the hermitian angle ϕ_m given in (4.25) over 1000 channel uses of a UE in a network of 21 BSs. We can see that the variance of ϕ_m over time is below 5 degree.

- **Impact of Speed:** Figures 4.6 and 4.7 show the cumulative density function and mean value of ϕ_m drawn from a simulation with 21 BSs setup for different UE speeds. It clearly shows that with the increase in UE speed, the variance of ϕ_m increases which implies the loss in alignment gains.

  Remarks: Following these results, we infer that although the interference coming from each BS is a stochastic process but the difference in direction of arrival of major component of interference at the UE has very low variance if the UEs in the system are experiencing slow time variant channels and the BSs perform channel dependent user scheduling and precoding.

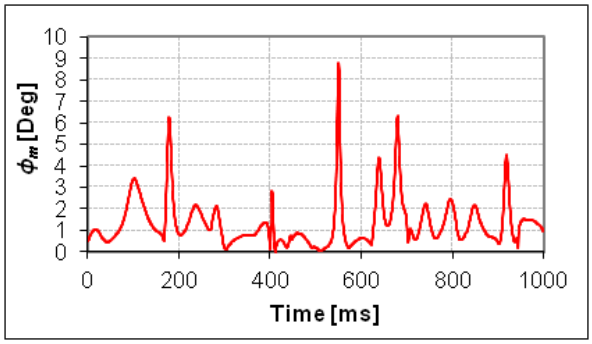

Figure 4.5: Trace of ϕ_m for UE speed = 3km/h and 1000 channel use

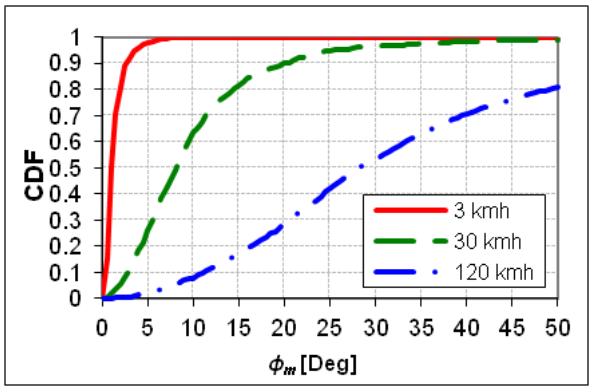

Figure 4.6: CDF of ϕ_m for different UE speeds

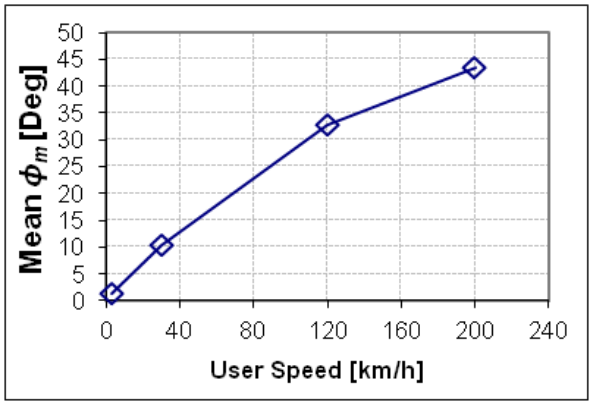

Figure 4.7: Mean ϕ_m value over the variation of UE speed

After explaining the characteristics of ICI in slow time variant environment, now we focus on the requirements of spatial dimensions for transmitter and receiver related to our approach. In near future we expect to have at least $N = 2$ receive antennas at the UEs. This is also specified by 3GPP for LTE-Advanced future releases (please see [29] and references therein). Therefore, from now on, we consider UEs with $N = 2$ receive antennas which gives us 2 spatial dimensions at the receiver to deal with the signal and interference. Only one dimension is available to deal with the interference. Therefore, we assume that $K = 2$ UEs are scheduled simultaneously on each resource so that we have one full component of MUI which is aligned with partial and outdated component of ICI. In case of $K > 2$, we can select the major MUI interferer and aligned this interferer to the ICI.

Assume that each BS is serving L active users. Let $\mathcal{S}_i = \{m, n\}$ be the set which contains the indices of the users selected by the ith BS for rank one transmission on one OFDM resource block. In LTE based OFDM system in *10 MHz* we have *50* physical resource blocks (PRBs). Hence in one transmission time interval (TTI), each BS has the opportunity to serve *50* different pairs of users. We assume block fading channel over one resource block. For the sake of simplicity, using the OFDM narrow band assumption, we focus our mathematical analysis on a single channel use, whereas simulation results will be given for a wideband OFDM system. Let $\mathbf{y}_m \in \mathbb{C}^{N\times 1}$ be the signal received by the mth UE served by the ith BS and it is given by,

$$\mathbf{y}_m = \mathbf{H}_{mi}\mathbf{p}_{mi}s_{mi} + \mathbf{H}_{mi}\mathbf{p}_{ni}s_{ni} + \sum_{j\neq i, j=1}^{I} \sum_{\forall h, h\in\mathcal{S}_j} \mathbf{H}_{mj}\mathbf{p}_{hj}s_{hj} + \mathbf{n}_m \tag{4.26}$$

where, $\mathbf{H}_{mi} \in \mathbb{C}^{N\times M}$ is the channel matrix between the ith BS and the corresponding mth UE, s_{mi} and s_{ni} are the transmitted signals by ith BS, $\mathbf{p}_{mi} \in \mathbb{C}^{M\times 1}$ and $\mathbf{p}_{ni} \in \mathbb{C}^{M\times 1}$ are the precoding vectors used by ith BS for the transmission towards UE m and UE n respectively, $(\sum_{j=1, j\neq i}^{I} \sum_{\forall h, h\in\mathcal{S}_j} \mathbf{H}_{mj}\mathbf{p}_{hj}s_{hj}) \in \mathbb{C}^{N\times 1}$ is the interfering term due to the transmission of the other $(I-1)$ BSs to their corresponding UEs and $\mathbf{n}_m$, $\mathcal{CN}(0, \eta^2)$ is the complex additive Gaussian noise. Except otherwise mentioned, we assume a power constraint at each BS, uniform power over all transmit antennas and that the precoding matrices are unitary with unit norm. The signal after receive combining can be represented as $y_m^{'}$ and is given by,

$$y_m^{'} = \mathbf{g}_m^H \mathbf{y}_m \tag{4.27}$$

where, $\mathbf{g}_m \in \mathbb{C}^{N\times 1}$ is the receiver-weights vector which is also unit norm. In the following we describe how do we compute $\{\mathbf{p}_{mi}$ and $\mathbf{p}_{ni}\}$ by aligning MUI and ICI. Moreover, we also discuss different receiver capabilities and receive combining strategies.

4.4 Transmit Precoding using Multi User Inter Cell Interference Alignment

In this section, we design the transmit precoding based on our approach. At first we assume that the receiver is able to estimate complete ICI perfectly. Then we proceed with the assumption that the receiver is able to perfectly estimate only the strongest cell interference.

4.4.1 Based on Multiuser Inter Cell IA (MUICIA)

We assumed that each BS is serving $K = 2$ UEs with single stream in one channel use. With I BSs, each UE experiences '$(I-1)K$' ICI streams. We have $(N-1)$ dimensions at the UE to confine all the interfering streams. However, for $N = 2$ and $I \geq N$ we have $(N-1) \leq (I-1)K$ which is an under-determined system. Therefore, we find a solution by taking the direction defining the major ICI component. Instead of dealing with individual ICI streams, we consider the eigenvector corresponding to the highest eigenvalue of total ICI covariance matrix $\mathbf{Q}_m^{ICI}$. This implies that we use *Partial* ICI information for the design of precoding. We use the word *Partial* in the sense that it is only an eigenvector corresponding to the highest eigenvalue of ICI covariance matrix. Even to make this partial ICI available at the BS is a problem as it is coupled with the design of precoding vectors in each BS. Hence in time t the current ICI cannot be made available at the BS (with non-iterative methods). Therefore, to decouple the problem, we propose a suboptimal solution inspired by [64] and based on the ICI characteristics presented in section 4.3. We use the *Outdated* ICI measured by the UE in time $(t-1)$. Hence we try to align the *Current* MUI with the *Partial and Outdated* ICI. The alignment condition at the *mth* UE served by *ith* BS can be written as:

$$at\ UE\ m{:}\ span(\mathbf{H}_{mi}(t)\mathbf{p}_{ni}(t)) = span(\mathbf{q}_m(t-1)) \tag{4.28}$$

Note that we have used the time index in the above condition to express the difference between the information used to design the precoding vectors with respect to the transmission time intervals (TTIs). However, later in this section and in the following document we will drop the time indices for simplicity. The symbol $\mathbf{p}_{ni} \in \mathbb{C}^{M\times 1}$ is the precoding vector used by *ith*

BS for nth UE, $\mathbf{q}_m \in \mathbb{C}^{N\times 1}$ is the eigenvector corresponding to the maximum eigenvalue of $\mathbf{Q}_m^{ICI}$ (the total inter-cell interference covariance matrix received by mth UE in TTI $(t-1)$). From the condition in equation (4.28) for mth UE we can derive the precoding vector for nth UE.

$$\mathbf{p}_{ni} = \mathbf{H}_{mi}^{-1}\mathbf{q}_m \tag{4.29}$$

Please note that the conditions for the existence of inverse of the channel matrix shall be satisfied. A remark on the feasibility is given previously in section (4.2). Similarly, the following alignment condition can be written for the nth UE and the precoding vector can be found for the mth UE.

$$at\ UE\ n{:}\ span(\mathbf{H}_{ni}^{(t)}\mathbf{p}_{mi}^{(t)}) = span(\mathbf{q}_n^{(t-1)}) \tag{4.30}$$

$$\mathbf{p}_{mi} = \mathbf{H}_{ni}^{-1}\mathbf{q}_n \tag{4.31}$$

The precoding vectors in equations (4.29) and (4.31) are further normalized (such that: $(||\mathbf{p}_m||= 1, ||\mathbf{p}_n||= 1)$) to ensure the total power constraint at the BS.

For the computation of receive vector let us focus on UE m. Let ψ_m be the post receiver *leakage interference power* in the desired signal space at UE m and it can be written as:

$$\psi_m = P_{ni}||\mathbf{g}_m^H\mathbf{H}_{mi}\mathbf{p}_{ni}||^2 + \sum_{j=1,j\neq i}^{I}\sum_{\forall h,h\in\mathcal{S}_j} P_{hj}||\mathbf{g}_m^H\mathbf{H}_{mj}\mathbf{p}_{hj}||^2 \tag{4.32}$$

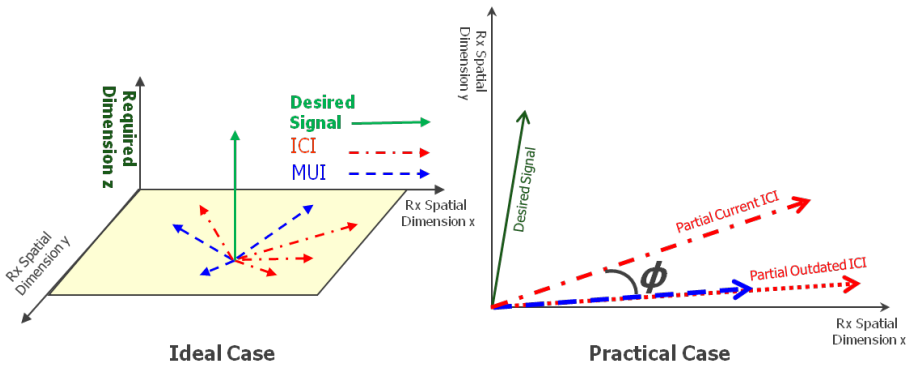

Figure 4.8: Signal vector space at the receiver with 2 Rx Antennas

For the complete suppression of interference power at UE m we need a receive vector $\mathbf{g}_m^H \in \mathbb{C}^{1\times N}$ such that $\psi_m = 0$. However, this condition $(\psi_m = 0)$ is difficult to fulfil in our

case because we have aligned the MUI only with the partial ICI. Moreover, the direction of arrival of interference in the current TTI differs from the direction of aligned interference by an angle ϕ_m given by equation (4.25). Figure 4.8 shows the vector representation of alignment situation at the *mth* UE in ideal and practical case for current transmission. Due to this imperfect alignment, the receiver cannot nullify the interference completely and as a result $\psi_m \neq 0$. However, if ϕ_m is very small as shown in section 4.3, this leakage interference will be negligible. Hence we can relax the condition over ψ_m and we can find the receiver matrix such that:

$$\mathbf{g}_m = \arg \min_{g_m : g_m \in C^{N\times 1}, ||g_m||=1} \psi_m \tag{4.33}$$

In order to minimize ψ_m, the received signal is projected in the direction of arrival of minimum interference. This direction is defined by the eigenvector corresponding to the lowest eigenvalue of the total interference (MUI and ICI) covariance matrix at UE m which is given by $\mathbf{Q}_m$ and can be written as,

$$\mathbf{Q}_m = P_{ni}(\mathbf{H}_{mi}\mathbf{p}_{ni})(\mathbf{H}_{mi}\mathbf{p}_{ni})^H + \mathbf{Q}_m^{ICI} \tag{4.34}$$

The receive vector can be found as the eigenvector corresponding to the minimum eigenvalue of $\mathbf{Q}_m$. We call this receiver type as *Interference Minimization* (IM) and the expression can be written as follows:

$$\mathbf{g}_m = arc\xi(\mathbf{Q}_m) \tag{4.35}$$

The function $arc\xi$ provides the eigenvector corresponding to the lowest eigenvalues of $\mathbf{Q}_m$. The objective function in equation (4.33) does not consider the improvements in desired signal energy. Therefore, we set our objective function to find the receive vector such that the signal to noise and interference ratio after receive processing is optimized. The solution to this optimization is already well known as MMSE based receiver (also known as Interference Rejection and Combining (IRC) receiver). In the previous chapter we named it as MMSE-I receiver. To keep the consistency with our publications that are referred in this chapter for detailed results, we call it as IRC receiver, the expression for IRC receiver is given as follows:

$$\mathbf{g}_m = (\mathbf{Q}_m + \eta^2\mathbf{I}_N)^{-1}(\mathbf{H}_{mi}\mathbf{p}_{mi}) \tag{4.36}$$

4.4.2 Based on Multiuser Strongest Cell IA (MUSCIA)

Current receiver algorithms can estimate the total average interference covariance with the help of received signal and desired signal covariance. The receiver that applies the receive vector given by equation (4.35) or (4.36) requires a perfect interference estimation algorithm. As mentioned earlier, there is an ongoing research in this direction [65] which enables the receiver to perfectly estimate the ICI and MUI. Here we can also realize the perfect estimation of interference with the help of orthogonal pilots in the system. However, we have to assume that the receiver is able to estimate all the strong and the weak interfering channels. Theoretically, it is possible. However, it is a complex task for the current practical receivers and it puts high requirements on the estimator. Therefore, we have considered two slightly modified receiver algorithms that are based on the assumption of perfectly estimating only the strongest cell interference covariance. Let j be the strongest interfering cell for the mth UE, the interference covariance of the strongest interfering cell is represented by $\mathbf{Q}_m^{SICI} \in \mathbb{C}^{N\times N}$ and is given as:

$$\mathbf{Q}_m^{SICI} = \sum_{j\in\mathcal{B}, j\neq i, \forall h, h\in\mathcal{S}_j} P_{hj}(\mathbf{H}_{mj}\mathbf{p}_{hj})(\mathbf{H}_{mj}\mathbf{p}_{hj})^H \tag{4.37}$$

The receiver can only estimate accurately the interference from the strongest interferer and feed this back to the BS. Therefore, the BS aligns the MUI with the strongest cell interference. Similar to equations (4.29) and (4.31), the new precoding vectors for each UE can be written as,

$$\mathbf{p}_{mi} = \mathbf{H}_{mi}^{-1}\tilde{\mathbf{q}}_m \tag{4.38}$$

$$\mathbf{p}_{ni} = \mathbf{H}_{ni}^{-1}\tilde{\mathbf{q}}_n \tag{4.39}$$

where, $\tilde{\mathbf{q}}_m \in \mathbb{C}^{N\times 1}$ and $\tilde{\mathbf{q}}_n \in \mathbb{C}^{N\times 1}$are the eigenvectors of corresponding to the maximum eigenvalue of matrices $\mathbf{Q}_m^{SICI}$ and $\mathbf{Q}_n^{SICI}$ respectively. Neglecting the interference from the weak interfering cells, the total interference covariance matrix at UE m can be represented by $\tilde{\mathbf{Q}}_m \in \mathbb{C}^{N\times N}$ and written as,

$$\tilde{\mathbf{Q}}_m = P_{ni}(\mathbf{H}_{mi}\mathbf{p}_{ni})(\mathbf{H}_{mi}\mathbf{p}_{ni})^H + \mathbf{Q}_m^{SICI} \tag{4.40}$$

The receive vector can be found by solving the optimization problem of maximizing the ratio of signal to noise plus strongest cell interference. We can express the solution as in equation

(4.41) and name it as Strongest Interference Rejection and Combining (SIRC).

$$\mathbf{g}_m = (\tilde{\mathbf{Q}}_m + \eta^2 \mathbf{I}_N)^{-1}(\mathbf{H}_{mi}\mathbf{p}_{mi}) \tag{4.41}$$

To estimate perfectly all the channels is a complex task however, an average of interfering channels can be estimated with somewhat lower effort. Let Γ_m represents the average interference power of all other cells except the strongest cell which can be perfectly estimated. The total interference covariance can be written as,

$$\hat{\mathbf{Q}}_m = P_{ni}(\mathbf{H}_{mi}\mathbf{p}_{ni})(\mathbf{H}_{mi}\mathbf{p}_{ni})^H + \mathbf{Q}_m^{SICI} + \Gamma_m \mathbf{I}_N \tag{4.42}$$

The receiver that uses $\hat{\mathbf{Q}}_m \in \mathbb{C}^{N\times N}$ in optimization can be named as Strongest and Average Interference Rejection and Combining (SAIRC).

$$\mathbf{g}_m = (\hat{\mathbf{Q}}_m + \eta^2 \mathbf{I}_N)^{-1}(\mathbf{H}_{mi}\mathbf{p}_{mi}) \tag{4.43}$$

4.5 Baseline Transmit Precoding Schemes

As a survey, we consider three baseline transmit precoding schemes which deal with MUI based on different optimisation functions. We do not compare with the schemes that deal with ICI as they require coordination between the cells and we have considered a system without any coordination. These baselines are non-alignment based state of the art transmit precodings for Multi User MIMO Systems (MU-MIMO).

4.5.1 Egoism: Maximum Ratio Transmission (MRT)

The precoding vector for each selected UE is designed to optimise the power towards the desired UE. Therefore, we call it an egoistic design as it does not consider the multi user interference caused to the other co-scheduled UE. The optimisation for the *mth* UE served by the *ith* BS can be written as:

$$\mathbf{p}_{mi} = \arg \max_{p_{mi}:||p_{mi}||^2=1} ||\mathbf{H}_{mi}\mathbf{p}_{mi}||^2 \tag{4.44}$$

The solution to (4.44) can be found by taking the SVD of $\mathbf{H}_{mi}$ and use the dominant right singular vector as $\mathbf{p}_{mi}$ for the corresponding UE. We consider total BS power constraint to normalize the precoder. In the following we refer this scheme as (MRT).

4.5.2 Altruism: Effective Zero forcing (EFZF)

This scheme is based on zero-forcing the effective MUI and is proposed in [39, 61]. The per-receive-antenna zero-forcing constraint is overcome by using the equivalent combined channel. Each UE decomposes the serving channel with SVD and uses the dominant left-singular vector as receive combiner. This combined channel (i.e. receive vector multiplied with channel matrix) is fed back by the UE to the BS. The combined channel of the mth UE can be represented by $\mathbf{v}_{mi} \in \mathbb{C}^{N\times 1}$ and is given by,

$$\mathbf{v}_{mi} = (\mathbf{u}_{mi}^{H}\mathbf{H}_{mi})^{H} \tag{4.45}$$

where, $\mathbf{u}_{mi} \in \mathbb{C}^{N\times 1}$ is the dominant vector from the left-singular vectors obtained from SVD of $\mathbf{H}_{mi}$. Similarly, the combined channel can be obtained by the nth UE and the complete combined channel matrix over the selected set $\mathcal{S}_i$ can be written as,

$$\tilde{\mathbf{H}}_i = [\mathbf{v}_{mi}\ \mathbf{v}_{ni}] \tag{4.46}$$

The pseudo-inverse of the combined channel matrix is given as follows:

$$\tilde{\mathbf{H}}_i^{\dagger} = \tilde{\mathbf{H}}_i^{H}(\tilde{\mathbf{H}}_i\tilde{\mathbf{H}}_i^{H})^{-1}$$

$$[\mathbf{p}_{mi}\ \mathbf{p}_{ni}] = \tilde{\mathbf{H}}_i^{\dagger} \tag{4.47}$$

The columns of the matrix $\tilde{\mathbf{H}}_i^{\dagger}$ are used as the precoding vectors for each UE. With the power constraint at BS we further normalized the precoding vectors.

4.5.3 Balance: Signal to Leakage and Noise Ratio (SLNR)

This scheme is based on maximising the Ratio of desired Signal to Leakage and Noise (SLNR). It is first proposed in [17]. The precoding is designed in such a way that the transmitted signal power towards the intended UE is maximized whereas the interference plus noise effect at unintended co-scheduled UEs which are served simultaneously on the same resources by the BS is minimized. The optimization function for precoding of the mth UE co-scheduled with the nth UE can be written as:

$$\mathbf{p}_{mi} = \arg \max_{p_{mi}:||p_{mi}||^2=1} \frac{||\mathbf{H}_{mi}\mathbf{p}_{mi}||^2 P_{mi}}{||\mathbf{H}_{ni}\mathbf{p}_{mi}||^2 P_{mi} + M\eta^2} \tag{4.48}$$

It is shown in [69] and references therein that the optimization in (4.48) is a generalized eigenvalue problem for which the solution is given as:

$$\mathbf{p}_{mi} = \xi\left(\left(\mathbf{H}_{ni}^{H}\mathbf{H}_{ni} + M\eta^{2}\mathbf{I}_{N}\right)^{-1}\mathbf{H}_{mi}^{H}\mathbf{H}_{mi}\right) \tag{4.49}$$

Where, the function, 'ξ' gives the dominant eigenvector, $\mathbf{H}_{ni} \in \mathbb{C}^{N\times M}$ is the channel between the ith BS and nth UE. The total power constraint at the BS is maintained through the normalization of the precoding matrix.

4.6 Rate Computation

The post receiver SINR for the mth UE for one channel use is given by,

$$SINR_{m} = \frac{|\mathbf{g}_{m}^{H}\mathbf{H}_{mi}\mathbf{p}_{mi}|^{2}P_{mi}}{|\mathbf{g}_{m}^{H}\mathbf{H}_{mi}\mathbf{p}_{ni}|^{2}P_{ni} + \sum\limits_{j=1,j\neq i}^{I}\sum\limits_{\forall h,h\in\mathcal{S}_{j}}|\mathbf{g}_{m}^{H}\mathbf{H}_{mj}\mathbf{p}_{hj}|^{2}P_{hj} + ||\mathbf{g}_{i}^{H}||^{2}\eta^{2}} \tag{4.50}$$

This SINR can be used to find the mth UE rate by Shannon SINR-Rate mapping. The ith BS rate R_i is the sum of the rates of UE m and UE n. The mean cell rate R_{avg} (cell spectral efficiency) for one channel use can be written as follows:

$$R_{avg} = \frac{1}{I}\sum_{\forall i,i=1}^{I} R_{i} \tag{4.51}$$

4.7 Performance Analysis of IA based Precoding Schemes

In this section, we demonstrate the performance of IA based precoding schemes (MUICIA, MUSCIA) and do a comparative analysis by performing a comparison with other baseline precoding schemes using the system simulations. At first we assume perfect receiver and analyse the impact of ICI. Later we discuss the impact of receiver capabilities.

4.7.1 Simulation Assumptions and Parameters

The performance evaluation is based on 3GPP based system level simulator. For the considered scenario we have used a site with co-located 3-sectorized antennas where each sector corresponds to a BS. The salient simulation parameters are depicted in Table 1. During a

Parameters	Values
Transmission Mode	Multi-user MIMO
Transmission Bandwidth	10 MHz
Physical Resource Blocks (PRB)	50
Subframe Duration	1 ms
Sub carrier Spacing	15 kHz
TX x RX Antennas	2×2
Scheduling	Random
Scheduled UEs per PRB	2
Scheduling Interval	1 ms
Channel Estimation	Perfect
UE Feed back	Instantaneous and Error Free
Link adaptation	Post Receiver Shannon Mapping
Re-Transmissions	No
Channel Model	Spatial Channel Model, Urban Micro
Transmission Layers	1 per UE
Speed	3 km/h
Traffic	Full Buffer

Table 4.1: Salient simulation parameters for the performance evaluation

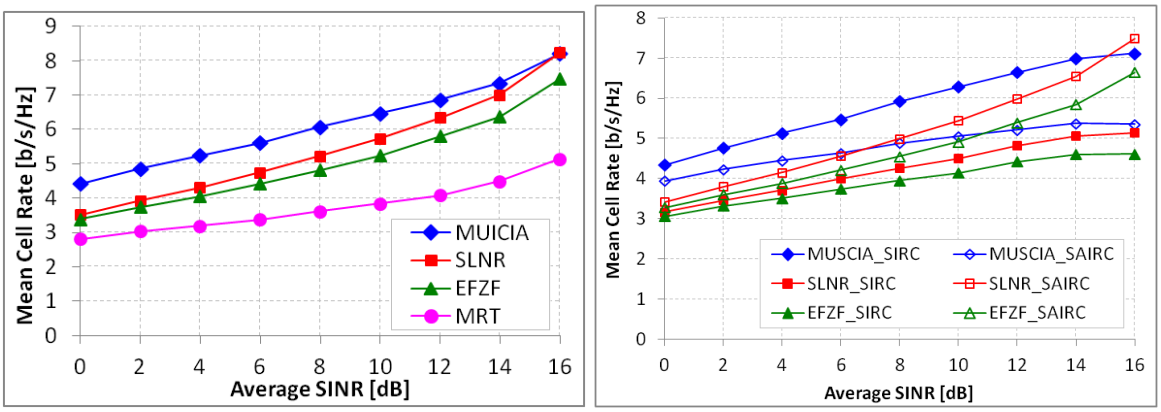

(a) MUICIA with IRC receiver

(b) MUSCIA with SIRC and SAIRC

Figure 4.9: Performance comparison of IA based precodings with base line precoding schemes illustrating the impact of ICI and the impact of different receiver realizations on the performance

simulation run several Monte Carlo drops of UEs are performed. At the start of a drop, the UEs are positioned in each cell according to the given input average SINR of the UE. The average SINR of the UE defines the position of the UE in the cell. The average SINR is given in dB, this is commonly known as *User Geometry*. This SINR does not depend upon the MUI. It depends upon the average received power from each BS in the system and thermal noise. The average receive power is inversely proportional to the distance dependent path loss, shadowing and other large scale parameters. These parameters are modelled as specified in [29]. Furthermore, the realization of all time and frequency selective spatial channels between the BSs and the UEs is done according to the spatial channel model given in [34].

4.7.2 Impact of Inter Cell Interference

Figure 4.9(a) presents the mean cell rates calculated in bits/s/Hz for different precoding schemes with perfect IRC based receiver realized by equation (4.36). It can be clearly seen that if the receiver can successfully suppress the interference directions then alignment with partial and outdated information still helps and our proposed scheme MUICIA provides almost 30% gains in lower and middle SINR regions over the best baseline which is SLNR. Smaller values of average SINR represent high ICI which means that the multiuser-system is limited by the ICI. In this situation, our proposed scheme aligns the ICI subspace with MUI and suppresses it with the help of IRC receiver.

4.7.3 Impact of Receiver Realization

As the IRC receiver is an ideal solution, we now consider more practical receivers. Figure 4.9(b) presents the performance comparison of MUSCIA with other baseline precodings using SIRC and SAIRC receivers. It can be seen that MUSCIA with SAIRC looses the performance as compared to SIRC. This is because the additional average interference perturbs the suppression direction where most of the interference is aligned. We see a very high loss in higher SINR regions because the influence of the strongest ICI is minimized in this region. Higher values of SINR represent a lower ICI which means that the system is now limited by the MUI. The SLNR based precoding with SAIRC performs very well in this situation as it finds the best compromise between the desired signal and the interference to the other UE. However it is still outperformed by MUSCIA with SIRC receiver. It shows that our approach is applicable even with practical considerations and provides considerable gains over the other baseline precoding schemes in high ICI scenarios. For further results on the performance of MUICIA with receiver algorithms we refer to our publication [21].

4.8 Multi User Selection

It is well known that the user selection diversity provides considerable gains in spectral efficiency of a MU-MIMO system. However, the dimension of selection diversity has not been explored for alignment based precoding in the previous sections of this chapter. Motivated by this fact, we extend our work by exploiting this dimension. At first, we employ a standard multi user selection algorithm [70] to select the users for transmission. The increase in the performance by the transmit precoding schemes can be noticed, however, the gains with the standard algorithm are marginal. Therefore, we propose three new algorithms for user selection in a MU-MIMO system. The details of the algorithms will be given in the subsection 4.8.1. If the instantaneous rate of each user can be perfectly estimated, the optimum subset of users (to maximize the system transmission rate) can be found by an exhaustive search over all the combinations. However, in a cellular system, measuring the instantaneous rates of each combination of users in a cell is a coupled problem.

Many low complexity sub optimal user selection algorithms have been presented in literature. The concept of semi orthogonal user selection (SUS) is presented in [16] for zero-forcing beamforming (ZF). It is designed to avoid the MUI by selecting the nearly orthogonal users (with high channel quality) with the help of a greedy search. The ZF-SUS asymptotically

achieves the performance of the optimum-DPC [16]. A variety of work has been presented in literature for the improvement and simplification of ZF-SUS. However, the practical problem with SUS is that it relies on the choice of an input correlation parameter to limit the searching space. The optimization of this parameter is cumbersome in a running system. Therefore, to avoid this problem, we consider the method in [70] as a standard method. The standard method is based on the concept of *Spatial Separability* inspired to find the spatially orthogonal users through an exhaustive search.

Most of the related work in literature on user selection like in above mentioned references has been done either for MISO multi user single cell systems with ZF or with the modelling of ICI as noise. We have considered MU-MIMO cellular system, which not only suffers from MUI but also from the ICI. Moreover, we do not restrict ourselves with ZF based precoding. At first, we show that in a MU-MIMO cellular system, the choice of user selection method does not depend only upon the feedback and computational complexity but it also depends upon the type of precoding scheme adopted by the transmitter. Hence this contribution serves two goals. The first is the proposal of new selection algorithms for MU-MIMO cellular system. The second is to analyse the impact of user selection methods on alignment based and non-alignment based transmit precoding schemes.

4.8.1 Pair Selection Algorithms

We consider a downlink OFDM based Multi user Multi Cell MIMO system similar to the one given in section 4.3. Let $\mathcal{U}_i$ represents the set containing the indices of $(L \geq M)$ active users in *ith* BS (please note again that the terms *BS*, *sector* and *cell* are equivalent here) such that $|\mathcal{U}_i| = L$. Each BS performs the user selection before transmission. The set $\mathcal{S}_i$ contains the indices of the selected users by the *ith* BS. Unlike previous chapter, we do not have any coordination between the BSs, it implies that the selection has to be made individually by each BS. This selection is not globally optimal, as the optimal selection would be based upon the system wide optimization of the objective function. However, in a cellular system it is highly complex and a coupled problem. Therefore, we rely on heuristic suboptimal solutions.

Spatially Orthogonal Users: (Standard)

As described earlier that in a MU-MIMO transmission, to minimize the MUI, we need to select the users which are facing spatially orthogonal channels. Therefore, at first we consider the method from [70] which works on the basis of spatial separability of the users. In case of MISO systems where we have vector channels, the spatial separability can be defined with

the help of Hermitian angle between the serving channel vectors of the users. In our case (multiple antenna UEs), with MIMO channel matrices, we define spatial separability by using the correlation between the channel matrices of the pair of users. Let Π_{mn} represents the correlation between the channels of UE m and UE n. The maximally separable users will have minimal correlation between their channels. We define the following objective function which finds the users with minimum Π_{mn}.

$$\mathcal{S}_i = \arg \min_{\{m,n\} \in \mathcal{S}_i, \mathcal{S}_i \subset \mathcal{U}_i, |\mathcal{S}_i| = K} \Pi_{mn} \tag{4.52}$$

The solution to the objective function in (4.52) can be found by defining the Π_{mn} as follows [70]:

$$\Pi_{mn} = ||\mathbf{H}_{mi}\mathbf{H}_{ni}^{H}||_F \tag{4.53}$$

In the following, we propose three new user selection methods. The first method is an improvement of the proposal in [70]. It is based on serving channel matrices to find the orthogonal users. The second is based on the maximization of alignment gain by using the strongest ICI, it selects the users by simple sorting process. The third is based on the maximization of post receiver SINR estimated by the BS with the help of serving channel and ICI information. This method is computationally more complex than the other two methods as it requires more feedback information and an exhaustive search. We proceed further by providing the details of each method.

1)- Minimum Transmit Side Colinearity: (Min-TxCol)

This algorithm is a slight modification to the standard algorithm. Similar to [70], our objective is to find a spatially separable pair using the information of serving channel matrices. However, instead of finding the total correlation between the channels of the users, we define a metric based on the estimation of transmit-side spatial structure of the MIMO Channel. As the spatial structure of MIMO channel can be tracked by the transmit-side correlation [71]. This metric is known as *Colinearity*. The measure of colinearity can be defined as the similarity between the subspaces spanned by the columns of the two matrices with same dimension [72]. Hence, two matrices which exhibit nearly spatial orthogonal structure should have minimum colinearity. Let Υ_{mn} represent the colinearity between the UEs m and n served by BS i, then we can write the objective function as follows:

$$\mathcal{S}_i = \arg \min_{\{m,n\} \in \mathcal{S}_i, \mathcal{S}_i \subset \mathcal{U}_i, |\mathcal{S}_i| = K} \Upsilon_{mn} \tag{4.54}$$

For the impact of transmit side correlation, we define $\mathbf{R}_m = \mathbf{H}_{mi}^H \mathbf{H}_{mi}$ be the matrix depending upon the channel between UE m and BS i. Similarly, $\mathbf{R}_n = \mathbf{H}_{ni}^H \mathbf{H}_{ni}$ be the matrix for UE n. The colinearity between these matrices can be written as [73]:

$$\Upsilon_{mn} = \frac{|Tr(\mathbf{R}_m \mathbf{R}_n^H)|}{||\mathbf{R}_m||_F ||\mathbf{R}_n||_F}$$

Like the standard method, the BS has to perform exhaustive search over all the combinations of the active users. Only the channel information from each user is required for the selection.

2)- Maximum ICI Condition Number: (Max-ICICond)

In case of MUICIA precoding, the cell aligns the MUI subspace to the ICI subspace. The degree of alignment will be higher for the UEs which will experience non-isotropic (coloured) ICI. Typically in a cellular system, the ICI is coloured when the UE experiences strong interference from one or two interfering cells. The presence of strong interferers can be detected with the help of the ratio of maximium to minimum eigenvalue of the ICI covariance matrix [74]. The *Condition Number* of the covariance matrix represents this ratio. For this purpose, we consider the condition number of the ICI covariance matrix. For mth UE it is given by,

$$\Psi_m = \sqrt{\frac{\lambda_m^{max}}{\lambda_m^{min}}}$$

where, λ_m^{max} and λ_m^{min} are maximum and minimum eigenvalues (with $\lambda_m^{min} > 0$) of the ICI covariance matrix from previous transmission $\mathbf{Q}_m^{ICI} \in \mathbb{C}^{N \times N}$. The cell sorts the UEs with respect to their condition numbers and finds the pair by using the following objective function:

$$\mathcal{S}_i = \arg \max_{\{m,n\} \in \mathcal{S}_i, \mathcal{S}_i \subset \mathcal{U}_i, |\mathcal{S}_i| = K} (\Psi_m + \Psi_n) \tag{4.55}$$

Where, Ψ_n represents the condition number for the nth UE. Only the condition number of the ICI covariance from the previous transmission is required as feedback. In contrast to the other methods, only simple sorting is required to find out the best pair.

3)- Expected Rate Maximisation (Max-ERate)

For this method, we write the following optimization function for the selection of the users in ith BS.

$$\mathcal{S}_i = \arg \max_{\mathcal{S}_i = \{m,n\}, \mathcal{S}_i \subset \mathcal{U}_i, |\mathcal{S}_i| = K} (\hat{R}_{mi} + \hat{R}_{ni}) \tag{4.56}$$

where, $\hat{R}_{mi}$ and $\hat{R}_{ni}$ represent the rates estimated by the *ith* BS for the pair of *mth* and *nth* UE. Let us focus on the *mth* UE served by the *ith* BS. The rate $\hat{R}_{mi}$ of the *mth* UE depends upon the post receiver $\widehat{SINR}_{mi}$ estimated by the BS. For this purpose, the BS calculates precoding vectors for all combinations ${}^{L}C_{K=2}$ based on the information fed back by the UEs. The expression for $\widehat{SINR}_{mi}$ is given by,

$$\widehat{SINR}_{mi} = \frac{|\hat{\mathbf{g}}_m^H \mathbf{H}_{mi} \hat{\mathbf{p}}_{mi}|^2 P_{mi}}{|\hat{\mathbf{g}}_m^H \mathbf{H}_{mi} \hat{\mathbf{p}}_{ni}|^2 P_{ni} + \Omega_m^2 + ||\hat{\mathbf{g}}_m^H||^2 \eta^2} \tag{4.57}$$

where, $\hat{\mathbf{g}}_m \in \mathbb{C}^{N \times 1}$ represents the receiver-weights vector estimated by the BS for UE m when paired with UE n, Ω_m^2 represents the residual ICI. We will discuss about $\hat{\mathbf{g}}_m$ and Ω_m^2 later in this section. The symbol $\hat{\mathbf{p}}_{mi} \in \mathbb{C}^{M \times 1}$ represents the precoding vector for UE m when it is paired with UE n. Similarly, $\hat{\mathbf{p}}_{ni} \in \mathbb{C}^{M \times 1}$is the precoding vector for UE n. The MUI faced by UE m when paired with UE n can be represented by $\hat{\mathbf{Z}}_{m(n)}$ and written as:

$$\hat{\mathbf{Z}}_{m(n)} = P_{ni} (\mathbf{H}_{mi} \hat{\mathbf{p}}_{ni}) (\mathbf{H}_{mi} \hat{\mathbf{p}}_{ni})^H \tag{4.58}$$

We assume that the BS is aware of the receiver algorithm used by the UEs. In practice, this assumption can be realized by defining UE categories as given in [59]. The ICI from the previous TTI is known to the BS. With the help of estimated MUI from equation (4.58) and ICI from previous transmission ($\mathbf{Q}_m^{ICI}$), the BS estimates the receive vectors. The receive vector for UE m when paired with UE n is represented by $\hat{\mathbf{g}}_m$ and is given in equation (4.59).

$$\hat{\mathbf{g}}_m = (\hat{\mathbf{Z}}_{m(n)} + \mathbf{Q}_m^{ICI} + \eta^2 \mathbf{I}_m)^{-1} (\mathbf{H}_{mi} \hat{\mathbf{p}}_{mi}) \tag{4.59}$$

The post receiver desired signal part received by UE m using the receiver vector from equation (4.59) has mean power:

$$\begin{aligned} |\hat{\mathbf{g}}_m^H \mathbf{H}_{mi} \hat{\mathbf{p}}_{mi}|^2 &= (\hat{\mathbf{g}}_m^H \mathbf{H}_{mi} \hat{\mathbf{p}}_{mi}) (\hat{\mathbf{g}}_m^H \mathbf{H}_{mi} \hat{\mathbf{p}}_{mi})^H \\ &= \hat{\mathbf{g}}_m^H (\mathbf{H}_{mi} \hat{\mathbf{p}}_{mi}) (\mathbf{H}_{mi} \hat{\mathbf{p}}_{mi})^H \hat{\mathbf{g}}_m \end{aligned} \tag{4.60}$$

Similar to equation (4.60), mean power of residual MUI part after receiver processing can be calculated as:

$$\begin{aligned} |\hat{\mathbf{g}}_m^H \mathbf{H}_{mi} \hat{\mathbf{p}}_{ni}|^2 &= \hat{\mathbf{g}}_m^H (\mathbf{H}_{mi} \hat{\mathbf{p}}_{ni}) (\mathbf{H}_{mi} \hat{\mathbf{p}}_{ni})^H \hat{\mathbf{g}}_m \\ &= \hat{\mathbf{g}}_m^H \hat{\mathbf{Z}}_{m(n)} \hat{\mathbf{g}}_m \end{aligned} \tag{4.61}$$

Similar to equation (4.61), we can write for the residual ICI as follows:

$$|\Omega_m|^2 = \hat{\mathbf{g}}_m^H(\mathbf{Q}_m^{ICI})\hat{\mathbf{g}}_m \tag{4.62}$$

The BS maps the estimated $\widehat{SINR}_{mi}$ using the Shannon rate as:

$$\hat{R}_{mi} = \log_2(1 + \widehat{SINR}_{mi}) \tag{4.63}$$

Similarly, $\hat{R}_{ni}$ can be computed and the objective function in equation (4.56) can be evaluated. As compared to the the other two methods, the required feedback information as well as the computational complexity is much higher in this method.

Remarks: Note that our primary objective is to find out how much capacity can be achieved with the help of additional user selection diversity in a MU-MIMO cellular system with multiple antenna UEs. Therefore, in all the above user selection methods our target is to maximize the system spectral efficiency. We expect that in a given $10MHz$ bandwidth, most of the users will be selected in a nominal fairness time due to the frequency diversity. However, with these methods, total fairness can not be guaranteed. In practice, user fairness is also an important metric and therefore the scheduler has to trade off between system spectral efficiency and user fairness. We leave the joint optimization of spectral efficiency and fairness with MUICIA based precoding for future research.

4.8.2 Performance of MUICIA with User Selection

In this section, we present the simulation results of the pair selection algorithms described in subsection 4.8.1. The same simulation methodology has been used as in subsection 4.7.1. Perfect channel estimation and instantaneous error-free feedback of CSI is assumed.

One complete simulation cycle consists of several Monte Carlo drops. Each drop consists of certain number of transmission time intervals (TTI). Full buffer traffic and a user speed of 3 km/h is simulated. The total frequency bandwidth is divided into J physical resource blocks (PRB) [29]. Each PRB contains W consecutive subcarriers with a frequency spacing of $15kHz$ (here in $10MHz$ including band gap: 576 subcarriers, $J = 50, W = 12$). With the user speed of 3 km/h, we have slow time variant and nearly frequency flat channels within a single PRB. However, we have frequency diversity due to high number of PRBs with in a TTI. We have the possibility of J different pair selections within a TTI if the number of active users is very high.

The UEs are dropped in the coverage area according to the given downlink wide band average SINR (represented here by σ in dB). This input SINR depends upon the average receive signal level from the serving cell, upon the average receive signal from all other cells and upon the thermal noise. As described in subsection 4.7.1, this parameter controls the position of the UEs in a cell coverage area. Typical values of σ lie between -5 to 17 dB for a frequency reuse-1 cellular system as in figure 3.1. Lower values of σ indicate that the UEs are close to the cell border and facing a high inter cell interference, representing *ICI-limited* region. Although MUI exists in the region but just to emphasize the strong influence of ICI at cell border we explicitly term the region as ICI-limited. Similarly, higher values of σ represent *MUI-limited* region i.e. the UEs are very close to the cell center. Middle order values of σ represent a region where both ICI and MUI have significant influence on the performance of the system.

In the following, we consider two cellular scenarios in order to analyse the impact of ICI on the performance of MUICIA. The first scenario is a system which consist of 3 cells. In such a system the users experience strongly directed (spatially coloured) ICI. The second scenario is a system with 21 cells. The users experience coloured ICI from the direct neighbouring cells but the interference from other cells change the characteristics of ICI. Hence it is interesting for us to investigate both scenarios as they impact the performance of alignment based transmission schemes. For further details on the performance comparison of MUICIA and user selection methods with other non-alignment based precodings we refer to our publications [22, 23] and the master thesis report [75].

3-Cells Scenario:

The 3-cells scenario is modelled by a site with co-located 3-sectorized antennas where each sector corresponds to a BS with unique cell ID. This is one of the baseline scenarios given in [29]. Figure 4.10(a) presents the performance improvements in cell spectral efficiency using MUICIA transmit precoding with different selection algorithms over the increasing number of active users in ICI-limited ($\sigma = 0dB$) and MUI-limited ($\sigma = 14dB$) regions. Notice that our proposed algorithms provide considerable gains in the performance as compared to the standard selection algorithm. In ICI-limited region, with 20 active UEs in the cell, we get almost 9% gains with Min-TxCol, user selection with Max-ICICond provides almost 30% gains and 70% gains are achieved with Max-ERate. In MUI-limited region, these gains are 12% with Min-TxCol, 20% gains are with Max-ICICond and 50% gains are with Max-ERate.

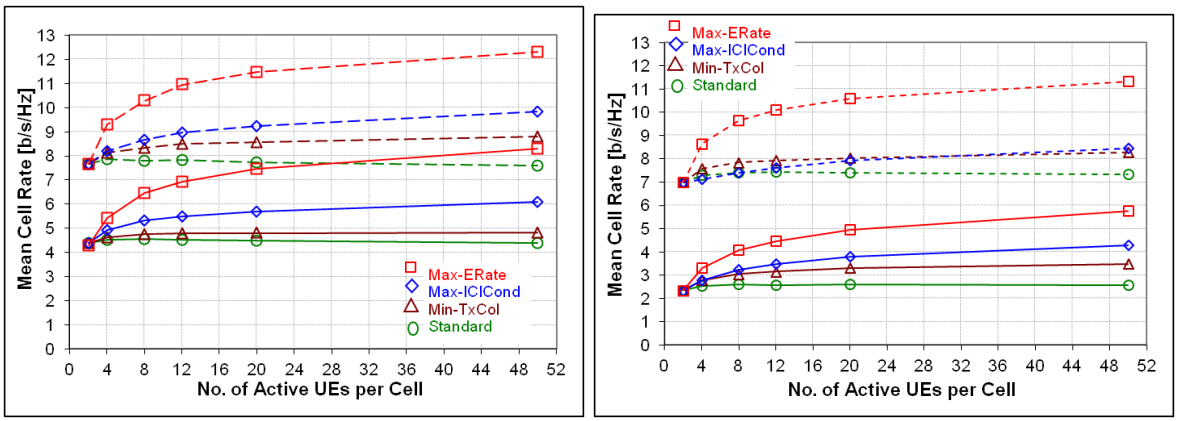

(a) 3-Cells scenario

(b) 21-Cells scenario

Figure 4.10: MUICIA precoding with pair selection algorithms in ICI limited ($\sigma = 0dB$; Smoothed lines) and MUI limited ($\sigma = 14dB$; Dashed lines) regions

The gains of Min-TxCol are increased in MUI-limited region whereas the gains of Max-ICICond are decreased in MUI-limited region. This is because in MUI-limited region, minimizing the MUI helps the transmission scheme. In both regions of operations, the Max-ICICond outperforms Min-TxCol which is based on classical orthogonality based selection. This is because Max-ICICond increases the alignment gain for MUICIA and suppression gain at the receiver by selecting active UEs experiencing strong ICI. Moreover, the gains of Max-ICICond are higher in ICI-limited region due to the strongly directed ICI. This is an important and interesting aspect which states that the selection of spatially separable users is not the best (in terms of spectral efficiency) for transmission in a MU-MIMO cellular system while using MUICIA. The selection with Max-ERate outperforms all other algorithms and it provides relatively better performance in MUI-limited region. It shows that with UE-category information and with slow time variant channels, transmission rate estimation can be done with high accuracy at the serving cell. This estimation helps to select users contributing to high spectral efficiency.

21-Cells Scenario:

The 21-cells scenario is modelled with the help of hexagonal grid of 7 sites each with co-located 3-sectorized antennas which corresponds to a large cellular network. Figure 4.10(b) presents the performance of MUICIA with all user selection algorithms in an ICI-limited and

MUI-limited region, in a 21-cell scenario. At $\sigma = 0$ dB, the user selection algorithm curves show the similar trends as of in 3-cell scenario in figure 4.10(a). The user selection with Max-ICICond outperforms the Min-TxCol. However, the performance gap between them has been decreased in 21-cell case. The situation of the performance comparison of Max-ICICond and Min-TxCol at $\sigma = 14$ dB in figure 4.10(b) is different than figure 4.10(a). We can see that in MUI-limited region, Min-TxCol outperforms Max-ICICond until 20UEs. This is because of the change in ICI characteristics due to the higher number of interfering cells in the system. The gains of MUICIA with Max-ICICond are considerably reduced due to the lack of aligned interference in the system.

4.9 Conclusion

In this chapter at first we have given a detailed account on the statistical characteristics of the interference seen by a user in a MIMO-cellular system. We have shown with the help of simulation results that interference characteristics are highly dependent upon the spatial structure of the environment, mobility of users and scheduling in the network. We have proposed a new transmit precoding scheme for MU-MIMO systems based on the interference alignment using the partial and outdated information about ICI. The results have shown that even with outdated alignment, our proposed scheme provides gains in higher ICI regions. We have also considered some practical limitations of the receivers and presented a modified scheme.

We have also proposed three user selection methods for MU-MIMO cellular system. With the help of extensive simulations we have shown that our proposed selection algorithms bring considerable gains to the performance of MUICIA as well as other baseline precodings. For a high number of active users, the Max-ERate based user selection method is computationally complex but it provides enormous gains in system performance. We have assessed the performance of MUICIA in a smaller and a larger cellular system scenario. In larger scenario we expect loss of interference alignment. The results have shown that MUICIA outperforms SLNR also in larger system for high and average ICI regions with Max-ERate method.

Chapter 5

Un-Coordinated Interference Alignment with Practical Constraints

In this chapter we consider the important issues related to the interference and channel state information at the receiver and the transmitter. At first we consider the estimation at the receiver and then we proceed by considering the imperfect information at the transmitter due to the non-ideal feedback. At the end we proceed towards real world channels. As a proof of concept and a step towards reality, we evaluate the performance of our scheme using measured channels in a lab trial test-bed.

5.1 Performance with Imperfect Information

In this section, we investigate the effects of channel and interference estimation errors at UE side. We consider the system as given in section 4.2 of the previous chapter and represented by the figure 4.1. We consider that the transmit and receive antennas are equal $M = N = 2$ and experiencing Rayleigh fading channels. The matrices, $\mathbf{H}_a \in \mathbb{C}^{2\times 2}$ and $\mathbf{H}_b \in \mathbb{C}^{2\times 2}$ represent these channels respectively for UE a and b. The coefficients of channel matrices are complex, uncorrelated and independent, they are drawn from a random Gaussian distribution with $\mathcal{CN}(0, 1)$. The vectors, $\mathbf{q}_a \in \mathbb{C}^{2\times 1}$ and $\mathbf{q}_b \in \mathbb{C}^{2\times 1}$ represent the directions of major ICI components received by the UE a and the UE b respectively due to the transmission in the strongest interfering cell, λ_a and λ_b represent the average ICI power in the directions of $\mathbf{q}_a$ and

$\mathbf{q}_b$ such that these are unit norm vectors ($||\mathbf{q}_a||= 1, ||\mathbf{q}_b||= 1$). We assume that interference power due to the other cells in the network is treated as noise. The vectors, $\mathbf{n}_a \in \mathbb{C}^{N\times 1}$ and $\mathbf{n}_b \in \mathbb{C}^{N\times 1}$ are the Gaussian noise vectors with $\mathcal{CN}(0, \eta^2)$ respectively for UE a and b.

5.1.1 Channel Estimation Errors at the Receiver

To simplify the analysis, at first we assume that both the UEs a and b are able to estimate the directions of ICI (i.e. $\mathbf{q}_a$ and $\mathbf{q}_b$) perfectly. Later we will consider also the impact of ICI estimation errors. We assume a perfect feedback. We model the estimation error of the desired channel at the receiver as the error of an LMMSE based biased estimator. The details of this estimation error model are given in [19]. Using this error model for our considered system from section 4.2, we can write the estimated channels for UE a and b as follows:

$$\widetilde{\mathbf{H}}_a = \sqrt{\beta}(\mathbf{H}_a + \mathbf{E}_a) \tag{5.1}$$

$$\widetilde{\mathbf{H}}_b = \sqrt{\beta}(\mathbf{H}_b + \mathbf{E}_b) \tag{5.2}$$

Where, $\widetilde{\mathbf{H}}_a \in \mathbb{C}^{2\times 2}$ and $\widetilde{\mathbf{H}}_b \in \mathbb{C}^{2\times 2}$ are the estimated channel matrices, $\mathbf{H}_a$ and $\mathbf{H}_b$ are the true serving channel matrices, $\mathbf{E}_a \in \mathbb{C}^{2\times 2}$ and $\mathbf{E}_b \in \mathbb{C}^{2\times 2}$ are the error matrices which are independent of $\mathbf{H}_a$ and $\mathbf{H}_b$ with all the complex coefficients are independent and drawn from a random Gaussian distribution with zero mean and variance σ_E^2 respectively for UE a and UE b, β is the scaling factor of biased estimator that is used to control the reliability of the estimation. The error variance is given by [19]:

$$\sigma_E^2 = \frac{\sigma_S^2}{T\mu} \tag{5.3}$$

Where, σ_S^2 is the average received signal power by the UEs, μ is the average input SINR and T represents the number of effective pilots that can be considered for a reliable channel estimation. Please note that we have used the same error variance and the same scaling factor for both UE a and UE b. This is because we assume that both the UEs have same input average SINR μ. The expression for scaling factor is given by:

$$\sqrt{\beta} = \frac{\mu T}{1 + \mu T} \tag{5.4}$$

Let us write the signal $\mathbf{y}_a(t) \in \mathbb{C}^{2\times 1}$ received by UE a in time t,

$$\mathbf{y}_a(t) = \mathbf{H}_a(t)\mathbf{p}_a(t)s_a + \mathbf{H}_a(t)\mathbf{p}_b(t)s_b + \sqrt{\lambda_a}\mathbf{q}_a(t) + \mathbf{n}_a(t) \tag{5.5}$$

where, $\mathbf{p}_a \in \mathbb{C}^{2\times 1}$ and $\mathbf{p}_b \in \mathbb{C}^{2\times 1}$ represent the precoding vectors for UE a and b. With the erroneous Channel State Information (CSI) due to the estimation error, the precoding vectors can be written as,

$$\mathbf{p}_a(t) = \frac{1}{\gamma_a}\widetilde{\mathbf{H}}_b^{-1}(t)\mathbf{q}_b(t-1)$$
$$\mathbf{p}_b(t) = \frac{1}{\gamma_b}\widetilde{\mathbf{H}}_a^{-1}(t)\mathbf{q}_a(t-1)$$

where, $\gamma_a = ||\widetilde{\mathbf{H}}_b^{-1}(t)\mathbf{q}_b(t-1)||$ and $\gamma_b = ||\widetilde{\mathbf{H}}_a^{-1}(t)\mathbf{q}_a(t-1)||$. Substituting the above precoding vectors in equation (5.5), we get the following form:

$$\begin{aligned}\mathbf{y}_a(t) = \frac{1}{\gamma_a}\mathbf{H}_a(t)\{\widetilde{\mathbf{H}}_b^{-1}(t)\mathbf{q}_b(t-1)\}s_a + \\ \frac{1}{\gamma_b}\mathbf{H}_a(t)\{\widetilde{\mathbf{H}}_a^{-1}(t)\mathbf{q}_a(t-1)\}s_b + \sqrt{\lambda_a}\mathbf{q}_a(t) + \mathbf{n}_a(t)\end{aligned} \tag{5.6}$$

Substituting equations (5.1) and (5.2) with time index in equation (5.6) we get:

$$\begin{aligned}\mathbf{y}_a(t) &= \frac{1}{\sqrt{\beta}\gamma_a}\mathbf{H}_a(t)\{\mathbf{H}_b(t) + \mathbf{E}_b(t)\}^{-1}\mathbf{q}_b(t-1)s_a + \\ &\frac{1}{\sqrt{\beta}\gamma_b}\mathbf{H}_a(t)\{\mathbf{H}_a(t) + \mathbf{E}_a(t)\}^{-1}\mathbf{q}_a(t-1)s_b + \sqrt{\lambda_a}\mathbf{q}_a(t) + \mathbf{n}_a(t) \\ &= \frac{1}{\sqrt{\beta}\gamma_a}\mathbf{H}_a(t)\mathbf{H}_b^{-1}(t)\{\mathbf{I} + \mathbf{E}_b(t)\mathbf{H}_b^{-1}(t)\}^{-1}\mathbf{q}_b(t-1)s_a + \\ &\frac{1}{\sqrt{\beta}\gamma_b}\mathbf{H}_a(t)\mathbf{H}_a^{-1}(t)\{\mathbf{I} + \mathbf{E}_a(t)\mathbf{H}_a^{-1}(t)\}^{-1}\mathbf{q}_a(t-1)s_b + \sqrt{\lambda_a}\mathbf{q}_a(t) + \mathbf{n}_a(t)\end{aligned} \tag{5.7}$$

$$\begin{aligned}\mathbf{y}_a(t) = \frac{1}{\sqrt{\beta}\gamma_a}\mathbf{H}_a(t)\mathbf{H}_b^{-1}(t)\{\mathbf{I} + \mathbf{E}_b(t)\mathbf{H}_b^{-1}(t)\}^{-1}\mathbf{q}_b(t-1)s_a \\ + \frac{1}{\sqrt{\beta}\gamma_b}\{\mathbf{I} + \mathbf{E}_a(t)\mathbf{H}_a^{-1}(t)\}^{-1}\mathbf{q}_a(t-1)s_b + \sqrt{\lambda_a}\mathbf{q}_a(t) + \mathbf{n}_a(t)\end{aligned} \tag{5.8}$$

For the sake of clarity, we denote $\mathbf{I}_N = \mathbf{I}$ and we drop the time index and substitute $\mathbf{q}_a(t-1) = \mathbf{q}_a^{'}$ and $\mathbf{q}_b(t-1) = \mathbf{q}_b^{'}$ in equation (5.8) as:

$$\mathbf{y}_a = \frac{1}{\sqrt{\beta}\gamma_a}\mathbf{H}_a\mathbf{H}_b^{-1}\{\mathbf{I} + \mathbf{E}_b\mathbf{H}_b^{-1}\}^{-1}\mathbf{q}_b^{'}s_a + \frac{1}{\sqrt{\beta}\gamma_b}\{\mathbf{I} + \mathbf{E}_a\mathbf{H}_a^{-1}\}^{-1}\mathbf{q}_a^{'}s_b + \sqrt{\lambda_a}\mathbf{q}_a + \mathbf{n}_a \tag{5.9}$$

By assumption, the channels are of full rank and their coefficients are fully independent, channel inverse exist with probability one. The error matrices are also full rank so the products $\mathbf{E}_a\mathbf{H}_a^{-1}$ and $\mathbf{E}_b\mathbf{H}_b^{-1}$ are also full rank and non-singular. Moreover, the summations

$\{\mathbf{I}+\mathbf{E}_a\mathbf{H}_a^{-1}\}^{-1}$ and $\{\mathbf{I}+\mathbf{E}_b\mathbf{H}_b^{-1}\}^{-1}$ are also non-singular. The conditions for Taylor series expansion state that if $\mathbf{A}$ be a matrix such that $\mathbf{A}^n \to 0$ when $n \to \infty$ then:

$$(\mathbf{I}+\mathbf{A})^{-1} = \mathbf{I}-\mathbf{A}+\mathbf{A}^2-\mathbf{A}^3+...$$

For $\mu \geq 0$ and $T > 1$, $\sigma_E^2 < 1$, we can have the following conditions:

$$(\mathbf{E}_a\mathbf{H}_a^{-1})^n \to 0; n \to \infty$$
$$(\mathbf{E}_b\mathbf{H}_b^{-1})^n \to 0; n \to \infty$$

Now we can apply the Taylor expansion and approximation $(\mathbf{E}_a\mathbf{H}_a^{-1})^x \approx 0$ and $(\mathbf{E}_b\mathbf{H}_b^{-1})^x \approx 0$, $\forall x > 1$ on the inverse of the sum of matrices in equation (5.9) and re-write it as follows:

$$\mathbf{y}_a \simeq \frac{1}{\sqrt{\beta}\gamma_a}\mathbf{H}_a\mathbf{H}_b^{-1}\{\mathbf{I}-\mathbf{E}_b\mathbf{H}_b^{-1}\}\mathbf{q}_b^{'}s_a + \frac{1}{\sqrt{\beta}\gamma_b}\{\mathbf{I}-\mathbf{E}_a\mathbf{H}_a^{-1}\}\mathbf{q}_a^{'}s_b + \sqrt{\lambda_a}\mathbf{q}_a + \mathbf{n}_a \quad (5.10)$$

Now we project the signal to the subspace where UE a is facing the minimum ICI. The vector $\mathbf{q}_{a_\perp}(t)$ which is orthogonal to $\mathbf{q}_a(t)$ represents this subspace.

$$\begin{aligned}\underbrace{\mathbf{q}_{a_\perp}^H\mathbf{y}_a}_{y_a^{'}} \simeq{}& \frac{1}{\sqrt{\beta}\gamma_a}\{\mathbf{q}_{a_\perp}^H\mathbf{H}_a\mathbf{H}_b^{-1}\mathbf{q}_b^{'} - \mathbf{q}_{a_\perp}^H\mathbf{H}_a\mathbf{H}_b^{-1}\mathbf{E}_b\mathbf{H}_b^{-1}\mathbf{q}_b^{'}\}s_a \\ &+ \frac{1}{\sqrt{\beta}\gamma_b}\{\mathbf{q}_{a_\perp}^H\mathbf{q}_a^{'} - \mathbf{q}_{a_\perp}^H\mathbf{E}_a\mathbf{H}_a^{-1}\mathbf{q}_a^{'}\}s_b + \sqrt{\lambda_a}\mathbf{q}_{a_\perp}^H\mathbf{q}_a + \mathbf{q}_{a_\perp}^H\mathbf{n}_a\end{aligned} \quad (5.11)$$

$$\begin{aligned}y_a^{'} \simeq{}& \frac{1}{\sqrt{\beta}\gamma_a}\{\mathbf{q}_{a_\perp}^H\mathbf{H}_a\mathbf{H}_b^{-1}\mathbf{q}_b^{'} - \mathbf{q}_{a_\perp}^H\mathbf{H}_a\mathbf{H}_b^{-1}\mathbf{E}_b\mathbf{H}_b^{-1}\mathbf{q}_b^{'}\}s_a \\ &+ \frac{1}{\sqrt{\beta}\gamma_b}\{\mathbf{q}_{a_\perp}^H\mathbf{q}_a^{'} - \mathbf{q}_{a_\perp}^H\mathbf{E}_a\mathbf{H}_a^{-1}\mathbf{q}_a^{'}\}s_b + \mathbf{q}_{a_\perp}^H\mathbf{n}_a\end{aligned} \quad (5.12)$$

We assume that the serving cell allocates unit power to the UEs, the SINR for UE a can be written as:

$$SINR_a \simeq \frac{|\frac{1}{\sqrt{\beta}\gamma_a}\{\mathbf{q}_{a_\perp}^H\mathbf{H}_a\mathbf{H}_b^{-1}\mathbf{q}_b^{'} - \mathbf{q}_{a_\perp}^H\mathbf{H}_a\mathbf{H}_b^{-1}\mathbf{E}_b\mathbf{H}_b^{-1}\mathbf{q}_b^{'}\}|^2}{|\frac{1}{\sqrt{\beta}\gamma_b}\{\mathbf{q}_{a_\perp}^H\mathbf{q}_a^{'} - \mathbf{q}_{a_\perp}^H\mathbf{E}_a\mathbf{H}_a^{-1}\mathbf{q}_a^{'}\}|^2 + ||\mathbf{q}_{a_\perp}^H||^2\eta^2}$$

$$SINR_a \simeq \frac{|\frac{1}{\sqrt{\beta}\gamma_a}\{\mathbf{q}_{a_\perp}^H\mathbf{H}_a\mathbf{H}_b^{-1}\mathbf{q}_b^{'} - \mathbf{q}_{a_\perp}^H\mathbf{H}_a\mathbf{H}_b^{-1}\mathbf{E}_b\mathbf{H}_b^{-1}\mathbf{q}_b^{'}\}|^2}{(\frac{1}{\sqrt{\beta}\gamma_b})^2|\mathbf{q}_{a_\perp}^H\mathbf{q}_a^{'} + (-1)\mathbf{q}_{a_\perp}^H\mathbf{E}_a\mathbf{H}_a^{-1}\mathbf{q}_a^{'}|^2 + \eta^2} \quad (5.13)$$

where, $(\mathbf{q}_{a_\perp}^H \mathbf{q}_a^{'}) \in \mathbb{C}^{1\times 1}$ and $(-\mathbf{q}_{a_\perp}\mathbf{E}_a\mathbf{H}_a^{-1}\mathbf{q}_a^{'}) \in \mathbb{C}^{1\times 1}$ are the complex numbers, we can apply the triangle inequality $|x+y| \leq |x|+|y|$ on equation (5.13) to numerically approximate the SINR:

$$SINR_a \approx \frac{|\frac{1}{\sqrt{\beta}\gamma_a}\{\mathbf{q}_{a_\perp}^H\mathbf{H}_a\mathbf{H}_b^{-1}\mathbf{q}_b^{'} - \mathbf{q}_{a_\perp}^H\mathbf{H}_a\mathbf{H}_b^{-1}\mathbf{E}_b\mathbf{H}_b^{-1}\mathbf{q}_b^{'}\}|^2}{(\frac{1}{\sqrt{\beta}\gamma_b})^2\{|\mathbf{q}_{a_\perp}^H\mathbf{q}_a^{'}|+|\mathbf{q}_{a_\perp}^H\mathbf{E}_a\mathbf{H}_a^{-1}\mathbf{q}_a^{'}|\}^2+\eta^2}$$

$$SINR_a \approx \frac{|\frac{1}{\sqrt{\beta}\gamma_a}\{\mathbf{q}_{a_\perp}^H\mathbf{H}_a\mathbf{H}_b^{-1}\mathbf{q}_b^{'} - \mathbf{q}_{a_\perp}^H\mathbf{H}_a\mathbf{H}_b^{-1}\mathbf{E}_b\mathbf{H}_b^{-1}\mathbf{q}_b^{'}\}|^2}{(\frac{1}{\sqrt{\beta}\gamma_b})^2\{|\mathbf{q}_{a_\perp}^H\mathbf{q}_a^{'}|^2+|\mathbf{q}_{a_\perp}^H\mathbf{E}_a\mathbf{H}_a^{-1}\mathbf{q}_a^{'}|^2+2|\mathbf{q}_{a_\perp}^H\mathbf{q}_a^{'}||\mathbf{q}_{a_\perp}^H\mathbf{E}_a\mathbf{H}_a^{-1}\mathbf{q}_a^{'}|\}+\eta^2} \quad (5.14)$$

The product $|\mathbf{q}_{a_\perp}^H\mathbf{q}_a^{'}|$ in equation (5.14) is the Hermitian angle between $\mathbf{q}_{a_\perp}$ and $\mathbf{q}_a^{'}$. It is related with $\phi_a \in [0, \pi/2]$ (i.e. Hermitian angle between $\mathbf{q}_a$ and $\mathbf{q}_a^{'}$) such that $|\mathbf{q}_{a_\perp}^H\mathbf{q}_a^{'}| = \cos(\pi/2-\phi_a) = \sin(\phi_a)$.

$$SINR_a \approx \frac{|\frac{1}{\sqrt{\beta}\gamma_a}\{\mathbf{q}_{a_\perp}^H\mathbf{H}_a\mathbf{H}_b^{-1}\mathbf{q}_b^{'} - \mathbf{q}_{a_\perp}^H\mathbf{H}_a\mathbf{H}_b^{-1}\mathbf{E}_b\mathbf{H}_b^{-1}\mathbf{q}_b^{'}\}|^2}{(\frac{1}{\sqrt{\beta}\gamma_b})^2\{\sin^2(\phi_a)+|\mathbf{q}_{a_\perp}^H\mathbf{E}_a\mathbf{H}_a^{-1}\mathbf{q}_a^{'}|^2+2\sin(\phi_a)|\mathbf{q}_{a_\perp}^H\mathbf{E}_a\mathbf{H}_a^{-1}\mathbf{q}_a^{'}|\}+\eta^2} \quad (5.15)$$

When $\phi_a = 0$, $(\sin\phi_a = 0)$ which means $\mathbf{q}_a$ and $\mathbf{q}_a^{'}$ are co-linear, however, there will still be some residual MUI power in desired signal space due to the channel estimation error and the expression for SINR is given by:

$$SINR_a^{(\phi_a=0)} \approx \frac{|\frac{1}{\sqrt{\beta}\gamma_a}\{\mathbf{q}_{a_\perp}^H\mathbf{H}_a\mathbf{H}_b^{-1}\mathbf{q}_b^{'} - \mathbf{q}_{a_\perp}^H\mathbf{H}_a\mathbf{H}_b^{-1}\mathbf{E}_b\mathbf{H}_b^{-1}\mathbf{q}_b^{'}\}|^2}{(\frac{1}{\sqrt{\beta}\gamma_b})^2|\mathbf{q}_{a_\perp}^H\mathbf{E}_a\mathbf{H}_a^{-1}\mathbf{q}_a^{'}|^2+\eta^2} \quad (5.16)$$

Comparing equation (5.16) with the expression of SINR with ideal CSI in equation (4.14) in section 4.2 we can see that there is an additional MUI term due to the channel estimation errors. When $\phi_a = \pi/2$, $(\sin\phi_a = 1)$ which means $\mathbf{q}_a$ and $\mathbf{q}_a^{'}$ are orthogonal, the SINR expression can be simplified as:

$$SINR_a^{(\phi_a=\frac{\pi}{2})} \approx \frac{|\frac{1}{\sqrt{\beta}\gamma_a}\{\mathbf{q}_{a_\perp}^H\mathbf{H}_a\mathbf{H}_b^{-1}\mathbf{q}_b^{'} - \mathbf{q}_{a_\perp}^H\mathbf{H}_a\mathbf{H}_b^{-1}\mathbf{E}_b\mathbf{H}_b^{-1}\mathbf{q}_b^{'}\}|^2}{(\frac{1}{\sqrt{\beta}\gamma_b})^2\{1+|\mathbf{q}_{a_\perp}^H\mathbf{E}_a\mathbf{H}_a^{-1}\mathbf{q}_a^{'}|^2+2|\mathbf{q}_{a_\perp}^H\mathbf{E}_a\mathbf{H}_a^{-1}\mathbf{q}_a^{'}|\}+\eta^2} \quad (5.17)$$

Now writing back the equation (5.15) with the time index:

$$\begin{aligned}
SINR_a(t) \approx & \left(|\frac{1}{\sqrt{\beta}\gamma_a}\{\mathbf{q}_{a_\perp}^H(t)\mathbf{H}_a(t)\mathbf{H}_b^{-1}(t)\mathbf{q}_b(t-1) - \right. \\
& \left.\mathbf{q}_{a_\perp}^H(t)\mathbf{H}_a(t)\mathbf{H}_b^{-1}(t)\mathbf{E}_b(t)\mathbf{H}_b^{-1}(t)\mathbf{q}_b(t-1)\}|^2\right) / \\
& \left((\frac{1}{\sqrt{\beta}\gamma_b})^2\{\sin^2(\phi_a)+|\mathbf{q}_{a_\perp}^H(t)\mathbf{E}_a(t)\mathbf{H}_a^{-1}(t)\mathbf{q}_a(t-1)|^2 + \right. \\
& \left.2\sin(\phi_a)|\mathbf{q}_{a_\perp}^H(t)\mathbf{E}_a(t)\mathbf{H}_a^{-1}(t)\mathbf{q}_a(t-1)|\}+\eta^2\right)
\end{aligned} \quad (5.18)$$

Notice that, when there are no estimation erros, $\sqrt{\beta} = 1$ and $\mathbf{E}_a = \mathbf{E}_b = \mathbf{O} \in \mathbb{C}^{2\times 2}$, the SINR in equation (5.18) will be equal to the ideal SINR in equation (4.20).

5.1.2 Interference Estimation Errors at the Receiver

Now we consider that in addition to the channel estimation error, the receiver has also an error in the estimation of ICI. We assume that the channel estimation errors and ICI errors are independent and uncorrelated. Therefore, in the previous section we modelled the channel estimation errors. Here we explain how we model the error in ICI estimation. We assume that the error lies only in the estimation of the direction of ICI whereas the average ICI power is perfectly estimated at the receiver. Let $\mathbf{e}_a(t) \in \mathbb{C}^{2\times 1}$ and $\mathbf{e}_b(t) \in \mathbb{C}^{2\times 1}$ be the random Gaussian error vectors with variance σ_e which affect the estimation of ICI in UE a and b respectively. The estimated ICI vectors for UE a and b are given as,

$$\widetilde{\mathbf{q}}_a(t) = \mathbf{q}_a(t) + \mathbf{e}_a(t) \tag{5.19}$$

$$\widetilde{\mathbf{q}}_b(t) = \mathbf{q}_b(t) + \mathbf{e}_b(t) \tag{5.20}$$

where, $\widetilde{\mathbf{q}}_a(t) \in \mathbb{C}^{2\times 1}$ and $\widetilde{\mathbf{q}}_b(t) \in \mathbb{C}^{2\times 1}$ are the estimated ICI vectors. We normalize the vectors such that $||\widetilde{\mathbf{q}}_a(t)|| = ||\widetilde{\mathbf{q}}_b(t)|| = 1$. We assume that the error in channel estimation and ICI estimation are independent. Intuitively, the variance of error for ICI estimation, σ_e, is directly related to average SINR (μ) because higher SINR implies weaker interference which implies an increase in ICI estimation error. On the other hand, intuitively, σ_e is inversely proportional to the Interference to Noise Ratio (INR), ζ, because higher INR implies stronger interference which implies a decrease in estimation error. An increase in the number of effective pilots T also decreases the estimation error. With these intuitions, the error variance of ICI estimation can be written as:

$$\sigma_e = \frac{\mu}{T\zeta} \tag{5.21}$$

Now we can re-write the equation (5.6) with channel and interference estimation errors as follows:

$$\begin{aligned}\mathbf{y}_a(t) = &\frac{1}{\gamma_a}\mathbf{H}_a(t)\{\widetilde{\mathbf{H}}_b^{-1}(t)\widetilde{\mathbf{q}}_b(t-1)\}s_a + \\ &\frac{1}{\gamma_b}\mathbf{H}_a(t)\{\widetilde{\mathbf{H}}_a^{-1}(t)\widetilde{\mathbf{q}}_a(t-1)\}s_b + \sqrt{\lambda_a}\mathbf{q}_a(t) + \mathbf{n}_a(t)\end{aligned} \tag{5.22}$$

Where, $\gamma_a = ||\widetilde{\mathbf{H}}_b^{-1}(t)\widetilde{\mathbf{q}}_b(t-1)||$ and $\gamma_b = ||\widetilde{\mathbf{H}}_a^{-1}(t)\widetilde{\mathbf{q}}_a(t-1)||$. Now we can project the receive vector on to $\widetilde{\mathbf{q}}_{a_\perp}(t)$ and perform the similar approximation for the inverses as in the

previous section. In the following we remove the time index and represent the $(t-1)$ quantities with a prime. The received signal after the receive processing analogous to equation (5.11) can be written as follows:

$$\begin{aligned} y_a^{'} = & \frac{1}{\sqrt{\beta}\gamma_a}\{\widetilde{\mathbf{q}}_{a_\perp}^H \mathbf{H}_a \mathbf{H}_b^{-1} \widetilde{\mathbf{q}}_b^{'} - \widetilde{\mathbf{q}}_{a_\perp}^H \mathbf{H}_a \mathbf{H}_b^{-1} \mathbf{E}_b \mathbf{H}_b^{-1} \widetilde{\mathbf{q}}_b^{'}\} s_a \\ & + \frac{1}{\sqrt{\beta}\gamma_b}\{\widetilde{\mathbf{q}}_{a_\perp}^H \widetilde{\mathbf{q}}_a^{'} - \widetilde{\mathbf{q}}_{a_\perp}^H \mathbf{E}_a \mathbf{H}_a^{-1} \widetilde{\mathbf{q}}_a^{'}\} s_b + \sqrt{\lambda_a}\widetilde{\mathbf{q}}_{a_\perp}^H \mathbf{q}_a + \widetilde{\mathbf{q}}_{a_\perp}^H \mathbf{n}_a \end{aligned} \tag{5.23}$$

Note that as oppose to equation (5.12), we see a residual ICI term $\sqrt{\lambda_a}\widetilde{\mathbf{q}}_{a_\perp}^H \mathbf{q}_a$ in equation (5.23) due to the estimation error in ICI. Assuming unit power transmission, the signal to interference and noise ratio can be written as:

$$SINR_a = \frac{|\frac{1}{\sqrt{\beta}\gamma_a}\{\widetilde{\mathbf{q}}_{a_\perp}^H \mathbf{H}_a \mathbf{H}_b^{-1} \widetilde{\mathbf{q}}_b^{'} - \widetilde{\mathbf{q}}_{a_\perp}^H \mathbf{H}_a \mathbf{H}_b^{-1} \mathbf{E}_b \mathbf{H}_b^{-1} \widetilde{\mathbf{q}}_b^{'}\}|^2}{|\frac{1}{\sqrt{\beta}\gamma_b}\{\widetilde{\mathbf{q}}_{a_\perp}^H \widetilde{\mathbf{q}}_a^{'} - \widetilde{\mathbf{q}}_{a_\perp}^H \mathbf{E}_a \mathbf{H}_a^{-1} \widetilde{\mathbf{q}}_a^{'}\}|^2 + \lambda_a |\widetilde{\mathbf{q}}_{a_\perp}^H \mathbf{q}_a|^2 + \eta^2} \tag{5.24}$$

Notice that, when there are no estimation erros, $\sqrt{\beta} = 1$, $\mathbf{E}_a = \mathbf{E}_b = \mathbf{O} \in \mathbb{C}^{2\times 2}$, $\mathbf{e}_a = \mathbf{e}_b = \mathbf{o} \in \mathbb{C}^{2\times 1}$ and $|\widetilde{\mathbf{q}}_{a_\perp}^H \mathbf{q}_a| = 0$, the SINR in equation (5.24) will be equal to the ideal SINR in equation (4.20).

5.1.3 Imperfect Information at the Transmitter

Now we consider the case when the CSI at the transmitter is uncertain due to the problems related to the feedback. For this purpose, we model the channel information as follows:

$$\widehat{\mathbf{H}}_a = \frac{1}{\sqrt{1-\varrho^2}}\widetilde{\mathbf{H}}_a + \frac{\varrho}{\sqrt{1-\varrho^2}}\widetilde{\mathbf{E}}_a \tag{5.25}$$

$$\widehat{\mathbf{H}}_b = \frac{1}{\sqrt{1-\varrho^2}}\widetilde{\mathbf{H}}_b + \frac{\varrho}{\sqrt{1-\varrho^2}}\widetilde{\mathbf{E}}_b \tag{5.26}$$

Where, $\widehat{\mathbf{H}}_a \in \mathbb{C}^{2\times 2}$ and $\widehat{\mathbf{H}}_b \in \mathbb{C}^{2\times 2}$ represent the uncertain channel information at the transmitter, $\widetilde{\mathbf{H}}_a \in \mathbb{C}^{2\times 2}$ and $\widetilde{\mathbf{H}}_b \in \mathbb{C}^{2\times 2}$ are the estimated channels by the receivers, $\widetilde{\mathbf{E}}_a \in \mathbb{C}^{2\times 2}$ and $\widetilde{\mathbf{E}}_b \in \mathbb{C}^{2\times 2}$, $\mathcal{CN}(0,1)$ are the error matrices with all independent complex coefficients drawn from a random Gaussian distribution with zero mean and unit variance, they are independent of $\mathbf{H}_a$ and $\mathbf{H}_b$ respectively for UE a and UE b, ϱ represents the uncertainty factor which lies between $0 \leq \varrho < 1$. When $\varrho = 0$, the transmitter has the same channel knowledge as the receiver. In a real network ϱ can account for the errors due to the limited feedback as well as the feedback delays. We assume that with the ICI information fed back

by the UE is also perturbed with the same uncertainty factor. With this assumption, we can write the imperfect ICI information at the transmitter as follows:

$$\widehat{\mathbf{q}}_a = \frac{1}{\sqrt{1-\varrho^2}}\widetilde{\mathbf{q}}_a + \frac{\varrho}{\sqrt{1-\varrho^2}}\widetilde{\mathbf{e}}_a \tag{5.27}$$

$$\widehat{\mathbf{q}}_b = \frac{1}{\sqrt{1-\varrho^2}}\widetilde{\mathbf{q}}_b + \frac{\varrho}{\sqrt{1-\varrho^2}}\widetilde{\mathbf{e}}_b \tag{5.28}$$

Where, $\widehat{\mathbf{q}}_a \in \mathbb{C}^{2\times 1}$ and $\widehat{\mathbf{q}}_b \in \mathbb{C}^{2\times 1}$, represent the uncertain ICI information at the transmitter such that $||\widehat{\mathbf{q}}_a|| = ||\widehat{\mathbf{q}}_b|| = 1$, $\widetilde{\mathbf{q}}_a \in \mathbb{C}^{2\times 1}$ and $\widetilde{\mathbf{q}}_b \in \mathbb{C}^{2\times 1}$ are the estimated ICI vectors by the receivers, $\widetilde{\mathbf{e}}_a \in \mathbb{C}^{2\times 1}$ and $\widetilde{\mathbf{e}}_b \in \mathbb{C}^{2\times 1}$, $\mathcal{CN}(0,1)$ are the error vectors with all independent complex coefficients drawn from a random Gaussian distribution with zero mean and unit variance, they are independent of $\mathbf{q}_a$ and $\mathbf{q}_b$ respectively for UE a and UE b. The precoding vectors for UEs a and b designed by the transmitter in time t can be written as:

$$\mathbf{p}_a(t) = \frac{1}{\widehat{\gamma}_a}\widehat{\mathbf{H}}_b^{-1}(t)\widehat{\mathbf{q}}_b(t-1)$$
$$\mathbf{p}_b(t) = \frac{1}{\widehat{\gamma}_b}\widehat{\mathbf{H}}_a^{-1}(t)\widehat{\mathbf{q}}_a(t-1)$$

where, $\widehat{\gamma}_a = ||\widehat{\mathbf{H}}_b^{-1}(t)\widehat{\mathbf{q}}_b(t-1)||_2$ and $\widehat{\gamma}_b = ||\widehat{\mathbf{H}}_a^{-1}(t)\widehat{\mathbf{q}}_a(t-1)||_2$. With the help of above precoding vectors we can re-write the signal $\mathbf{y}_a(t) \in \mathbb{C}^{2\times 1}$ received by UE a in time t similar to equation (5.22) as:

$$\begin{aligned}\mathbf{y}_a(t) = &\frac{1}{\widehat{\gamma}_a}\mathbf{H}_a(t)\{\widehat{\mathbf{H}}_b^{-1}(t)\widehat{\mathbf{q}}_b(t-1)\}s_a + \\ &\frac{1}{\widehat{\gamma}_b}\mathbf{H}_a(t)\{\widehat{\mathbf{H}}_a^{-1}(t)\widehat{\mathbf{q}}_a(t-1)\}s_b + \sqrt{\lambda_a}\mathbf{q}_a(t) + \mathbf{n}_a\end{aligned} \tag{5.29}$$

For simplification we drop the time index in the following and let $\kappa = \frac{1}{\sqrt{1-\varrho^2}}$ and $\omega = \frac{\varrho}{\sqrt{1-\varrho^2}}$. Substituting (5.25) and (5.26) in (5.29) we get:

$$\begin{aligned}\mathbf{y}_a &= \frac{1}{\widehat{\gamma}_a}\mathbf{H}_a\{\kappa\widetilde{\mathbf{H}}_b + \omega\widetilde{\mathbf{E}}_b\}^{-1}\widehat{\mathbf{q}}_b^{'}s_a + \frac{1}{\widehat{\gamma}_b}\mathbf{H}_a\{\kappa\widetilde{\mathbf{H}}_a + \omega\widetilde{\mathbf{E}}_a\}^{-1}\widehat{\mathbf{q}}_a^{'}s_b + \sqrt{\lambda_a}\mathbf{q}_a + \mathbf{n}_a \\ &= \frac{1}{\kappa\widehat{\gamma}_a}\mathbf{H}_a\{\widetilde{\mathbf{H}}_b + \frac{\omega}{\kappa}\widetilde{\mathbf{E}}_b\}^{-1}\widehat{\mathbf{q}}_b^{'}s_a + \frac{1}{\kappa\widehat{\gamma}_b}\mathbf{H}_a\{\widetilde{\mathbf{H}}_a + \frac{\omega}{\kappa}\widetilde{\mathbf{E}}_a\}^{-1}\widehat{\mathbf{q}}_a^{'}s_b + \sqrt{\lambda_a}\mathbf{q}_a + \mathbf{n}_a \\ &= \frac{1}{\kappa\widehat{\gamma}_a}\mathbf{H}_a\{\widetilde{\mathbf{H}}_b + \widehat{\mathbf{E}}_b\}^{-1}\widehat{\mathbf{q}}_b^{'}s_a + \frac{1}{\kappa\widehat{\gamma}_b}\mathbf{H}_a\{\widetilde{\mathbf{H}}_a + \widehat{\mathbf{E}}_a\}^{-1}\widehat{\mathbf{q}}_a^{'}s_b + \sqrt{\lambda_a}\mathbf{q}_a + \mathbf{n}_a\end{aligned} \tag{5.30}$$

$$\mathbf{y}_a = \frac{1}{\kappa\widehat{\gamma}_a}\mathbf{H}_a\widetilde{\mathbf{H}}_b^{-1}\{\mathbf{I} + \widehat{\mathbf{E}}_b\widetilde{\mathbf{H}}_b^{-1}\}^{-1}\widehat{\mathbf{q}}_b^{'}s_a + \frac{1}{\kappa\widehat{\gamma}_b}\mathbf{H}_a\widetilde{\mathbf{H}}_a^{-1}\{\mathbf{I} + \widehat{\mathbf{E}}_a\widetilde{\mathbf{H}}_a^{-1}\}^{-1}\widehat{\mathbf{q}}_a^{'}s_b + \sqrt{\lambda_a}\mathbf{q}_a + \mathbf{n}_a \tag{5.31}$$

Where, $\widehat{\mathbf{E}}_a(t) = \frac{\omega}{\kappa}\widetilde{\mathbf{E}}_a(t)$ and $\widehat{\mathbf{E}}_b(t) = \frac{\omega}{\kappa}\widetilde{\mathbf{E}}_b(t)$. At the receiver, we can project the receive vector on to $\widetilde{\mathbf{q}}_{a_\perp}(t)$ and perform the similar approximation for the inverses as in the previous section. The received signal after the receive processing analogous to equation (5.23) can be written as follows:

$$\begin{aligned} y_a^{'} = & \frac{1}{\kappa\widehat{\gamma_a}}\{\widetilde{\mathbf{q}}_{a_\perp}^H \mathbf{H}_a \widetilde{\mathbf{H}}_b^{-1}\widehat{\mathbf{q}}_b^{'} - \widetilde{\mathbf{q}}_{a_\perp}^H \mathbf{H}_a \widetilde{\mathbf{H}}_b^{-1}\widehat{\mathbf{E}}_b \widetilde{\mathbf{H}}_b^{-1}\widehat{\mathbf{q}}_b^{'}\} s_a \\ & + \frac{1}{\kappa\widehat{\gamma_b}}\{\widetilde{\mathbf{q}}_{a_\perp}^H \mathbf{H}_a \widetilde{\mathbf{H}}_a^{-1}\widehat{\mathbf{q}}_a^{'} - \widetilde{\mathbf{q}}_{a_\perp}^H \mathbf{H}_a \widetilde{\mathbf{H}}_a^{-1}\widehat{\mathbf{E}}_a \widetilde{\mathbf{H}}_a^{-1}\widehat{\mathbf{q}}_a^{'}\} s_b + \sqrt{\lambda_a}\widetilde{\mathbf{q}}_{a_\perp}^H \mathbf{q}_a + \widetilde{\mathbf{q}}_{a_\perp}^H \mathbf{n}_a \end{aligned} \tag{5.32}$$

With unit power transmission, we can write the SINR as in equation (5.24):

$$SINR_a = \frac{|\frac{1}{\kappa\widehat{\gamma_a}}\{\widetilde{\mathbf{q}}_{a_\perp}^H \mathbf{H}_a \widetilde{\mathbf{H}}_b^{-1}\widehat{\mathbf{q}}_b^{'} - \widetilde{\mathbf{q}}_{a_\perp}^H \mathbf{H}_a \widetilde{\mathbf{H}}_b^{-1}\widehat{\mathbf{E}}_b \widetilde{\mathbf{H}}_b^{-1}\widehat{\mathbf{q}}_b^{'}\}|^2}{\frac{1}{\kappa\widehat{\gamma_b}}\{\widetilde{\mathbf{q}}_{a_\perp}^H \mathbf{H}_a \widetilde{\mathbf{H}}_a^{-1}\widehat{\mathbf{q}}_a^{'} - \widetilde{\mathbf{q}}_{a_\perp}^H \mathbf{H}_a \widetilde{\mathbf{H}}_a^{-1}\widehat{\mathbf{E}}_a \widetilde{\mathbf{H}}_a^{-1}\widehat{\mathbf{q}}_a^{'}|^2\} + \lambda_a|\widetilde{\mathbf{q}}_{a_\perp}^H \mathbf{q}_a|^2 + \eta^2} \tag{5.33}$$

Comparing equation (5.33)) with equation (5.24)), we can see that even after the uncertainty of information at the transmitter, the residual ICI remains the same at the receiver. Moreover, notice that when the transmitter has perfect information and the receiver can have perfect estimates of channel and ICI information, the SINR in equation (5.33) will be equal to the ideal SINR in equation (4.20).

5.1.4 Results with Imperfect Information

We consider the system as shown in figure 4.1 for numerical simulations of 5000 channel realizations with Rayleigh fading. The direction of arrival of major component of ICI in two consecutive transmissions is uniformly distributed in the interval $[0, \phi_{max}]$. As described in the previous chapter, we control the *colourdness* of ICI with the help of INR (ζ). Both the UEs have a given input average SINR (μ) and an average INR (ζ). We divide our performance analysis in two steps. In the first step we consider only the channel estimation errors at the receiver and analyse the performance of MUICIA with the approximated SINR from equation (5.18) and with simulations. For step one, we consider the interference minimization (IM) receiver $\mathbf{q}_{a_\perp}^H$. In the second step, with the help of uncertainty model, we consider estimation errors at the receiver (both channel and ICI estimation) and the design of precoding vectors with the imperfect information at the transmitter. In this study we also compare the performance of MUICIA precoding with SLNR precoding. For the fair comparison of precodings, we use IRC algorithm at the receivers as it is optimum for the baseline precoding.

Analysis with Channel Estimation Errros at the Receiver

Figure (5.1) presents the performance of MUICIA for the range of ϕ_{max} which is varying from 0 to 90 degrees. Additionally, we compare the performance with two other schemes which can be seen as an upper bound (OPTIMAL) and a lower bound (LB-Perfect) for the considered system. The OPTIMAL is a hypothetical optimum scheme which transmits equal power to both the UEs in their eigenmodes and perfectly nullify both MUI and ICI. The LB-Perfect also transmits the power in the eiqenmodes but it does not treat the interference power at the receiver rather it simply uses the MRC combiner.

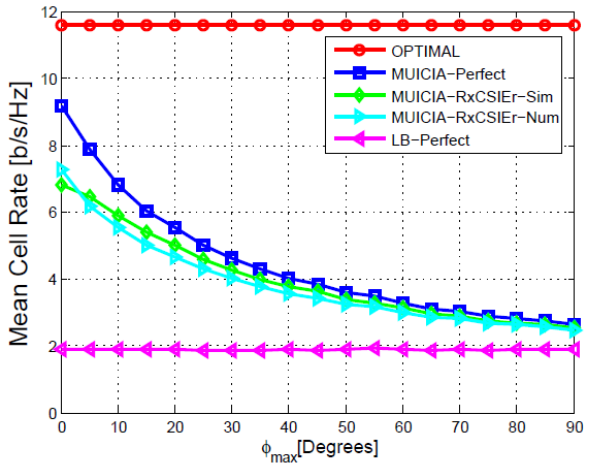

Figure 5.1: Mean cell rate performance over ϕ_{max} for SINR=10 dB, INR=20 dB and T=16

In figure 5.1, when $\phi_{max} = 0$, we observe higher loss in the performance due to channel estimation errors at the receiver. With the increase in ϕ_{max}, the loss due to misalignment is dominant. The performance with numerical approximation is also close to the simulation performance. Figure 5.2(a) shows the performance comparison over SINR. Note that in a real system, the typical SINR values are below 20 dB, we have simulated this range only to find the required SINR which can achieve ideal performance. We can see that the performance increases with the increase in SINR. However, the increase in performance is saturated at very high SINRs even for the perfect system. This is because for a given INR, an increase in SINR causes the decrease in interference which reduces the alignment gains. Notice that the impaired channel performance approaches the perfect performance as the error variance decreases with the increase in SINR. At low SINRs, our approximation is weak therefore the numerical error performance is higher than the simulation results. However, at high SINRs,

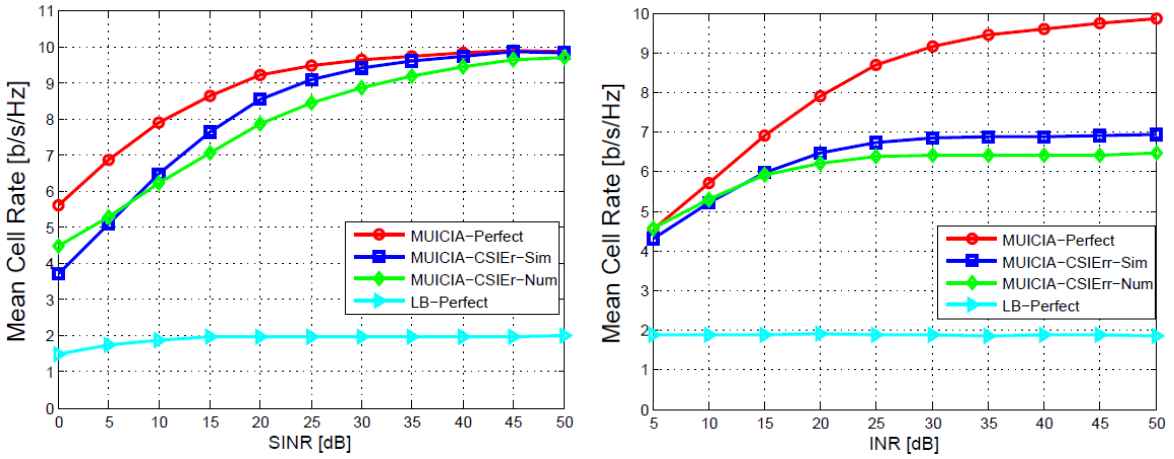

(a) Performance over SINR, INR=20 dB

(b) Performance over INR, SINR=10 dB

Figure 5.2: Mean cell rate performance, ϕ_{max}=5 Degrees and T=16

the numerical performance is below the simulation performance.

Figure 5.2(b) shows the performance comparison over INR. Again note that in a real system, the typical INR values are below 30 dB, we have simulated this range only to find the required INR which can achieve ideal performance. The increase in INR increases the performance due to the increase in the alignment gain. However, the increase in performance is saturated at very high INRs even for the perfect system. As the increase in INR does not decreases the error variance, therefore the impaired channel performance only asymptotically approaches the ideal performance. The numerical approximation overlaps the simulation performance at INR values below 20 dB. However, a little gap is maintained over high INRs.

Figure 5.3 shows the performance comparison over the effective number of pilots that can be used for the estimation of one channel coefficient. Please note that the performance of MUICIA and lower bound with perfect estimation is independent of the number of pilots. In an LTE based 2-by-2 MIMO system, upto 16 pilot symbols (CSRS) are inserted within a PRB for channel estimation as shown in section 2.2. The minimum transmission bandwidth in LTE is *1.25 MHz* which contains 6 PRBs (48 pilot symbols per antenna). For slow time variant and less frequency selective channels, channel estimation algorithms can use multiple PRBs in one transmission time. From figure 5.3 we see that the increase in the number of effective pilots increases the performance. This is because the error variance is decreased with the increase in T. The performance with channel estimation error asymptotically approaches

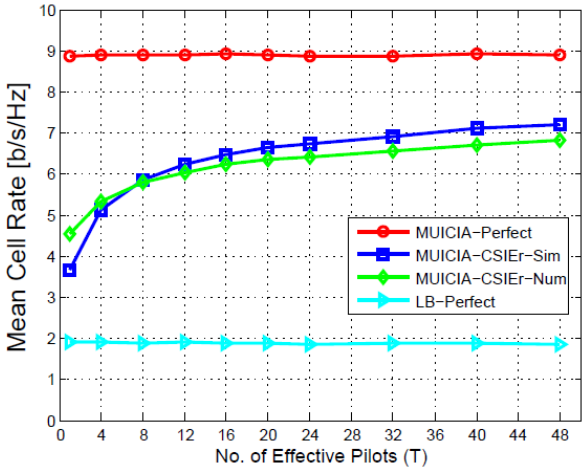

Figure 5.3: Mean cell rate performance over the available pilots for SINR=10 dB, INR=20 dB and ϕ_{max}=5 Degrees

the ideal performance.

Analysis with Imperfect Information at the Transmitter

With the help of simulations, now we consider the estimation errors (both channel and ICI estimation errors) at the receiver as well as the impaired information at the transmitter. At first, we compare the performance of MUICIA with a hypothetical upper bound (OPTIMAL) and a lower bound (LB-Perfect). For this purpose, we use IM receiver. The legend **RxErr** represents the channel and ICI estimation errors only at the receiver. The imperfect information at the transmitter due to the estimation errors and feedback errors is represented by **RxTxErr**.

Figure 5.4 presents the performance of MUICIA for the range of ϕ_{max}. For the case of RxTxErr, the uncertainty factor $\varrho = 0.1$. We can see an additional loss of performance with impaired information at the transmitter. We observe that for higher values of ϕ_{max} the loss due to the misalignment is dominant and the impaired performance approaches the ideal lower bound performance.

Now for the other system parameters, we compare the performance of MUICIA with the performance of SLNR. For onward comparisons, we use the IRC receiver for all the precdoing schemes(as IRC is a better receiver for the baselines precoding SLNR, so it is fair to use IRC for all the precoding schemes). Figure 5.5(a) presents the performance comparison over the uncertainty factor ϱ. For lower values of ϱ, the impaired MUICIA performance is even

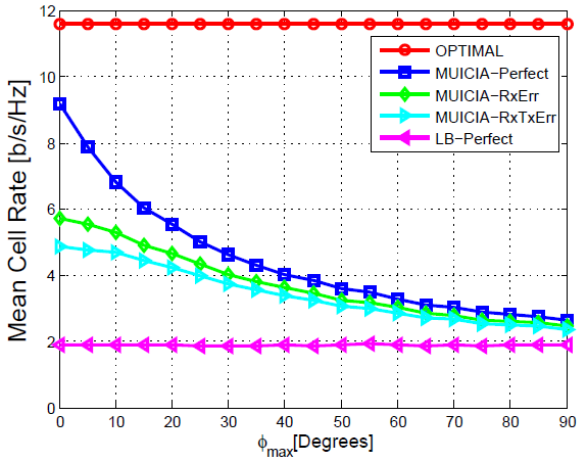

Figure 5.4: Performance of MUICIA, SINR=10 dB, INR=20 dB, $\varrho = 0.1$ and T=16

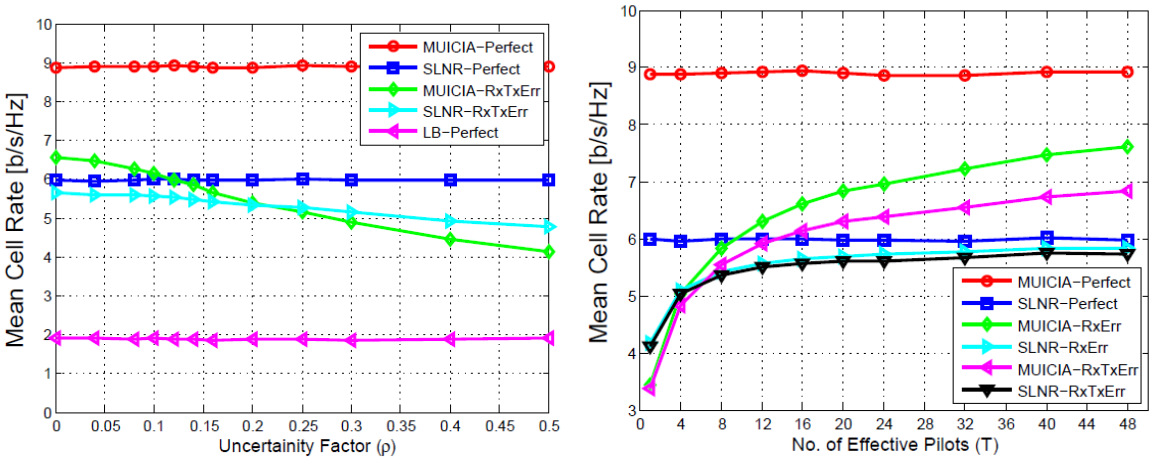

(a) Performance over uncertainty ϱ, T=16 dB

(b) Performance over T, ϱ=0.1 dB

Figure 5.5: Performance comparison of all precodings with IRC receiver, SINR=10 dB, INR=20 dB and ϕ_{max}=5 Degrees

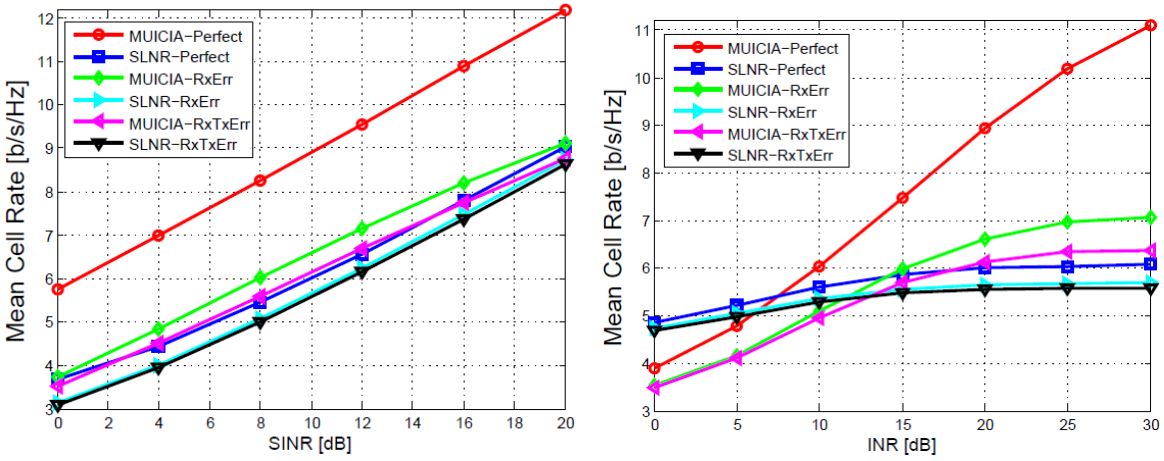

(a) Performance over SINR, INR=20 dB

(b) Performance over INR, SINR=10 dB

Figure 5.6: Performance comparison of all precodings with IRC receiver, ϕ_{max}=5 Degrees, T=16 and ϱ=0.1

better than the ideal SLNR performance. However, if the uncertainty is very high, the SLNR outperforms MUICIA.

Figure 5.5(b) presents the performance comparison over the number of available pilots. Notice that there is almost no gap in the performance of SLNR with and without impaired information at the transmitter. For less than four pilots, SLNR outperforms the MUICIA. It shows that SLNR is robust to estimation errors as compared to MUICIA. However, for more than eight pilots, MUICIA is over SLNR. It implies that, slow moving UEs can use higher number of pilots for estimation and thus MUICIA is a better choice in this case.

Figure 5.6(a) presents the performance comparison over SINR. Notice that MUICIA suffers a huge loss in the performance due to the impairments over the whole range of SINR. The percentage loss in the performance of MUICIA is higher than SLNR. Both schemes asymptotically approach the ideal performance. With $T = 16$ (two consecutive PRBs can be used for estimation), even with impaired information, MUICIA outperforms SLNR.

Figure 5.6(b) presents the performance comparison over INR. For INR below 10 dB, SLNR outperforms even the ideal MUICIA. However, for higher INR values, MUICIA outperforms the SLNR. It is clear because the alignment gains are higher when the interference is dominant. In a co-channel heterogeneous scenario, where the users of low power pico cells are facing strong macro interference, we expect higher values of INR.

An overall observation about the performance with impaired information is that MUICIA has a very high percentage loss in the performance as compared to the SLNR. The simulation results show that the SLNR based precoding is very robust with respect to the practical constraints. However, for some conditions, for example with slow time and frequency variant channels, MUICIA with practical constraints is even better than ideal SLNR performance.

5.2 Performance with Limited Feedback

In closed loop systems, the term *Limited Feedback* is used to express the constraint that only a limited system resources can be used to provide the feedback information. In FDD based downlink transmission, very limited uplink resources are available to provide the feedback. Using the limited resources, perfect information cannot be fed back to the transmitter. Due to this reason, all the closed loop schemes suffer loss in the performance if the feedback is limited. In the previous section we have already performed initial analysis using the uncertainty based feedback imperfection model. Here we extend the analysis where we consider the practical system with practical feedback methods.

In general, the feedback information required for the closed loop transmission consists of complex coefficients. Vector quantization is one of the method which is used to quantize this information. The UE quantizes the feedback information with respect to the vector codebooks which are known to both the UE and the serving cell. The UE sends only the index of the quantized vector. The performance of the transmission mainly depends upon the size of the codebook (number of bits), number of coefficients, average SINR of UE, feedback rate and the sensitivity of the precoding to quantization errors. The design of the codebooks also impacts the performance. A detailed explanation of the terms and methods over limited feedback and different types of feedback information is given in [76].

We consider two types of feedback frameworks. One is based on Random Vector Quantization (RVQ) [77] where the codebooks are generated randomly for each link. The other framework exploits the channel properties to design the codebooks. It is known as *Hierarchical Codebook Design*. Many studies have shown that for slow time variant channels the hierarchical codebook framework is more effective in terms of reducing the feedback load computational complexity. We consider the hierarchical design proposed in [78] for our analysis.

The major goal of our contribution is to evaluate the feasibility of MUICIA in limited feedback systems. We accomplish this goal by the evaluation of the performance of MUICIA and also by the comparison of this performance with a state of the art transmit precoding. This precoding is based on effective zero-forcing [61] as described in the previous chapter. With the help of system simulations, at first we use the RVQ and evaluate the performance for the number of bits available for feedback and for the given input average SINR of the UEs. We further apply the hierarchical codebook design and show the enhancements in the performance over RVQ. Moreover, we also analyse the effects of parameters specific to the hierarchical codebook design and provide a proposal for the choice of these parameters. Our results indicate that with a reasonable feedback load, better performance can be achieved with MUICIA in practical systems. Here we report only the selective results. For the detailed assessment of performance we refer to our publication [24] and the master thesis report [79].

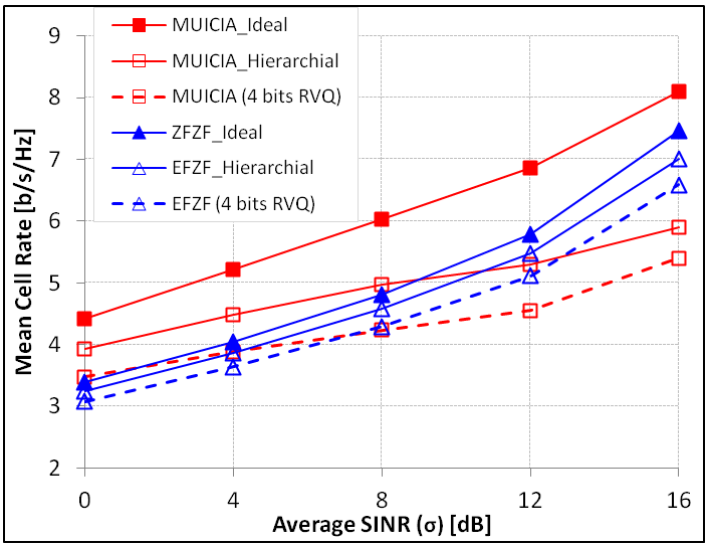

Figure 5.7: Performance comparison of MUICIA and EFZF with limited feedback based on RVQ (4 bits) and Hierarchical codebook design. For hierarchical codebook, Refresh Time = 5ms, B1=4 bits and B2=3 bits

In figure 5.7 we consider an area covered with three cells arranged in a tri-sector manner where the UEs are dropped according to the given user geometry (input average SINR represented by σ) which is plotted on the x-axis. Figure 5.7 presents performance comparison of MUICIA with EFZF. In ideal case, MUICIA completely outperforms EFZF. With hierarchical codebooks, MUICIA outperforms EFZF until $\sigma = 10dB$. In this case, the performance of

MUICIA with limited feedback is even better than the ideal performance of EFZF. However, with RVQ, EFZF mostly outperforms MUICIA. However, MUICIA s still better than EFZF in ICI-limited region. This is because of the loss in alignment gains due to the imperfect feedback. This indicates that with limited feedback, MUICIA can be used for the UEs which are facing strong ICI. We also observe that the hierarchical codebook design is beneficial for both transmit precoding schemes, in particular for MUICIA. Moreover, MUICIA provides sustainable gains as compared to EFZF if high and moderate amount of feedback resources is available. However, if the feedback resources are sparse, then EFZF outperforms MUICIA. This implies that in urban and dense urban scenarios where the users have low mobility profile and higher downlink data demand we can use MUICIA.

5.3 Performance with Measured Channels

Until now we have evaluated the performance of systems analytically or with simulations. In this section, we use the measured channels for the evaluation of multi user multi cell system. For this purpose, we use our proprietary software-defined wireless measurement test-bed. The measurement test-bed utilizes OFDM based radio air-interface. Following are the objectives that we target in this section.

- Proof of concept for MUICIA.
- Assessment of MUICIA with suitable training overhead.
- Impact of reduced training overhead on the performance.

5.3.1 Technical Description for the Measurement Platform

Our measurement test-bed consists of a combination of hardware and software modules. A transmission site is constructed with the help of three transmit antenna arrays as shown in figure 5.8. Each array consists of two antenna elements which are horizontally polarized. The antenna hardware is fed with the help of a Remote Radio Head (RRH) which is connected with a proprietary eNB emulator. Each cell is serving two multiple antenna UEs. Each UE has a cross polarized patch antenna array. The performance results are evaluated only for *cell b* (marked as grey in figure 5.8) therefore, we focus on the UEs served by *cell b* and refer to them as test-UEs. The antennas of test-UEs are receiving signals from their serving cell which is *cell b* and also the signals from the interfering cells which are *cell a* and *cell c*. The

impact of transmit precoding and interference from the interfering cells is considered with the help of the software platform.

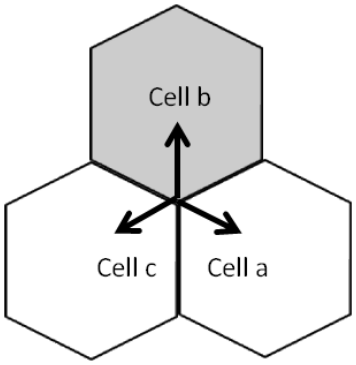

Figure 5.8: A site with three co-located sectorized antennas, cell b is serving cell whereas cell a and c are interferers

Figure 5.9 shows the complete measurement platform. The measurement platform is operated with the help of a control computer which hosts the software defined wireless platform. It is used to take parameter settings as input and to display performance graphs as output. In each working cycle (iteration/transmission), training pilots are encapsulated in a downlink transmission frame of $10ms$ duration. The frame is configured by the transmit processing module in the software which is shown as a sub-block in figure 5.9. The configured frame is OFDM-modulated and transmitted in the air with the help of an eNB emulator and the RRH. The hardware of UEs receive the frame and forward it to the software for further receive processing as shown in figure 5.9. The transmit processing block and the receive processing block are further described in the following subsections.

5.3.2 Precoding in Interfering Cells

The interfering cells are also transmitting the training symbols which are used by the test-UEs to estimate the interfering channels. In practice, the ICI experienced by a UE varies due to a number of factors. In order to clearly understand the impact of precoding in interfering cells on the temporal variations in ICI and on the alignment for a given frequency sub carrier, we model the precoding vectors in interfering cells as follows:

$$\mathbf{p}_{mh}(t) = \cos\phi(t)\mathbf{p}_{mh}(t-1) + \sin\phi(t)\mathbf{p}_{mh_{\perp}}(t-1) \tag{5.34}$$

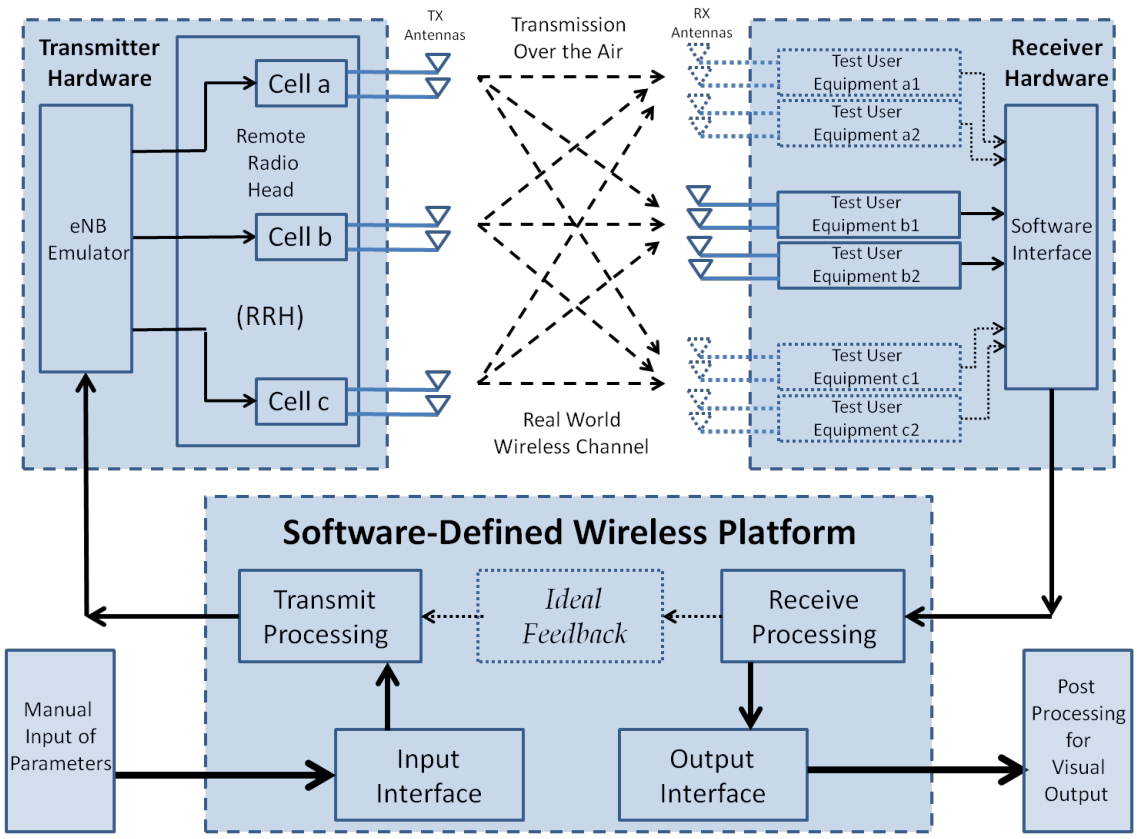

Figure 5.9: Block diagram for the measurement test-bed

Where, m represents the UE index and $h = \{a, c\}$ represents the cell index, t represents the time index for the transmission frame, $\phi(t)$ is the random phase distributed uniformly between $[0, \phi_{max}]$, $\mathbf{p}_{mh}(t) \in \mathbb{C}^{M\times 1}$ is the precoding vector in time t, $\mathbf{p}_{mh_\perp}(t-1) \in \mathbb{C}^{M\times 1}$ is the vector orthogonal to $\mathbf{p}_{mh}(t-1)$. Different levels of ICI variations can be model with the help of ϕ_{max}. In the following, we provide details over the variation levels for ICI.

Time In-Variant(TIV) ICI: This is the case where random precoding vectors are generated for each interfering UE and the same vectors are used for all the transmission frames at a given measurement position. We consider this case for the purpose of best performance comparison only.

Low Time Variant ICI (LTV): In this case, the precoding vectors are updated in every transmission with the help of equation (5.34). For slow temporal variations, we select the value of ϕ_{max}=5°. It implies that the random precoding vectors are varying between 0 to 5° in each consecutive transmission at a given measurement position.

Medium Time Variant ICI (MTV): For medium temporal variations in ICI, ϕ_{max}=15°.

High Time Variant ICI (HTV): For high variations in ICI, ϕ_{max}=30°.

Random ICI (RAND): In this case, the precoding vectors for each interfering UE are selected in each transmission from a uniform random distribution (i.e. $\mathbf{p}_{mh}(t)$ and $\mathbf{p}_{mh}(t-1)$ are totally independent). It represents the worst case precoding.

5.3.3 Transmit Processing

As shown in figure 5.9, the transmit processing block mainly generates the transmission frame that is to be transmitted in the air. Each cell transmits the training symbols which are embedded in a TDD based transmission frame. The length of the frame is similar to the LTE frame which is 10 ms. The TDD structure of the frame is also similar to one of the LTE-TDD frame type. Please refer to *configuration 1* in the *uplink-downlink configuration Table 4.2-2* in [38]. The symbol structure within the frame is proprietary. One frame consists of synchronisation symbols, training symbols and data symbols. As we do not use data for evaluation so the data symbols are empty. The TDD frame is divided into two downlink and two uplink periods. We have used only one downlink period for the transmission. There is no transmission in the uplink period. The frame structure is shown in figure 5.10.

The synchronization symbols and the training symbols (pilots) are based on Constant Amplitude Zero Auto-Correlation Waveforms (CAZAC) sequences. Each transmit antenna sends the pilots in a given symbol time. To differentiate the transmit antennas, different

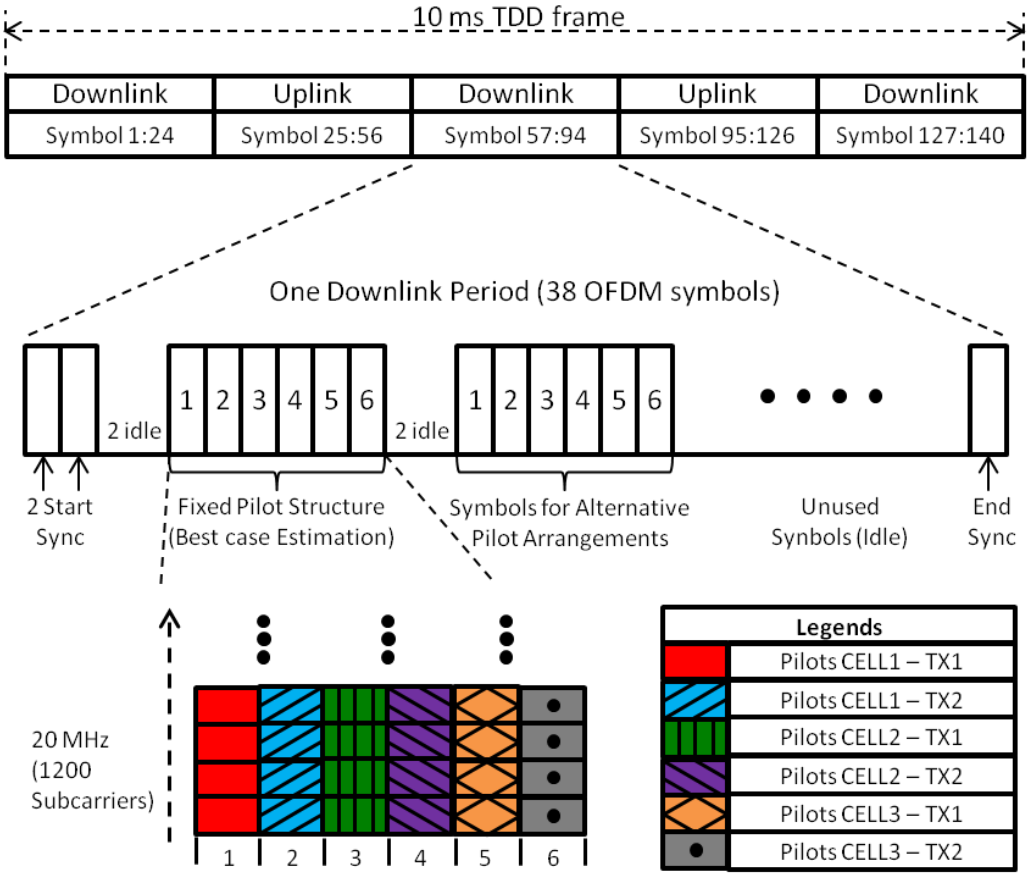

Figure 5.10: Frame Structure

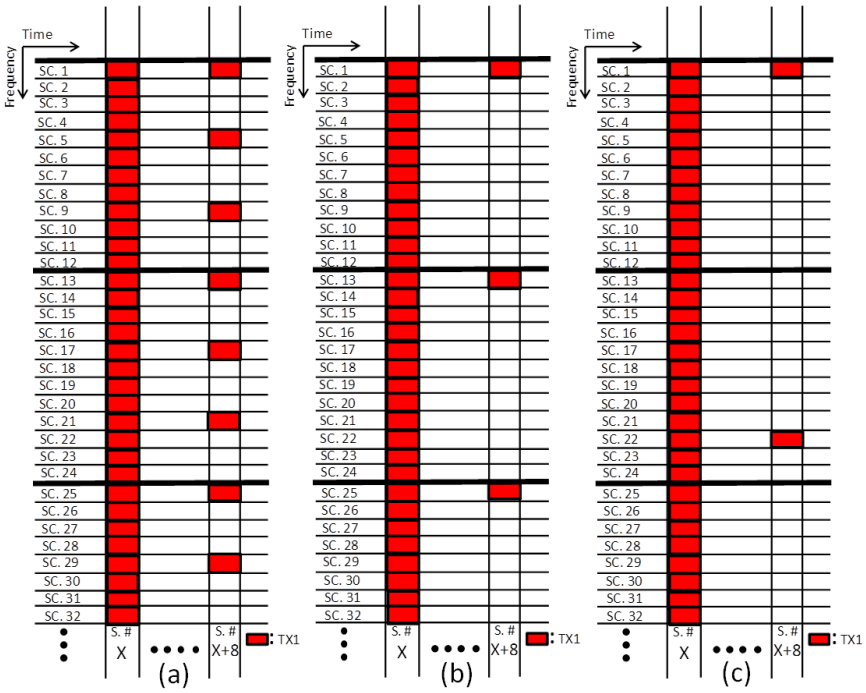

Figure 5.11: Pilot Arrangements

symbols are used for each antenna. Figure 5.10 shows the pilot placement in the transmission frame. The transmission bandwidth which is *20 MHz* is divided into equally spaced sub carriers. For the purpose of analysis, two sets of symbols in the same downlink period are used for the transmission of pilots. Both sets are shown in the frame structure figure 5.10 for a single subcarrier. The first set has a basic pilot spacing where pilots are transmitted on every sub carrier. We assume that the channels estimated from this set are almost ideal. These estimates are used as reference for the performance evaluation. The second set can be used for any other spacing of pilots. We have assess the performance with three different pilot spacings. For *cell b* these pilot spacings are shown in figure 5.11.

Pilot Every 4th Sub Carrier (PS04): The first arrangement can be seen in figure 5.11(a), here we have pilots on every 4th sub carrier.

Pilot Every 12th Sub Carrier (PS12): The second arrangement has pilots every *12th* sub carrier as shown in figure 5.11(b). One PRB in LTE contains 12 sub carriers. This arrangement represents one pilot over the total sub carriers in a PRB.

Pilot Every 21st Sub Carrier (PS21): A complete PRB contains *12* x *14* OFDM resource elements and for 2-Tx antennas there are 8 pilots per antenna per PRB. It implies that

we have one pilot per antenna over *21* resource elements in a PRB. The third arrangement in figure 5.11(c) represents this case where we have a pilot every *21st* sub carrier.

The sub carrier spacing and the OFDM symbol generation follows the LTE specifications [38]. Salient OFDM related parameters are given in the table 5.1.

System Parameters	Values
Carrier Frequency	2.6 GHz
Transmission Bandwidth	20 MHz
Subcarrier Spacing	15 kHz
Useful Symbol Duration	$\sim$ 66.67 μ s
FFT size	2048
Sampling Frequency	30.72 MHz
Long Cyclic Prefix	160 samples
Short Cyclic Prefix	144 samples

Table 5.1: OFDM system parameters.

5.3.4 Receive Processing

The signals received by the test-UE hardware are supplied to the receive processing module shown in figure 5.9. The receiver processing is done in two stages. The first stage estimates the channel and the second stage uses the estimated channels to compute further information for performance evaluation. The channel estimation stage is done in three steps which are explained below in this section.

Synchronization: In practice, synchronization symbols are used for frame synchronization. We have not used the frame synchronization symbols and rather used the common clock generator for the transmitter and receiver equipment which is affordable in an indoor measurement test-bed. However, we have used synchronization symbols for downlink period synchronization with in the frame.

Frequency Offset Corrections: After the timing synchronization, synchronization of the carrier frequency is required to avoid any inter carrier interference. With the help of cyclic prefix, we estimate the frequency offset and perform correction as given in [80].

Channel Estimation: The channels are estimated with the help of pilot symbols. The receiver is already aware of the training sequences. As the pilots are orthogonal in time, we estimate the channel coefficients separately for each TX-RX link. Let $h_{(u,v)i}$ be the channel

coefficient between the uth antenna element of test-UE i and the vth antenna element of cell i. Let $x_{(v)i}$ be the transmitted training symbol and $y_{(u)i}$ be the received signal which is given by:

$$y_{(u)i} = h_{(u,v)i}x_{(v)i} + n_{(u)i} \tag{5.35}$$

Where, $n_{(u)i}$ is the noise at the uth receive antenna element. As $x_{(v)i}$ is known to the receiver, we can write the estimated channel coefficient $\tilde{h}_{(u,v)i}$ in the following form:

$$\tilde{h}_{(u,v)i} = h_{(u,v)i} + \frac{n_{(u)i}}{x_{(v)i}} \tag{5.36}$$

The estimated coefficients are used for further processing as explained in the next section.

Performance Evaluation: The precoding vectors and the receiver vectors are computed for each OFDM time-frequency resource element using the estimated channels for a given pilot arrangement in the second set of training symbols as shown in figure 5.11. With the help of the perfect channels estimated from the first set of pilots, we compute the output SINR for each resource element using equation (4.50). Please note that the performance is evaluated only for *cell b* which is using MUICIA (or baseline precodings) as transmit precoding. This SINR is used to compute the capacity with the help of SINR to Shannon rate mapping.

5.3.5 Measurement Scenarios

Here we consider two scenarios with a 3-Cell arrangement. Figure 5.12(a) shows the layout of the cells on the measurement grid. We refer to our publication [25] and the master thesis project [81] for further measurement results with limited feedback, user mobility and different cellular arrangements.

Measurement Scenario 1: In this scenario, channel measurements are taken with one UE fixed at one position of the grid, while the measurements for the other UE are taken at each given position of the grid (1000 iterations of measurement per position).

Measurement Scenario 2: In this scenario, measurements are taken on certain positions on the gird. The positions are selected such that both the UEs have same average SINR for one set of measurements (1000 iterations of measurements with both UEs at two different particular positions corresponding to same average SINR values).

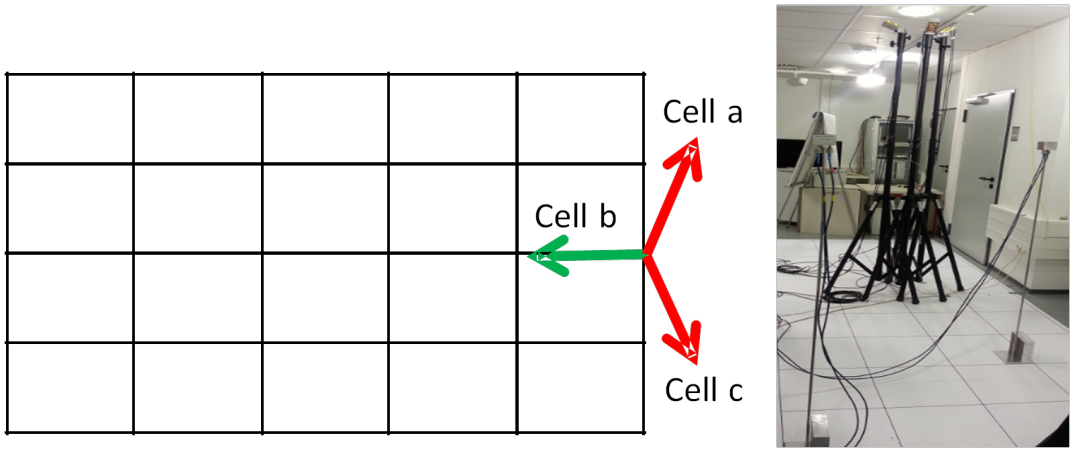

(a) Placement of BSs on measurement grid, arrows represent the bore-sight directions of transmit arrays

(b) Real world picture of the transmitters and the grid

Figure 5.12: Schematic and real view of the measurement grid

5.3.6 Measurement Results and Anaylsis

The assessments of the results is performed with three objectives. The first objective is the proof of concept for MUICIA and to show that partial and outdated ICI is still useful. The second is to compare the performance of MUICIA with other non-alignment based baseline precodings. The third objective is to assess the performance with reduced training overhead.

Proof of Concept: At first we evaluate the impact of variation in ICI on the statistical characteristics of the *Hermitian Angle* between the eigenvectors corresponding to the maximum eigenvalue of ICI covariance matrix in two consecutive transmissions. We have discussed these characteristics in section 4.3. Figure 5.13(a) presents the CDF curves of the angle based on 5000 measurement samples for a resource element allocated to a UE placed on a random position in the measurement grid. Different graphs in the figure represent different levels of variations of ICI which are modelled with the help of precoding vectors as explained in the subsection 5.3.2. We can see that for randomly selected precoding vectors in each transmission (RAND), the variation in ICI is very high and the span of angle is very large. The case of HTV is very close to RAND. These results are in line with the simulation results presented in section 4.3.

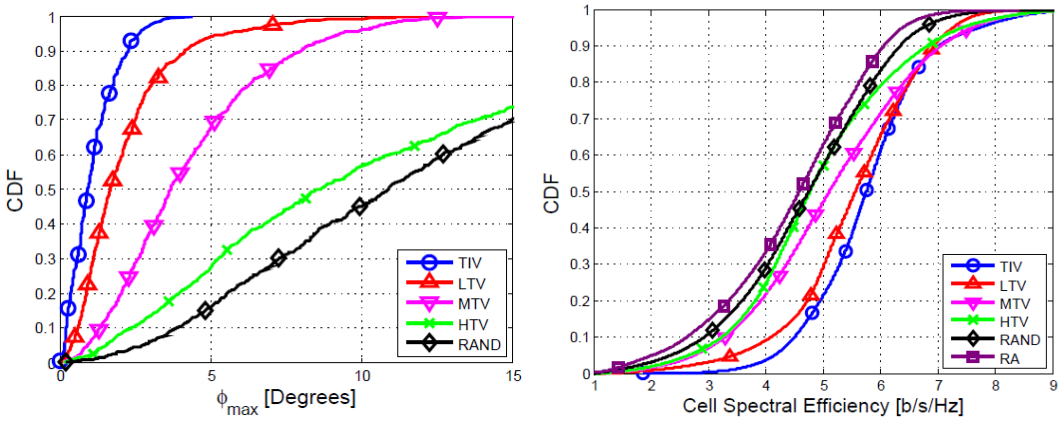

(a) The CDF of Hermitian Angle (4.25) for a re- source element at some measurement position on the grid.

(b) Performance with cell spectral efficiency. RA represents alignment with any random vector.

Figure 5.13: Proof of concept for the use of partial and outdated ICI. Note that the markers are used only to differentiate the curves. They do not represent the measurement samples.

Further to the proof of concept, now we evaluate the impact of different levels of ICI variations on the performance of MUICIA precoding which aligns partial and outdated ICI with MUI. For comparison, we have also considered a scheme which aligns the MUI with any randomly generated vector (totally uncorrelated with ICI). We call it *Random Alignment* (RA). Figure 5.13(b) shows the CDF of cell spectral efficiency for the positions of the UEs on the measurement grid corresponding to average SINR of *1 dB* and *5 dB* respectively for the two UEs. At first notice that, performance with RAND (highly time variant ICI) is still better than RA throughout the CDF. This proves that alignment with the partial and outdated ICI vector is better even when ICI is highly time variant. From left to right in the figure performance increases when the variation in ICI decreases. Highly varying ICI causes the losses due to misalignment. If we compare the worst (RA) and the best (TIV) case then a performance gain on different percentile of CDF is $\{(\%percentile, \%gain), (10, 80), (50, 26), (90, 16)\}$.

Performance Comparison: In order to justify the alignment and use of partial and outdated ICI, we compare the performance of MUICIA with other non-alignment based multi-user transmit precodings which only deal with the MUI. Figure 5.14 presents the performance comparison of MUICIA in two scenarios with the pilot spacing of *4* sub carriers. As given in measurement scenario 1, one of the UEs is fixed at a grid position corresponding to an average SINR of *7 dB*, while the other UE is placed at all the positions of measurement grid (in an

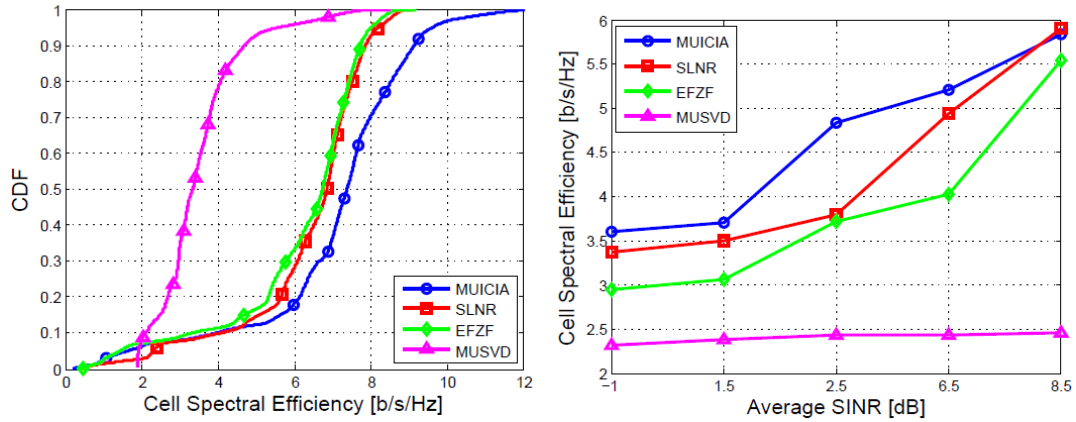

(a) Performance comparison in scenario 1.

(b) Performance comparison in scenario 2.

Figure 5.14: Performance comparison of MUICIA with other baselines, $\phi_{max} = 5$. Note that the markers are used only to differentiate the curves. They do not represent the measurement samples.

average SINR range of *[0,13]* dB). The CDF in figure 5.14(a) is composed of the cell spectral efficiency samples of all the frequency sub carriers for all the iterations of measurements for all the positions in the grid. The results show that until *10th percentile* of the CDF, the performance of all the schemes is almost overlapping. However, above the *10th percentile*, MUICIA outperforms all the other precoding schemes.

Now we consider the measurement scenario 2 where both UEs are placed in the grid such that they have the same average SINR. Figure 5.14(b) presents the mean cell spectral efficiency over the average SINR of the UEs. Notice that these results are clearly in-line with the simulation results shown in figure 4.9(a) in subsection 4.7.2. The impact of ICI reduces with the increase in average SINR and therefore, performance of SLNR approaches to MUICIA.

Impact of Training Overhead: Previous results have shown that SLNR is the best baseline, therefore for better display of the graphs, in this performance analysis we compare MUICIA only with SLNR. The measurements with different training overheads (*different number of total pilots per symbol*) are performed for different positions of the two UEs. One UE is positioned in the grid such that the range of SINR is *[1.6,6]* dB and the other UE is placed such that the range is *[-2,6]* dB. Both the UEs are static for one set of measurement at their respective positions in the grid. Each CDF graph in figure 5.15 is composed of

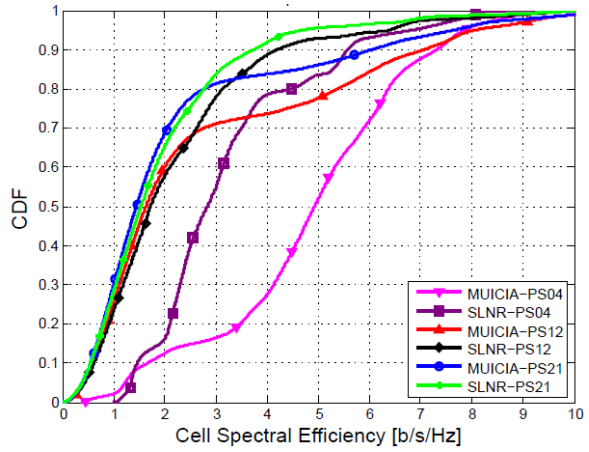

Figure 5.15: Performance comparison with different pilot spacings. Note that the markers are used only to differentiate the curves. They do not represent the measurement samples. $\phi_{max} = 5$

the cell spectral efficiency samples of all the frequency sub carriers for all the iterations of measurements for all the selected positions in the grid. The decrease in training overhead

Pilot Spacing		**4th SC**	**12th SC**	**21st SC**
Mean Cell Rate[b/s/Hz]	***MUICIA***	5.68	2.28	1.76
	SLNR	3.24	1.82	1.52

Table 5.2: Impact of reduced training overhead on overall mean cell rate.

(increase in pilot spacing) increases the error in channel estimation. Therefore, we can see that the performance of both the schemes decreases with the reduction in the pilots. However, we see that the percentage loss in the performance of MUICIA is higher than the SLNR. This is because MUICIA is dependent upon the estimated channels from not just the serving cell (as is the case with SLNR) but also on the channels from the interfering cells.

Now we focus on the comparison of the two schemes with the same pilot spacing. In figure 5.15 with PS04, there is a performance overlap till *10th percentile* and after that MUICIA outperforms SLNR. This overlap region extends till *70th percentile* with PS12 and after that MUICIA is better than SLNR. With PS21, the two schemes overlap till *80th percentile* and then MUICIA delivers better results. The table 5.2 lists the overall mean cell performance of both MUICIA and SLNR with different training overheads. Although the percentage gain of MUICIA falls with increase in pilot spacing, it still shows a relatively higher mean cell performance than SLNR.

5.4 Conclusion

In this chapter, we have considered the practical system constraints in three different ways. In the first step, we have evaluated the impact of estimation errors at the receiver and the impact of the imperfect information at the transmitter on the performance of MUICIA and other baselines. The results show that MUICIA is sensitive to the imperfect information. However, even with practical constraints MUICIA outperforms other baselines with proper selection of parameters. In the second step, we have considered the limited feedback model with two different codebook designs (RVQ and hierarchical). The results show that hierarchical design is better for both the transmit precoding schemes. Moreover, in high ICI regions, MUICIA outperforms the baseline even with only *4 bits* feedback. The third step is based on the measurements where we evaluate the performance with real measured channels. At first we prove that the partial and outdated ICI is still useful for precoding design. Then we show that even with reduced training overhead, MUICIA outperforms the baselines.

Chapter 6

Performance of Un-Coordinated Alignment in Heterogeneous Networks

In this chapter, we consider the application of the multi user inter cell interference alignment scheme in a Heterogeneous Network (HetNet). We consider 3GPP based HetNet architecture and show the potential gains of interference alignment over other precoding schemes. The state of the art interference management techniques in HetNet are based on interference coordination between the cells, in time or frequency domain. We compare the performance of interference alignment with interference coordination and show that sustainable gains can be achieved with alignment.

6.1 Introduction

The exponential growth in the demand of wireless capacity urges the network operators to deploy additional access nodes. The decrease in cell size and increase in cell density enhances the capacity. Therefore, for the purpose of capacity, the new nodes are deployed to cover small but dense traffic areas. They operate with a range of transmit power which is very low as compared to the macro cells *macros*. Hence, these low power nodes are known as small cells or pico cells *picos*. The pico cells are overlaid on the well planned Homogeneous Macro Network (HomoNet). This new blend of already existing coverage infrastructure and the additional pico cells governs the name of Heterogeneous Network (HetNet). One example

deployment is shown in figure 6.1.

The overall situation in a co-channel HetNet deployment scenario is that on one hand, we insert resources (bandwidth and equipment) by deploying additional pico cells and expect to get manifold gains in the network capacity. On the other hand, additional picos also bring extra inter cell interference (ICI) in the network which may limit the achievable expected performance. Moreover, the users served by the low-power pico cells also experience ICI by high-power macros. Especially, the cell-edge users of pico suffer very high ICI due to macro transmissions.

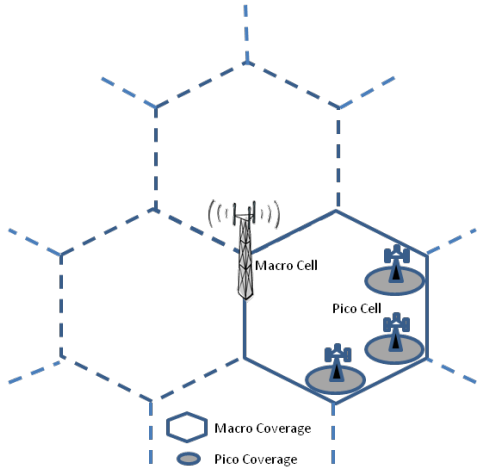

Figure 6.1: Deployment of co-channel pico cells in a macro coverage area

Enhanced interference coordination (eICIC) mechanisms in time and frequency domains have been proposed to overcome the problem of ICI [82]. One example is time domain interference coordination which is also known as *Almost Blank Subframe* (ABS). The main advantage of eICIC mechanisms is that they provide a solution to the ICI problem. However, the disadvantage is that they restrict the resource utilization in the network and require coordination between the cells through backhaul.

Interference Alignment (IA) as proposed in [5] is one of the techniques to deal with ICI in HomoNets. There are other studies in literature that have extended the idea of IA to HetNets. However, the solutions proposed by these studies also require coordination between the cells for the channel information exchange and the design of transmit precoding matrices. Unlike these contributions on interference alignment, in chapter 4, we have proposed an *uncoordinated* transmit precoding scheme based on interference alignment which manages

both the Multi User Interference (MUI) and the ICI in a HomoNet. We referred to it as Multi User Inter Cell Interference Alignment (MUICIA) in the previous chapters.

In this chapter, we extend our work by the application of MUICIA in HetNet with manifold objectives . We put up the following open questions as a formulation of our objectives.

1. What is the impact of transmit power heterogeneity on the performance of MUICIA?
2. What are the comparative performance gains of different user selection methods with MUICIA when we deploy additional picos?
3. How does uncoordinated MUICIA behave in comparison with non-alignment based transmission in the presence of co-channel deployed HetNets?
4. Is MUICIA able to provide low complexity, fair resource utilization and higher efficiency solution for interference management in HetNet?

We use simulation based analysis to answer the above questions.

6.2 System Model and Performance Metric

Let I be the total number of cells covering a given service area where each cell is using multiple antennas for the spatial multiplexing of users (MU-MIMO) in OFDM based downlink transmissions. Let $\mathcal{J}$ be the set containing the indices of macro cells whereas $\mathcal{R}$ be the set that contains the indices of pico cells such that ($|\mathcal{J}|+|\mathcal{R}|= I$). Let P_{Macro} be the maximum power available in macro cell for an OFDM sample transmission whereas the respective power in pico is P_{Pico} such that ($P_{Macro} > P_{Pico}$). Let each cell is equipped with M transmit antennas whereas the UEs in the service area are equipped with N receive antennas. Let there be L active UEs ($L \geq M$) in the coverage of each cell. Only $K(\leq M)$ UEs are selected simultaneously on the same resource for transmission by each cell. Let $\mathcal{S}_i$ represent the set which contains the indices of users selected for transmission by the ith cell such that ($|\mathcal{S}_i|= K$). Each cell transmits single stream towards each selected UE. The signal received by the mth UE ($m \in \mathcal{S}_i$) on one OFDM resource sample when co-scheduled with other ($K-1$) UEs is denoted by $\mathbf{y}_m \in \mathbb{C}^{N\times 1}$ and is given by:

$$\mathbf{y}_m = \mathbf{H}_{mi}\mathbf{p}_{mi}s_{mi} + \sum_{n\in S_i, n\neq m, n=1}^{K} \mathbf{H}_{mi}\mathbf{p}_{ni}s_{ni} + \sum_{j\neq i, j=1}^{I}\sum_{h\in S_j, h=1}^{K} \mathbf{H}_{mj}\mathbf{p}_{hj}s_{hj} + \mathbf{n}_m \qquad (6.1)$$

Where, $\mathbf{H}_{mi} \in \mathbb{C}^{N\times M}$ is the MIMO channel matrix between the ith cell and the corresponding mth UE, s_{mi} is the transmit symbol, $\mathbf{p}_{mi} \in \mathbb{C}^{M\times 1}$ is the precoding vector, $(\sum_{n\in S_i, n\neq m, n=1}^{K} \mathbf{H}_{mi}\mathbf{p}_{ni}s_{ni}) \in \mathbb{C}^{N\times 1}$ is the MUI term due to the transmission to other UEs in $\mathcal{S}_i$, $(\sum_{j\neq i, j=1}^{I}\sum_{h\in S_j, h=1}^{K} \mathbf{H}_{mj}\mathbf{p}_{hj}s_{hj}) \in \mathbb{C}^{N\times 1}$ is the total ICI term due to the transmission of the other $(I-1)$ cells to their corresponding UEs, S_j is the set of users selected by the cell j such that $|\mathcal{S}_j| = K$ and $\mathbf{n}_m \in \mathbb{C}^{N\times 1}$ is the Gaussian noise term with zero mean and variance η^2.

For the comparison of MUICIA with state of the art, we consider two different non-alignment based transmit precodings which deal with MUI, namely Signal to Leakage and Noise Ratio (SLNR)[17] and Effective Zero Forcing (EFZF)[61]. We also consider Singular Value Decomposition (SVD) based precoding where the precoding vectors are simply the right singular vectors of the channel matrix. For all kind of precoding designs we assume equal power allocation, the precoding vector for the mth UE can be written as:

$$\mathbf{p}_{mi} = \sqrt{(P_T/K)}\hat{\mathbf{p}}_{mi}$$

Where, $\hat{\mathbf{p}}_{mi} \in \mathbb{C}^{M\times 1}$ is the precoding vector with unit norm, (P_T/K) is the power allocated to each UE in $\mathcal{S}_i$, the transmit power constraint for ith cell can be written as,

$$P_T = \begin{cases} P_{Macro} & \text{if } i \in \mathcal{J} \\ P_{Pico} & \text{if } i \in \mathcal{R} \end{cases}$$

The signal after receive-processing can be written as,

$$y_m^{'} = \mathbf{g}_m^H \mathbf{y}_m$$

where, $\mathbf{g}_m \in \mathbb{C}^{N\times 1}$ is the receive vector which is based on the maximization of post receiver signal to interference and noise ratio (SINR) and is given by,

$$\mathbf{g}_m = (\mathbf{Q}_m + \eta^2\mathbf{I}_N)^{-1}\mathbf{H}_{mi}\mathbf{p}_{mi}$$

where, $\mathbf{Q}_m \in \mathbb{C}^{N\times N}$ represents the total interference covariance arriving at the mth UE. The post receiver SINR can be written as:

$$SINR_{mi} = \frac{(P_T/K)|\mathbf{g}_m^H\mathbf{H}_{mi}\hat{\mathbf{p}}_{mi}|^2}{(P_T/K)\sum_{n\in S_i, n\neq m, n=1}^{K}|\mathbf{g}_m^H\mathbf{H}_{mi}\hat{\mathbf{p}}_{ni}|^2 + Z_{ICI} + ||\mathbf{g}_m^H||^2\eta^2}$$

The symbol Z_{ICI} is the ICI after receive processing:

$$Z_{ICI} = \sum_{j\neq i, j=1}^{I}\sum_{h\in S_j, h=1}^{K}(P_T/K)|\mathbf{g}_m^H\mathbf{H}_{mj}\hat{\mathbf{p}}_{hj}|^2 \tag{6.2}$$

6.3 Important Aspects of Heterogeneous Networks

The co-channel HetNet is emerging as a promising solution to provide both coverage and capacity. The macro layer is usually deployed with proper network planning which allows further optimization and interference control in the network. However, the deployment of picos appears to be more random [83] as they are deployed in response to the traffic demand in macro coverage area. Hence the ICI in the network grows uncontrolled. In the following subsections, we explain the ICI related problems in co-channel HetNets and the techniques available at hand to solve them.

6.3.1 Cell Association and Range Expansion

Typically both the macro and pico layers use the same amount of bandwidth in a co-channel deployment scenario. It yields an unfair distribution of network resources, due to the small coverage area of low-power pico cells. Hence, it is important to offload macro traffic to pico cells, so that the additional resources introduced in the system can be well exploited. Typically the cell association is done on the basis of Reference Signal Received Power (RSRP) from each cell [82]. Due to very low power of picos, only the UEs very near to the pico BS are associated with it and therefore pico coverage is very small. To overcome this problem, a concept of range expansion for pico cells is introduced to achieve load balancing between the two cellular layers. The range expansion is achieved through cell-biasing [82]. With the help of an additional offset value (referred as ***Cell Bias***), an early handover is triggered from macro to pico. This *Bias* (in dB) artificially makes pico cell more attractive than macro for user association. A positive bias value extends the pico coverage and offloads the macro traffic. However, applying bias value results in low SINR for pico cell-edge UEs, because of obvious high ICI from high power macros. This gives rise to the requirements of interference management in HetNets.

6.3.2 Enhanced Inter Cell Interference Coordination (eICIC)

Enhanced Inter Cell Interference Coordination (eICIC) mechanisms have been proposed in [82] and [84]. These methods control power allocation, scheduling, beamforming etc. but we categorized them broadly in frequency domain and time domain methods. In the following, we briefly explain the time domain interference coordination.

The basic idea behind time domain interference coordination is that the macro cell periodically stops the data transmission in certain transmission time intervals (TTIs) also called *Subframes*. The pico utilizes these subframes to schedule those UEs which are most affected by macro interference. As some of the control information e.g. pilots are still transmitted by the macro in the coordinated subframes, therefore these subframes are referred as *Almost Blank Subframes* (ABS). A real time coordination is done via backhaul (e.g. X2 interface in LTE [82]) between macro and pico to set the percentage of ABS frames and also the patterns or periods. The cells maintain adaptive interference coordination depending upon the traffic load. Each macro mainly coordinates with the picos which are overlaid in its coverage area.

6.3.3 User Scheduling during ABS

In order to take benefits of ABS and deal with ICI, picos may adopt user scheduling schemes which utilizes ABS. In [85] an scheduling technique has been presented for pico cells. We have used this scheme in our evaluations as it supports eICIC. In the following we provide the details of comparative systems (eICIC and IA) with respect to the user scheduling and coordination requirements.

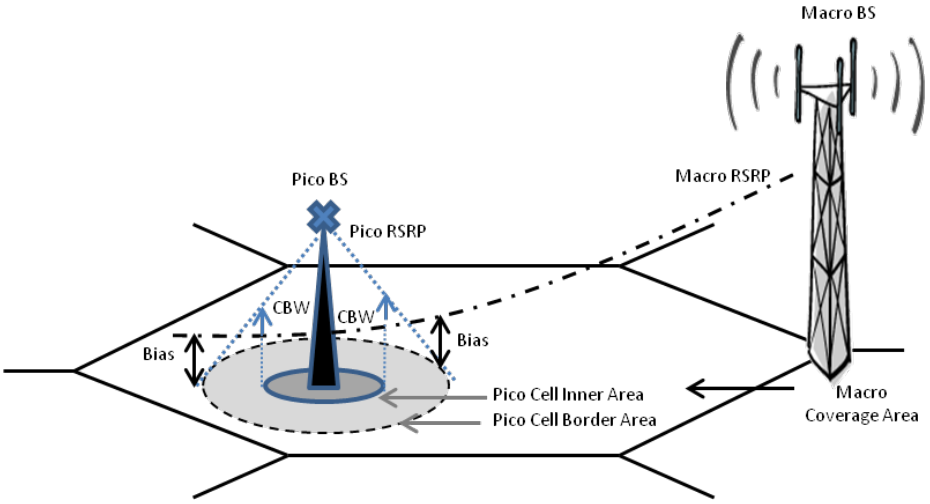

Figure 6.2: Effect of range expansion on cell association of the users to pico cells

For Interference Coordination via eICIC:

The purpose of ABS is to help the pico users affected by the interference from macro. Therefore, pico classifies its users as $cell-inner$ and $cell-border$. The cell-border users are

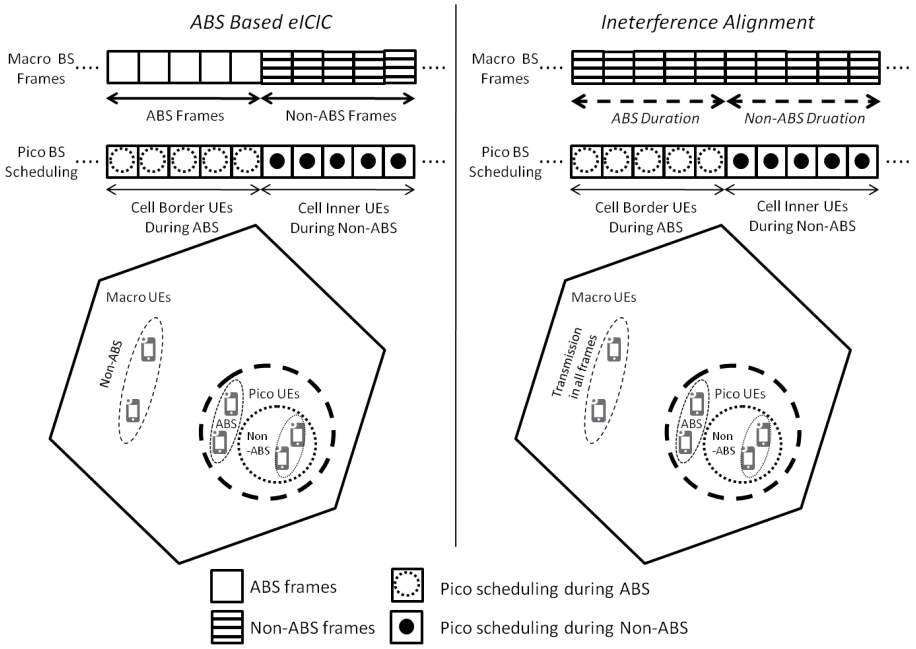

Figure 6.3: Strict scheduling representation in pico for ABS (left) and IA (right)

the main victims of macro transmissions. This is done with the help of an offset known as *Cell Border Window* (CBW) [82, 85]. Figure 6.2 illustrates the impact of Bias and CBW. The pico schedules the cell-border UEs during ABS and this scheduling method is referred as *Strict-Scheduling* in [85]. For our comparative study of IA and eICIC, we employ strict scheduling in pico cells. The coordination between pico and macro is required to exchange information like load, ABS length, ABS frame position and ABS pattern. We have evaluated eICIC for a fixed ABS pattern in all the macros. We have used SLNR and EFZF as non alignment based transmit precoding schemes in both macro and pico. These schemes do not require any inter cell coordination, the coordination is required only for eICIC. We also evaluate the performance with different Bias and CBW values to analyse the impact of these offsets.

For Interference Alignment via MUICIA:

To establish a fair comparison between eICIC and IA based techniques, we adopt strict scheduling in picos during the ABS frame times also with IA based precoding technique (MUICIA). However, note that in case of IA based precoding, macro cells are still serving their users with full power. The ABS time in picos with MUICIA is used just to ensure the scheduling of the same users. There is no coordination between the cells required for

the design of MUICIA. Figure 6.3 schematically represents the strict scheduling method for both non-alignment based and alignment based system. We emphasize that although strict scheduling is not required for IA based transmissions, but for the sake of comparison and the selection of same users we also use the strict scheduling for MUICIA. In fact this is the worst case for the MUICIA as the leverage of selecting any users in pico will also provide additional diversity gains to MUICIA.

6.4 Performance Results and Analysis

The performance results in this section would help us to answer the questions that we have formulated in section 6.1. We merge the third question with the first question by performing joint analysis of the impact of heterogeneous transmit power on alignment based and non-alignment based transmit precoding schemes in HetNets. We proceed further by analysing the percentage gains of IA in macro coverage area. A performance comparison of IA based interference management with enhanced interference coordination is presented at the end. Before presenting the simulation results for analysis, at first we describe the HetNet simulation scenario and our system assumptions.

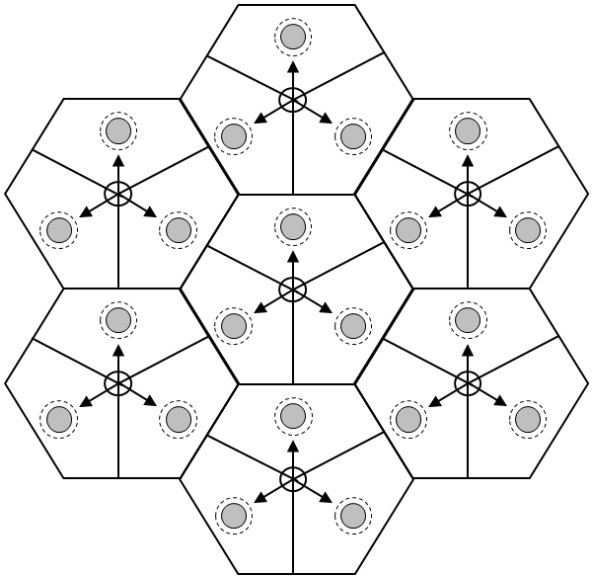

Figure 6.4: HetNet with one pico per macro coverage area. Gray areas represent the pico coverage. Dotted lines represent the cell range expansion of pico cells with the help of a bias value

6.4.1 Simulation Assumptions

Parameter	Values	
	Macro cell	Pico cell
Cellular Layout	Hexagonal grid	
Frequency Reuse factor	One	
Inter-site distance (ISD)	500 m	not defined
Pico nodes per macro cell	N/A	one per macro cell
Pico placement	N/A	0.3 lSD (from macro BS)
UE speed	3 km/h	
Antenna pattern	3D	omni directional
Channel Model	3GPP Spatial Channel Model (SCM)	
Channel Scenario	Urban Macro	Urban Micro
Carrier Frequency	2.0 GHz	
Bandwidth (P_T)	10 MHz	10 MHz
Total BS TX power (P_T)	46dBm	30dBm
Antenna Configuration	2 tx, 2 rx antenna ports	
User scheduling per PRB	$K = 2, macro$ UEs	$K = 2, pico$ UEs

Table 6.1: Salient simulation parameters for the performance evaluation

The system model as described in section 6.2 is a MIMO based closed loop multi user downlink cellular system. We use a drop based event driven system level simulation methodology based on 3GPP in [29] for HetNets. We consider the scenario with 7 sites arranged in a hexagonal grid with wraparound. Each site consists of 3-sectorized antennas such that each sector corresponds to a macro cell with unique cell ID. This gives us the usual homogeneous macro cellular layer. For the modelling of HetNets, one low-power pico cell is placed under the coverage of each high-power macro. The pico cell is positioned at a distance of 0.3 ISD (150 m) and along the bore-sight direction of the antenna array of the macro which depicts a scenario where ICI management is highly required. Figure 6.4 represents the simulated network model. Users are randomly dropped over the simulation area with the help of a uniform distribution. However, the UE positioning is managed such that the number of UEs associated to pico cells are according to the defined hotspot probability which is (1:2) for (macr:pico) [29]. We assume that each transmitter is equipped with M=2 transmit antennas and each UE is equipped with N=2 receive antennas. Each cell selects a pair of UEs ($K = 2$)

out of the set of active UEs for multi user transmission simultaneously on a time-frequency OFDM resource element. The OFDM resource structure is the same as in the previous chapters. We consider full buffer traffic and an ideal channel estimation and feedback by the UEs to their serving cells. Important simulation parameters are mentioned in table 6.1. Further propagation and antenna related parameters can be referred from [29].

6.4.2 Impact of Heterogeneity

Our primary step is to analyse the impact of ICI caused by the macro at the pico users for different multi user transmit precoding schemes. Therefore, cell range expansion has not been considered for this study i.e. $bias = 0$ dB. However, a hotspot probability of 1:2 is assumed to justify the need of a pico cell as specified by 3GPP. The comparative analysis done in this section is based on two different performance metrics namely the 'Cell Edge Throughput' [Mbit/s] and 'Mean Cell Rate' [bit/s/Hz] of the system.

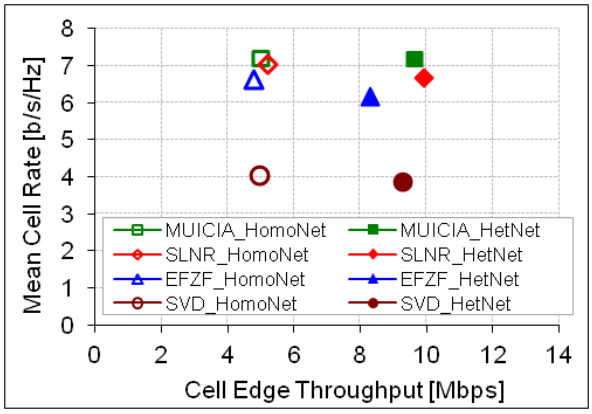

Figure 6.5: Comparison of MUICIA with other Precodings in Homo and HetNets

Figure 6.5 presents the performance of MUICIA in comparison with other precodings in two scenarios; only macro-layer (HomoNet) and HetNet. As per the expectations, HetNet achieves enhanced cell-edge user throughput for all transmit precoding schemes. If we focus on the performance comparison of MUICIA with SLNR then we see that in HomoNet there is almost no performance gap. However, in HetNets, MUICIA outperforms SLNR and other baselines in terms of mean cell rates. This is due to the extra alignment gain achieved by the UEs associated to pico cells. The ICI experienced by the pico UEs is strong and dominant from the macro transmissions. Therefore, it facilitates alignment and suppression at the receiver. Consequently in HetNet, MUICIA has a sustainable performance lead from SLNR

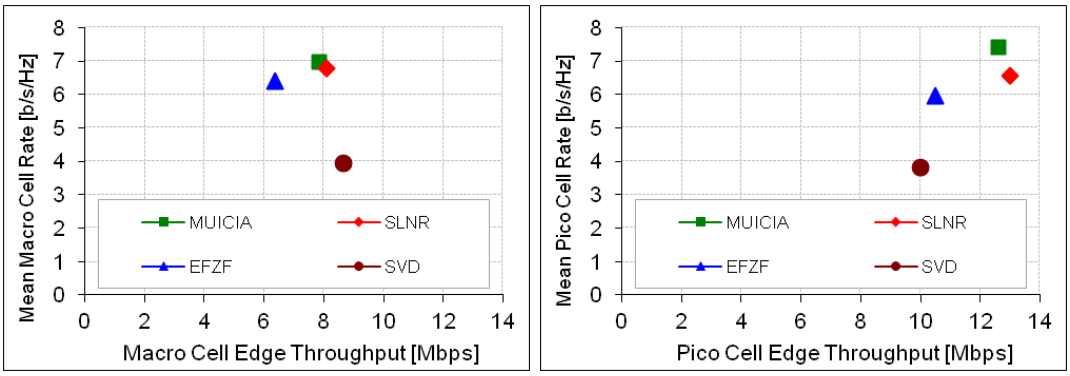

(a) Only Macro Cells (b) Only Pico Cells

Figure 6.6: Individual performance of only macro layer and only pico layer in HetNets

and EFZF as compared to HomoNet. This effect can be seen clearly in figure 6.6(b) which presents mean cell rate of only pico cells in HetNet. We can see that MUICIA outperforms SLNR by approximately 15% and EFZF by approximately 25%. This lead of MUICIA in pico translates the performance gap in the overall HetNet. In figure 6.6(a), for all precodings, the mean cell rate of macro cells in HetNet suggests no particular gain as compared to HomoNet. This is because even in the presence of pico cells, the interference from high-power macros is dominant. However, we see an increase in cell edge throughput in HetNet which is because of the decrease in number of active UEs per cell. Moreover, we see that the performance of MUICIA is almost similar to SLNR. For further results related to the impact of heterogeneity on the performance MUICIA and other precodings we refer to our publications [26] and the master thesis project [75].

6.4.3 Spectral Efficiency Gains in Macro Coverage Area

Figure 6.7 shows the gains in spectral efficiency per macro area using MUICIA with different user selection methods in HetNet. As we have one pico per macro, we expect that we achieve 100% or higher gains in the performance per macro coverage area. However, due to the additional ICI, we do not reach this point. There are two main effects here, a) the influence of macro ICI over pico, b) as we are using MUICIA also in macro cells, so there is a loss in alignment gains for macro UEs because of the increase in interference floor due to the pico cells. Hence we see that with $MaxICICondNum$ based user selection the loss in macro mean cell rate due to the additional pico interference is compensated by the gain in the pico

cells. Therefore for higher number of active users, we approach 100% gains. We see that the highest % increase in the performance of $MaxICICondNum$ algorithm and the lowest in the $MaxERate$ algorithm. As $MaxERate$ is already close to optimal, it has less comparative gains with additional picos.

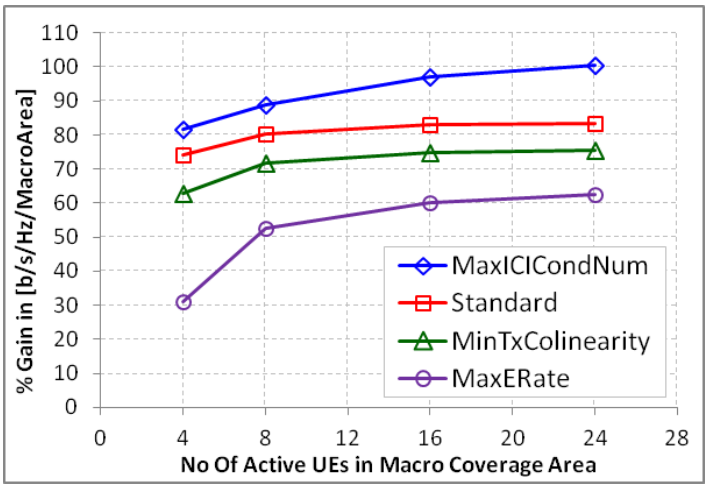

Figure 6.7: Percentage performance gains in macro coverage area with MUICIA precoding and different user selection methods

6.4.4 Interference Alignment vs Interference Coordination

In this section, we compare the interference management in HetNets through eICIC and IA. We take the same placement strategy for pico cells as in subsection 6.4.2 but here we use cell range expansion and a CBW for pico cells. In a real network scenario having eICIC, a particular ABS pattern at the macro is adopted through real time coordination with its overlaid pico. The percentage of ABS and the ABS pattern depends on pico bias offset and load distribution in the network. However, here we consider a fixed pattern and variable percentage of ABS, which varies from 0% to 100%. We select this range for ABS in order to find out the minima and maxima of the system performance.

As SLNR and EFZF are the state of the art transmit precodings, so we take them as non-alignment based multi user transmit precoding schemes and manage the ICI with eICIC based management. The MUICIA is taken as IA based transmit precoding scheme which also performs as ICI management technique. We emphasize that the strict scheduling is not

required for IA based transmission. But, for the sake of fair comparison we also apply the strict scheduling for MUICIA as explained in subsection 6.3.3.

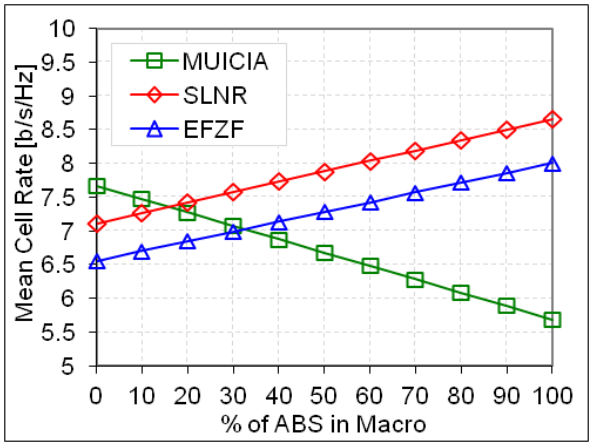

Figure 6.8: Overall Performance Comparison of MUICIA with ABS based eICIC in HetNet

Figure 6.8 presents the performance comparison of eICIC with MUICIA in terms of mean cell rate of overall HetNet with $bias = 5dB$ and $CBW = 3dB$. The two extreme points on the X-axis represent two different user selection scenarios in pico cells. The minimum abscissa, 0 % ABS means pico selects only cell-inner UEs. The maximum abscissa, 100 % ABS means pico selects only cell-border UEs. Please note that, in case of MUICIA, the percentage of ABS in figure 6.8 represents only the effect of strict scheduling in pico cells. Whereas, in case of SLNR and EFZF, in addition to strict scheduling in pico, 0 % ABS refers to *FULL* macro transmission and 100 % ABS refers to *NO* macro transmission. Positive rising slopes of SLNR and EFZF in figure 6.8, illustrate the gains coming from pico due to the increasing percentage of ABS. However, this enhancement comes at the cost of three other system metrics which are the decrease in spectral efficiency of macro, decrease in network resource utilization and the decrease in the fairness of cell-inner UEs of pico cells. Hence, eICIC is a trade-off between the increase in HetNet mean cell rate with the decrease in other system utilities. In figure 6.8, we can see that MUICIA outperforms SLNR until approximately 20 % ABS and EFZF until approximately 35 % ABS. This means MUICIA has an upper hand over eICIC until the cross over points without compromising macro spectral efficiency. For further results related to the impact of CBW and bias we refer to our publication [27] and the master thesis project [75].

6.4.5 Conclusion

We have assessed the performance of IA based transmit precoding in a closed loop MU-MIMO downlink cellular HetNet. For this purpose, we have selected MUICIA which is an uncoordinated IA based transmit precoding scheme. The simulative analysis suggests that the interference alignment based transmission schemes (e.g. MUICIA) yield higher gains in the power mismatch scenario of HetNet as compared to the homogeneous scenarios. The alignment based user selection method, $MaxICICondNum$, enhances the performance of low-power pico cells by selecting users experiencing strong and aligned ICI from high power macro cells.

With the help of system simulations, we have not only evaluated the individual performance of MUICIA but also compared it with state of the art MU-MIMO precodings (SLNR, EFZF and SVD). Our results indicate that with respect to the overall system performance, MUICIA provides higher gains in HetNets due to the specific ICI characteristics of HetNet. It simply implies that in case of strong interference scenarios as in HetNets, alignment based transmission schemes are better than the non-alignment based schemes. Moreover, it serves two purposes at a time. First, as a transmit precoding scheme and secondly as an interference management scheme without any additional effort or requirements. In particular, comparison with eICIC shows that MUICIA outperforms the eICIC technique with a sustainable gain upto 20% ABS values.

With these results, we infer that interference alignment can also be considered as a candidate for interference management technique in parallel with enhanced interference coordination schemes introduced by 3GPP for co-channel HetNet scenarios. The uncoordinated interference management approach through interference alignment has a prime advantage over coordinated approaches.

Chapter 7

Conclusion

In this work we have focused on the performance assessment and improvement of OFDM based closed loop downlink transmission in a multi user multi antenna cellular network. The technical contribution starts from Chapter 3 where we have assess the performance of *Coordinated* IA based transmit precoding scheme. The results have shown that IA outperforms the baseline schemes only in a single site scenario. However, the baseline schemes are outperforming IA under the assumption of a larger (more realistic) number of sites and BSs. These results draw important conclusions about the application of *Coordinated* IA to mitigate ICI in practical systems. It implies that IA can only be applied in very limited practical scenarios with very low or almost zero mobility. These results lead to a reconsideration of the benefits of *Coordinated* IA in real-world systems. After the assessment of IA, we have also proposed heuristic user selection methods which improve the performance of IA by using the diversity in the system.

In Chapter 4 we have focused on a cellular system where each cell is performing multi user MIMO transmissions. In this scenario, we have proposed a new *Uncoordinated* IA based transmit precoding scheme that aligns the multi user interference with partial and outdated inter cell interference. The results have shown that even with outdated alignment, our proposed scheme outperforms the baselines and provides substantial gains in spectral efficiency specially in higher ICI regions. We have also considered some practical limitations of the receivers and presented a modified scheme. Even after the limitations our scheme provides considerable gains over the other baselines.

In addition to the proposal of an *Uncoordinated* alignment based transmit precoding scheme, we have also proposed three user selection methods for MU-MIMO cellular system.

Using the user selection methods, we have assessed the performance of our scheme in a smaller and a larger cellular system scenario. In larger scenario we expect the loss of interference alignment due to the whiteness of interference space. However, the results have shown that unlike the *Coordinated* IA in Chapter 3 our proposal outperforms the baseline also in large cellular system for high and average ICI regions. These results provide a strong statement for further research to transform the gains of interference alignment in a larger cellular scenario.

In Chapter 4, we proved analytically and with the help of system simulations that our alignment based proposal provides gains over the non-alignment based schemes. In Chapter 5, we continue this line of action by providing the proof of concept for our proposal with the help of measured channels. We evaluate and assess our scheme using a software defined indoor measurement lab trial test-bed. The results from measurements show that our scheme outperform baselines even with a training overhead similar to the current LTE system.

In the last technical chapter that is Chapter 6, we have assessed the application of MUICIA in a co-channel heterogeneous cellular network as an interference management scheme. The first observation of the results show that alignment based precoding provide higher gains in heterogeneous networks due to the special interference characteristics. Additionally, we have compared the performance of MUICIA as an *interference alignment* based solution with Time-Domain eICIC which is an *interference coordination* based solution. The results show considerable gains with MUICIA over eICIC. This study helps us to consider future solutions which can combine both techniques in order to further optimize the future systems.

In a nutshell, we can state that the outcome of this work provides an essential understanding on the application of interference alignment based solutions in cellular networks. Moreover, we have provided an interference alignment based transmit precoding design with user selection algorithms that enhances the system performance as compared to the state of the art solutions. However, we still foresee many directions that can be followed for future research in this area. With respect to the *Coordinated* IA, further gains can be explored with dynamic clustering and user selection algorithms. The *Uncoordinated* IA that we have proposed is limited to schedule two users simultaneously on a single radio resource. Further research is required to pull up these limits. In this study, we have focused mainly on linear solutions mainly due to delay, feedback overhead and computational complexity constraints. However, we envision that future technologies will relax these barriers and iterative solutions for these problems may further optimize the system performance.

References

[1] V.H. MacDonald. "Advanced Mobile Phone Service: The Cellular Concept". *Bell System Technical Journal*, 58, No.1:15–43, Jan. 1979.

[2] K.S. Gilhousen, I.M. Jacobs, R. Padovani, A.J. Viterbi, Jr. Weaver, L.A., and III Wheatley, C.E. "On the capacity of a cellular CDMA system". *IEEE Transactions on Vehicular Technology*, 40(2):303–312, May. 1991.

[3] G. Boudreau, J. Panicker, Ning Guo, Rui Chang, Neng Wang, and S. Vrzic. "Interference coordination and cancellation for 4G networks". *IEEE Communications Magazine*, 47(4):74–81, May. 2009.

[4] M.A. Maddah-Ali, A.S. Motahari, and A.K. Khandani. "Communication Over MIMO X Channels: Interference Alignment, Decomposition, and Performance Analysis". *IEEE Transactions on Information Theory*, 54(8):3457–3470, Jul. 2008.

[5] V.R. Cadambe and S.A. Jafar. "Interference Alignment and Spatial Degrees of Freedom for the K User Interference Channel". In *Proceedings of IEEE International Conference on Communication (ICC)*, pages 971–975, Jun. 2008.

[6] M. Mouly and M.B. Pautet. *"The GSM System for Mobile Communication"*. Telecom Publishing, 2nd edition, Dec. 1992.

[7] Harri Holma and Antti Toskala. *"WCDMA for UMTS: HSPA Evolution and LTE"*. John Wiley & Sons, Inc., New York, NY, USA, Aug. 2010.

[8] H. Holma and A. Toskala. *"LTE Advanced: 3GPP Solution for IMT-Advanced"*. John Wiley & Sons, Inc., New York, NY, USA, Aug. 2012.

[9] Abdelbaset S. Hamza, Shady S. Khalifa, Haitham S. Hamza, and Khaled Elsayed. "A Survey on Inter-Cell Interference Coordination Techniques in OFDMA-Based Cellular Networks". *IEEE Tutorials on Communication Surveys*, 15(4):1642–1670, Nov. 2013.

[10] L.C. Godara. "Application of antenna arrays to mobile communications. II. Beamforming and direction-of-arrival considerations". *Proceedings of the IEEE*, 85(8):1195–1245, Aug. 1997.

[11] L.C. Godara. "Applications of antenna arrays to mobile communications. I. Performance improvement, feasibility, and system considerations". *Proceedings of the IEEE*, 85(7):1031–1060, Jul. 1997.

[12] G. J. Foschini and M. J. Gans. "On limits of wireless communications in a fading environment when using multiple antennas". *Wireless Personal Communications*, 6:311–335, Mar. 1998.

[13] I. Emre Telatar. "Capacity of multi-antenna Gaussian channels". *European Transactions on Telecommunications*, 10:585–595, Dec. 1999.

[14] S. Alamouti. "A simple transmit diversity technique for wireless communications". *IEEE Journal on Selected Areas in Communications*, 16(8):1451–1458, Oct. 1998.

[15] Q.H. Spencer, A.L. Swindlehurst, and M. Haardt. "Zero-forcing methods for downlink spatial multiplexing in multiuser MIMO channels". *IEEE Transactions on Signal Processing*, 52(2):461–471, Feb. 2004.

[16] Taesang Yoo and A. Goldsmith. "On the optimality of multiantenna broadcast scheduling using zero-forcing beamforming". *IEEE Journal on Selected Areas in Communications*, 24(3):528 – 541, Mar. 2006.

[17] M. Sadek, A. Tarighat, and A.H. Sayed. " Leakage-Based Precoding Scheme for Downlink Multi-User MIMO Channels". *IEEE Transactions on Wireless Communications*, 6(5):1711 –1721, May. 2007.

[18] D. Aziz, F. Boccardi, and A. Weber. "System-level performance study of interference alignment in cellular systems with base-station coordination". In *Proceedings of IEEE International Symposium on Personal, Indoor and Mobile Radio Communications (PIMRC)*, pages 1155–1160, Sept. 2012.

[19] D. Aziz, S. Sentuerk, A. Weber, and T. Wild. "A simple model for imperfect channel state information and its application for the assessment of Interference Alignment". In *Proceedings of IEEE International Conference on Wireless and Mobile Computing, Networking and Communications (WiMob)*, pages 507–511, Oct. 2012.

[20] D. Aziz and A. Weber. "Multiuser transmit precoding based on outdated interference alignment"'. In *Proceedings of IEEE International Congress on Ultra Modern Telecommunications and Control Systems and Workshops (ICUMT)*, pages 148–153, Oct. 2012.

[21] D. Aziz and A. Weber. "Transmit precoding based on outdated interference alignment for two users multi cell MIMO system". In *Proceedings of IEEE International Conference on Computing, Networking and Communications (ICNC)*, pages 708–713, Jan. 2013.

[22] D. Aziz, M. Mazhar, and A. Weber. "Impact of multi user selection on the performance of transmit precoding in MU-MIMO cellular systems". In *Proceedings of IEEE Wireless Communications and Networking Conference (WCNC)*, pages 3191–3196, Apr. 2013.

[23] D. Aziz, M. Mazhar, and A. Weber. "Performance Enhancement of Multi User Multi Cell Interference Alignment with Pair Selection". In *Proceedings of IEEE Vehicular Technology Conference (VTC Fall)*, Sep. 2013.

[24] D. Aziz, R. Atanasov, and A. Weber. "Performance Assessment of Multi User Multi Cell Interference Alignment with Limited Feedback". In *Proceedings of IEEE Vehicular Technology Conference (VTC Spring)*, May 2014.

[25] D. Aziz, S. Ahmed, C. Hoek, G. Herzog, and J. Koppenborg. "Performance Assessment of Multi User Inter Cell Interference Alignment with Measured Channels". In *Proceedings of IEEE International Symposium on Personal, Indoor and Mobile Radio Communications (PIMRC)*, Sep. 2014.

[26] D. Aziz, M. Mazhar, and A. Weber. "Multi User Inter Cell Interference Alignment in Heterogeneous Cellular Networks". In *Proceedings of IEEE Vehicular Technology Conference (VTC Spring)*, May 2014.

[27] D. Aziz, M. Mazhar, and A. Weber. "Interference Management through Interference Alignment based Transmit Precoding in Multi User Heterogeneous Cellular Networks". In *Proceedings of IEEE European Wireless Conference*, May 2014.

[28] T. Huschka. "Ray tracing models for indoor environments and their computational complexity". In *Proceedings of IEEE International Symposium on Personal, Indoor and Mobile Radio Communications (PIMRC)*, pages 486–490 vol.2, Sep. 1994.

[29] 3GPP. "Further Advancements for E-UTRA - Physical Layer Aspects", Technical Report. TR 36.814, V 9.0.0, Mar. 2010.

[30] IST-WINNER II Deliverable 1.1.2 v.1.2. "WINNER II Channel Models, Part-II". Final Technical Report, Sep. 2007.

[31] M. Gudmundson. "Correlation model for shadow fading in mobile radio systems". *Electronics Letters*, 27(23):2145–2146, Nov. 1991.

[32] S. Klein, S. Uygungelen, and C.M. Mueller. "A Novel Sampling Method for the Spatial Frequencies of Sinusoid-Based Shadowing Models". In *Proceedings of IEEE Vehicular Technology Conference (VTC Spring)*, pages 1–5, May 2010.

[33] Peter Almers, Ernst Bonek, A Burr, Nicolai Czink, Mérouane Debbah, Vittorio Degli-Esposti, Helmut Hofstetter, P Kyö, D Laurenson, Gerald Matz, et al. "Survey of channel and radio propagation models for wireless MIMO systems". *EURASIP Journal on Wireless Communications and Networking*, 2007, Feb. 2007.

[34] 3GPP. "Spatial Channel Model for MIMO Simulations", Technical Report. TR 25.996, V 9.0.0, Mar. 2010.

[35] A.F. Molisch, H. Asplund, R. Heddergott, M. Steinbauer, and T. Zwick. "The COST259 Directional Channel Model-Part I: Overview and Methodology". *IEEE Transactions on Wireless Communications*, 5(12):3421–3433, Dec. 2006.

[36] William Tranter, K. Shanmugan, Theodore Rappaport, and Kurt Kosbar. *"Principles of Communication Systems Simulation with Wireless Applications"*. Prentice Hall Press, Upper Saddle River, NJ, USA, first edition, Aug. 2002.

[37] Robert W. Chang. "Synthesis of Band-Limited Orthogonal Signals for Multichannel Data Transmission". *Bell Systems Technical Journal*, 45:1775–1796, Dec. 1966.

[38] 3GPP. "Physical channels and modulation", Technical Specifications. TS 36.211, V11.5.0, Mar. 2012.

[39] M. Trivellato, F. Boccardi, and H. Huang. Zero-forcing vs unitary beamforming in multiuser MIMO systems with limited feedback. In *Proceedings of IEEE International Symposium on Personal, Indoor and Mobile Radio Communications (PIMRC)*, pages 1–6, Sep. 2008.

[40] Farhan Khalid and Joachim Speidel. "Advances in MIMO Techniques for Mobile Communications - A Survey". *IJCNS*, 3(3):213–252, Mar. 2010.

[41] P. Marsch and G.P. Fettweis. *"Coordinated Multi-Point in Mobile Communications: From Theory to Practice"*. Cambridge University Press, Aug. 2011.

[42] A. Host-Madsen and A. Nosratinia. "The multiplexing gain of wireless networks". In *Proceedings of IEEE International Symposium on Information Theory (ISIT)*, pages 2065–2069, Sep. 2005.

[43] O. El Ayach, S.W. Peters, and R.W. Heath. "The Feasibility of Interference Alignment Over Measured MIMO-OFDM Channels". *IEEE Transactions on Vehicular Technology*, 59(9):4309–4321, Nov. 2010.

[44] R. Tresch and M. Guillaud. "Clustered interference alignment in large cellular networks". In *Proceedins of IEEE International Symposium on Personal, Indoor and Mobile Radio Communications (PIMRC)*, pages 1024–1028, Sep. 2009.

[45] T. Wild. "Comparing Downlink Coordinated Multi-Point Schemes with Imperfect Channel Knowledge". In *Proceedings of IEEE Vehicular Technology Conference (VTC Fall)*, pages 1–5, Sep. 2011.

[46] C.M. Yetis, Tiangao Gou, S.A. Jafar, and A.H. Kayran. "Feasibility Conditions for Interference Alignment". In *Proceedings of IEEE Global Telecommunications Conference (GLOBECOM)*, pages 1–6, Dec. 2009.

[47] V.R. Cadambe and S.A. Jafar. Interference Alignment and Degrees of Freedom of the K - User Interference Channel. *IEEE Transactions on Information Theory*, 54(8):3425–3441, Aug. 2008.

[48] M. H M Costa. "Writing on dirty paper (Corresp.)". *IEEE Transactions on Information Theory*, 29(3):439–441, May 1983.

[49] N. Hassanpour, J.E. Smee, Jilei Hou, and Joseph B. Soriaga. "Distributed Beamforming Based on Signal-to Caused-Interference Ratio". In *Proceedings of IEEE International Symposium on Spread Spectrum Techniques and Applications (ISSSTA)*, pages 405–410, Aug. 2008.

[50] K. Gomadam, V.R. Cadambe, and S.A. Jafar. "Approaching the Capacity of Wireless Networks through Distributed Interference Alignment". In *Proceedings of IEEE Global Telecommunications Conference (GLOBECOM)*, pages 1 –6, Dec. 2008.

[51] R. Tresch and M. Guillaud. "Cellular Interference Alignment with Imperfect Channel Knowledge". In *Proceedings of IEEE International Conference on Communications (ICC) Workshops*, pages 1–5, Jun. 2009.

[52] B. Nosrat-Makouei, J.G. Andrews, and R.W. Heath. "MIMO Interference Alignment Over Correlated Channels With Imperfect CSI". *IEEE Transactions on Signal Processing*, 59(6):2783–2794, Mar. 2011.

[53] Sevil Sentuerk. "Feasibility of Interference Alignment in Future Cellular Networks". *Unpublished Master Thesis Report to the Institute of Telecommunication, University of Stuttgart*, Mar. 2012.

[54] P. Baracca, F. Boccardi, and V. Braun. "A dynamic joint clustering scheduling algorithm for downlink CoMP systems with limited CSI". In *Proceedings of IEEE International Symposium on Wireless Communication Systems (ISWCS)*, pages 830–834, Aug. 2012.

[55] Uk Jang, Kang-Yong Lee, Kee-Seong Cho, and Won Ryu. "Transmit Beamforming Based Inter-Cell Interference Alignment and User Selection with CoMP". In *Proceedings of IEEE Vehicular Technology Conference (VTC Fall)*, pages 1–5, Sep. 2010.

[56] Jung Hoon Lee and Wan Choi. "Opportunistic Interference Aligned User Selection in Multiuser MIMO Interference Channels". In *Proeccedings of IEEE Global Telecommunications Conference (GLOBECOM)*, pages 1–5, Dec. 2010.

[57] J. Schreck and G. Wunder. "Iterative interference alignment for cellular systems with user selection". In *Proceedings of IEEE International Conference on Acoustics, Speech and Signal Processing (ICASSP)*, pages 2833–2836, Mar. 2012.

[58] Jie Gong, Sheng Zhou, Zhisheng Niu, Lu Geng, and Meng Zheng. "Joint Scheduling and Dynamic Clustering in Downlink Cellular Networks". In *Proceedings of IEEE Global Telecommunications Conference (GLOBECOM)*, pages 1–5, Dec. 2011.

[59] 3GPP. "E-UTRA User Equipment (UE) radio access capabilities", Technical Report. TR 36.306, V 11.1.0, Mar. 2011.

[60] Rui Zhang, J.M. Cioffi, and Ying-Chang Liang. "Throughput comparison of wireless downlink transmission schemes with multiple antennas". In *Proceedings of IEEE International Conference on Communications (ICC)*, 4, pages 2700–2704 Vol. 4, Jun. 2005.

[61] F. Boccardi, H. Huang, and M. Trivellato. "Multiuser eigenmode transmission for mimo broadcast channels with limited feedback". In *Proceedings of IEEE Workshop on Signal Processing Advances in Wireless Communications (SPAWC)*, pages 1 –5, Jun. 2007.

[62] Changho Suh, M. Ho, and D. Tse. "Downlink Interference Alignment". In *Proceedings of IEEE Global Telecommunications Conference (GLOBECOM)*, pages 1 –5, Dec. 2010.

[63] A. Bayesteh, A. Mobasher, and Yongkang Jia. "Downlink multi-user interference alignment in two-cell scenario". In *Proceedings of IEEE Canadian Workshop on Information Theory (CWIT)*, pages 182 –185, May 2011.

[64] M.A. Maddah-Ali and D. Tse. "Completely stale transmitter channel state information is still very useful". In *Proceedings of IEEE Annual Allerton Conference on Communication, Control, and Computing (Allerton)*, pages 1188 –1195, Oct. 2010.

[65] 3GPP. "Network-Assisted Interference Cancellation and Suppression for LTE", Technical Report. TR 36.866, V 0.1.0, Apr. 2013.

[66] K.E. Baddour and N.C. Beaulieu. "Autoregressive modeling for fading channel simulation". *IEEE Transactions on Wireless Communications*, 4(4):1650–1662, Jul. 2005.

[67] A. Galntai and Cs. J. Hegeds. "Jordan's principal angles in complex vector spaces". *Numerical Linear Algebra with Applications*, 13(7):589–598, Sep. 2006.

[68] T. K Y Lo. "Maximum ratio transmission". *IEEE Transactions on Communications*, 47(10):1458–1461, Oct. 1999.

[69] M. Sadek, A. Tarighat, and A.H. Sayed. "Active Antenna Selection in Multiuser MIMO Communications". *IEEE Transactions on, Signal Processing*, 55(4):1498–1510, Apr. 2007.

[70] Q.H. Spencer and A.L. Swindlehurst. "Channel allocation in multi-user MIMO wireless communications systems". In *Proceedings of IEEE International Conference on Communications (ICC)*, 5, pages 3035 – 3039 Vol.5, Jun. 2004.

[71] M. Herdin, N. Czink, H. Ozcelik, and E. Bonek. "Correlation matrix distance, a meaningful measure for evaluation of non-stationary MIMO channels". In *Proceedings of IEEE Vehicular Technology Conference (VTC Spring)*, 1, pages 136 – 140 Vol. 1, Jun. 2005.

[72] G. Golub and C. van Loan. *"Matrix computations"*. London: The Johns Hopkins University Press, 1996.

[73] N. Czink, B. Bandemer, G. Vazquez-Vilar, L. Jalloul, C. Oestges, and A. Paulraj. "Spatial separation of multi-user MIMO channels". In *Proceedings of IEEE International Symposium on Personal, Indoor and Mobile Radio Communications (PIMRC)*, pages 1059–1063, Sep. 2009.

[74] Yonghong Zeng and Ying-Chang Liang. "Eigenvalue-based spectrum sensing algorithms for cognitive radio". *IEEE Transactions on Communications*, 57(6):1784 –1793, Jun. 2009.

[75] Mustansir Mazhar. "Advanced Multi User Algorithms for Next Generation MIMO Cellular Networks". *Unpublished Master Thesis Report to the Institute for Integrated Signal Processing Systems (ISS), RWTH Aachen University*, Jul. 2013.

[76] D.J. Love, R.W. Heath, V. K N Lau, D. Gesbert, B.D. Rao, and M. Andrews. "An overview of limited feedback in wireless communication systems". *IEEE Journal on Selected Areas in Communications*, 26(8):1341–1365, Oct. Oct. 2008.

[77] Chun Kin Au Yeung and D.J. Love. "Performance Analysis of Random Vector Quantization Limited Feedback Beamforming". In *Proceedings of IEEE Asilomar Conference on Signals, Systems and Computers*, pages 408–412, Nov. 2005.

[78] Kyeongjun Ko and Jungwoo Lee. "Hierarchical codebook design for fast search with Grassmannian codebook". In *Proceedings of IEEE Wireless Communications and Networking Conference (WCNC)*, pages 873–877, Apr. 2012.

[79] Radoslav Atanasov. "Performance of Interference Alignment with Limited Feedback". *Unpublished Master Thesis Report to the Institute of Telecommunication, University of Stuttgart*, Jan. 2012.

[80] Magnus Sandell, Jan-Jaap van de Beek, and Per Ola Brjesson. "Timing and Frequency Synchronization in OFDM Systems Using the Cyclic Prefix". In *Proceedings of International Symposium on Synchronization*, 42, pages 2908–2914, Dec. 1995.

[81] Syed Ammar Iqbal Ahmed. Multi-User Inter-Cell Interference Alignment (MUICIA) with Measured Channels. *"Unpublished Master Thesis Report to the Institute of Telecommunication, University of Stuttgart"*, Jan. 2014.

[82] 3GPP. "Evolved Universal Terrestrial Radio Access (E-UTRA) and Evolved Universal Terrestrial Radio Access Network (E-UTRAN); Overall description", Technical Specifications . TS 36.300, V 10.0.0, Dec. 2010.

[83] R.W. Heath and M. Kountouris. "Modeling heterogeneous network interference". In *Proceedings of IEEE Information Theory and Applications Workshop (ITA)*, pages 17–22, Feb. 2012.

[84] D. Lopez-Perez, I. Guvenc, G. De la Roche, M. Kountouris, T.Q.S. Quek, and Jie Zhang. "Enhanced intercell interference coordination challenges in heterogeneous networks". *IEEE Wireless Communications Magazine*, 18(3):22–30, Jun. 2011.

[85] A. Weber and O. Stanze. "Scheduling strategies for HetNets using eICIC". In *Proceedings of IEEE International Conference on Communications (ICC)*, pages 6787–6791, Jun. 2012.